ABSTRACT

Title of Dissertation: **ELECTROADHESION OF HYDROGELS TO BIOLOGICAL TISSUES: A DISCOVERY THAT COULD ENABLE SUTURELESS SURGERY**

Leah Klein Borden, Doctor of Philosophy, 2022

Directed By: Professor Srinivasa R. Raghavan,
Department of Chemical and Biomolecular Engineering

This study concerns the topic of electroadhesion (EA), which refers to adhesion induced by an electric field. Previous research had demonstrated that a DC electric field could be used to adhere a cationic hydrogel to an anionic hydrogel. Here, we extend this phenomenon to new systems. First, we adhere cationic gels to animal (bovine) tissues by simply applying a DC field of ~ 10 V across a gel-tissue pair for 10 to 20 s. This adhesion persists indefinitely after the electric field is removed. Moreover, if the field is re-applied with reversed polarity, the EA is eliminated, and the materials can be separated. Because tissues have anionic character, only cationic gels can be stuck to them by EA. We also show that gels can be stuck over cuts or tears in tissues using EA, which can enable tissue repair (surgery) to be performed without the need for sutures or staples.

Electroadhesion goes far beyond just bovine tissues. We have found that gels can be adhered by EA to tissues from various animals, including mammals (e.g., cow, pig, mouse); birds (e.g., chicken); fish (e.g., salmon); reptiles (e.g., lizards); amphibians (e.g., frogs), as well as various invertebrates (e.g., shrimp, worms). In addition, gels can also be adhered to plant tissue, including fruits (e.g., plums) and vegetables (e.g.; carrot), and also to fungi (mushrooms). In mammals, EA is strong for certain tissue types, such as arteries, intestines, and cornea across a

range of species. Conversely, weak or no adhesion is observed with other mammalian tissues such as adipose and brain. These differences reveal some common themes in regard to EA: for instance, the higher the fraction of anionic polymers (proteins and/or polysaccharides) in the biological material, the higher the EA strength. Interestingly also, because tissues often have anisotropic structure, adhesion by EA can be strong in one tissue orientation, but weak or non-existent in the perpendicular one.

Lastly, we delve into the mechanism behind EA. The EA strength between a cationic gel and an anionic material (gel or tissue) can be systematically enhanced in several ways. These include increasing the polymer concentration in the cationic gel as well as the cationic charge density. We also conduct experiments to unravel the contributions to EA from the charged polymer chains and the counterions. When cationic and anionic gels are contacted in the EA orientation and a high voltage of ~ 100 V is applied, the gels undergo “zipping”, i.e., they rapidly lock into adhesion due to electrostatic interactions in a manner that resembles the closing of a zip. Our findings suggest the following sequence of events for EA between gels. First, the DC field pulls counterions away from the gel-gel interface, which strongly polarizes the cationic and anionic chains at the interface. These chains then form a dense electrostatic complex (ESC), leading to adhesion of the gels. When the field is turned off, the ESC persists because it is thermodynamically stable. This explains why the adhesion remains strong and can even be permanent. Future work will investigate the applicability of EA towards surgeries, first in animals, and then potentially in humans.

ELECTROADHESION OF HYDROGELS TO BIOLOGICAL TISSUES: A DISCOVERY THAT COULD ENABLE SUTURELESS SURGERY

by

Leah Klein Borden

Dissertation submitted to the Faculty of the Graduate School of the
University of Maryland, College Park, in partial fulfillment
of the requirements for the degree of
Doctor of Philosophy
2022

Advisory Committee:

Professor Srinivasa R. Raghavan, Department of Chemical & Biomolecular Engineering, Chair
Professor Peter Kofinas, Department of Chemical & Biomolecular Engineering
Professor Ian White, Fischell Department of Bioengineering
Professor Paul Albertus, Department of Chemical & Biomolecular Engineering
Professor John P. Fisher, Fischell Department of Bioengineering, Dean's Representative

“I am among those who think that science has great beauty”

Marie Curie

Acknowledgements

I would like to begin with my appreciation to my PhD advisor Dr. Srini Raghavan. Dr. Raghavan's mentoring and advising style provided me as his 26th PhD student with the opportunities to explore areas of research that were of great interest to me. This allowed me grow not only as a researcher and scientist, but also as a mentor and entrepreneur. Dr. Raghavan insisted on our strong understanding of fundamentals as well as being able to present scientific knowledge in an approachable manner. This winning combination has been an invaluable lesson I learned over these last 5 years, and I will carry these lessons in my scientific adventures and career.

I would also like to acknowledge my thesis committee: Dr. Peter Kofinas on productive advising and writing my recommendation letters, Dr. Ian White for a fruitful collaboration on the electric field parameters as well as assisting in developing the medical device for the animal studies, Dr. John Fisher on generously allowing me to use instruments in his lab as well as insight about the field of tissue engineering, and Dr. Paul Albertus for his feedback on electrochemistry – a field I still find difficult.

I would also like to thank my collaborators, Dr. Anthony Sandler, for generously opening his lab for our use and sharing the animal facility resources towards our project together. I would like to thank Dr. Michele Saruwatari for designing experiments and preforming the surgical and biological procedures, for insight and dedication during the animal studies.

I am highly indebted to my colleagues from the Raghavan group, both present and past, for all the help I received related to my research activities. I am especially thankful to Dr. Hema

Choudhary and Dr. Nikhil Subraveti, my batch mates, for walking through these times with me. I am thankful for your support, friendship, sharing happiness and sorrows throughout over our 5 years together. It wouldn't be the same without you.

I have great appreciation to my fellow researchers and mentees who worked with me on Electroadhesion. First and foremost, Uma Kokilepersaud. Your willingness to learn and help has moved electroadhesion forward and helped me in many ways. You have been my go-to person throughout nearly my entire time in the lab. I will always remember your contribution. I would like to acknowledge Oliver Viyer for your time working on EA. My undergrad mentees Claire Rutkowski for your friendship, Sam Grasso for your insightful work, Lena Akil, Maya Wheeler and Eitan Traum for your contributions. I would also like to thank David Boegner for being the contact person orchestrating the collaborative work at the White Lab.

I am also thankful to Dr. Niti Agrawal for a great time at ACS in Florida, Dr. Sohyun Ahn for introducing me to good restaurants in the DMV area, Dr. Ben Thompson for research discussions, Faraz Burni for always willing to entertain complex research ideas and excellent Biriyani at each potluck, Sairam Ganesh for your positive attitude, Wenhao Xu for discussing and contemplating common research questions, Morine Nader for your help on electroadhesion during my time writing the dissertation, Mahima Srivastava for taking over Safety Officer duties, Medha Rath, Eylul Utlu, and Christine Zhou for good times together.

Finally, I would like to express my appreciation to my family. Words cannot express my gratitude for your unconditional love, support, and your numerous sacrifices. James, without your

support I would have not been able to pursue this path. I am forever grateful for you, my dear. Benjamin and Elana, you have brought me the greatest joy that life can offer. All my hard work is towards a better future for you, my loves. Mom, for being part of my life's journey. Dad, for introducing me to chemistry in a world with no science. Finally, my sweet sisters Bracha and Rivka Baila, you both have been my rock at hard times, and I appreciate you.

Table of Contents

Table of Figures

List of Abbreviations

AAm	Acrylamide
Alg	Alginate
APS	Ammonium persulfate
ASTM	American Society for Testing and Materials
BIS	N,N'-methylenebis(acrylamide)
Ca^{2+}	Calcium ion
$CaCl_2$	Calcium chloride dihydrate
Co-mono	Co-monomer
DC	Direct current
DI	Deionized water
DMA	Dynamic mechanical analyzer
EA	Electroadhesion
ECM	Extracellular matrix
EPA	Electrophoretic adhesion
$FeCl_3$	Iron (III) Chloride
GAG	Glycosaminoglycan
IPN	Interpenetrating network
JR	Johnsen-Rahbek
LAP	Laponite XLG nanoparticles
MB^+	Methylene blue dye

O_{II}^-	Orange (II) dye
PBS	Phosphate buffered saline
PO	Post-operative
PSA	Pressure sensitive adhesives
PU	Poly-urethane
QDM	Quaternized dimethylamino etheyl methacrylate
RB	Rhodamine blue
s-IPN	Semi interpenetrating network
SA	Sodium acrylate
SB	Strawberry
TEMED	N,N,N',N'-tetramethylethylene-diamine
VDW	Van Der Waals

Chapter 1

Introduction and Overview

1.1 Problem Description and Motivation

Adhesives have been used since prehistoric times to stick materials together,[1] and the associated property is called adhesion.[2,3] The first adhesives[4] were made around 200,000 years ago by Neanderthals from birch-bark tar and used to stick stone tools to wooden handles.[5] Currently, numerous kinds of adhesives are available, and these can be derived from natural or synthetic sources.[6-15] Adhesives can stick dry or wet materials,[11-13,16] rough and smooth surfaces,[15,17] and be applied by pressure or drying.[8-10] It is common knowledge that if two solids do not stick when contacted, an adhesive is required to stick the solids together.

Can two non-sticky materials be adhered without using an adhesive at all? This is exactly the scenario we will discuss in this dissertation. For example, consider a cationic hydrogel and an anionic hydrogel. These are not sticky on their own. Rather, the materials develop adhesion to one another only upon exposure to a DC electric field (~ 10 V applied for just 10 to 20 s).[18,19] This property is therefore called *electroadhesion* (EA).[18,20-24] Interestingly, the hydrogels stay adhered indefinitely after the field is removed. Moreover, this adhesion can be reversed by reversing the polarity of the DC field, implying that EA is a reversible phenomenon. EA was first reported in 2010 by Asoh and Kikuchi.[18] However, in the decade since the original publication, it has attracted little attention because adhesion of oppositely charged hydrogels does not have an obvious purpose or application. In other words, the research community regarded EA as a scientific oddity, but not much more.

1.2 Proposed Approach

In this work, we set out to further investigate the phenomenon of electroadhesion. We will show that EA can be applied to numerous materials apart from hydrogels. Specifically, we have used EA to adhere cationic hydrogels to various biological tissues, including tissues from animals and plants. We have also delved into the fundamental mechanism behind EA, which applies both to gel-gel and gel-tissue adhesion. The utility of gel-tissue EA is shown by *in vitro* experiments: hydrogel patches are adhered over cuts tissues using EA, which can enable a new approach to surgery. The three Chapters of this dissertation deal with the following aspects:

1.2.1 Electroadhesion of Gels to Bovine Tissues: A New Way to Seal Cuts and Tears

In Chapter 3, we extend EA from gel-gel to gel-tissue systems. We report our discovery that cationic hydrogels can be adhered using EA to various bovine tissues.[19] The key results are shown in Figure 1.1. A piece from a bovine aorta (blood vessel) is examined together with a cationic hydrogel (QDM). The two do not stick on contact (Figure 1.1A). Next, the two are connected to a DC power source and a potential of 10 V is applied for ~ 20 s in a specific orientation. The gel and tissue now develop a strong adhesion (Figure 1.1B), which is permanent after the pair is removed from the field. If the pair is reinserted into the same DC field, but with the polarity reversed, the gel and tissue can be detached after ~ 20 s (Figure 1.1C). We show that cationic gels can be adhered strongly by EA to a variety of tissue types such as aorta, cornea, lung, and cartilage, but adhesion is weak or non-existent with other tissues such as the liver, spleen, brain, and fat. We then also studied *in vitro* models of EA-based repair. Cuts were made in model tubes, and gel-patches were stuck over the cuts using EA. We then pumped fluid through the repaired tube and showed that the gel-patches could withstand fluid pressure.

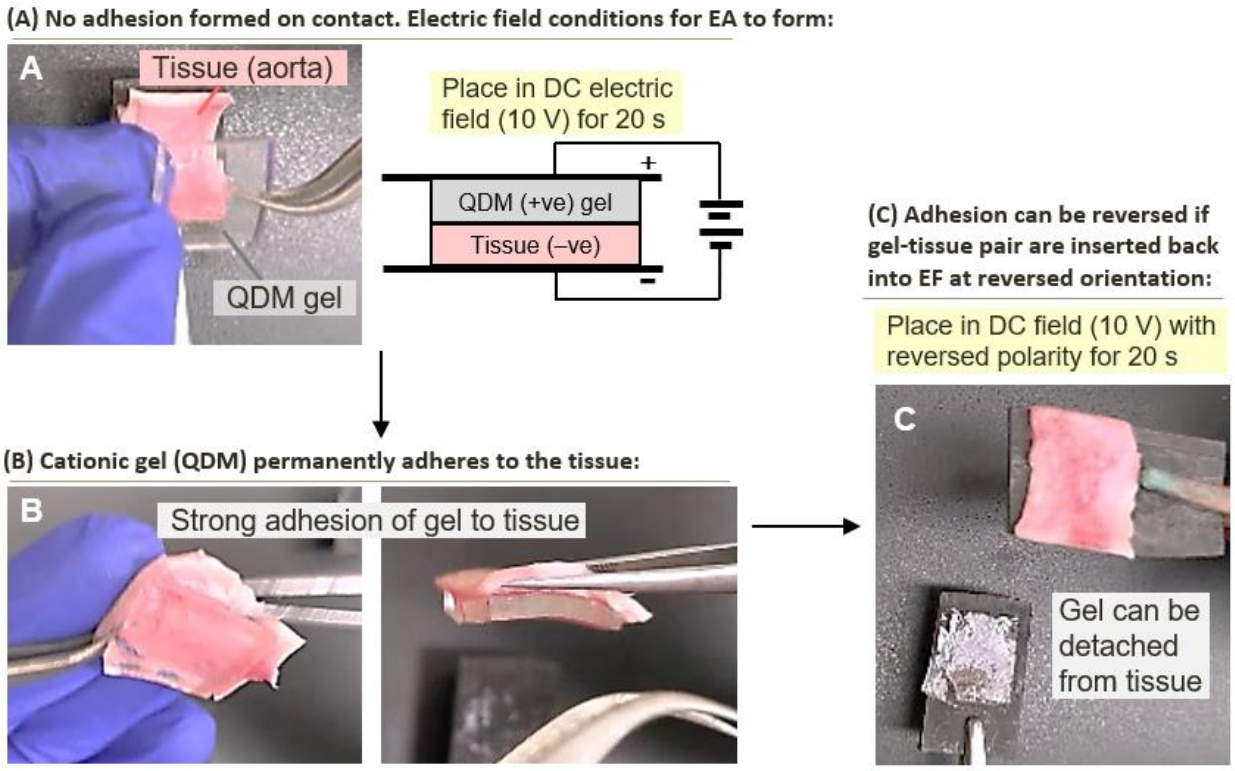

Figure 1.1. Electroadhesion between a cationic gel and animal tissue. (A) The gel (denoted by QDM) and tissue (bovine aorta) do not adhere upon contact. The two are then exposed to a 10 V DC field for ~ 20 s. The gel is touching the positive electrode, and the tissue the negative electrode. (B) The materials develop strong adhesion, which persists after the field is removed. (C) The adhered pair is placed back in the field, but the polarity is reversed (gel touches the negative electrode and the tissue the positive electrode). The same 10 V DC is applied for ~ 20 s, whereupon the adhesion is reversed, and the gel and tissue can be separated.

1.2.2 Electroadhesion of Gels to Tissues from Various Animals and Plants

In Chapter 4, we further extend our discovery and show that gels can be adhered by EA to tissues from various kingdoms in nature, including animals, plants, and fungi (Figure 1.2A). Examples of animal tissues include those of mammals (e.g., cow, pig, mouse); birds (e.g., chicken); fish (e.g., salmon, cod); reptiles (e.g., lizards); amphibians (e.g., frogs), as well as various invertebrates (e.g., shrimp, worms, scallop, cicada). Examples of plant tissue include fruits (e.g., plums) and vegetables (e.g.; carrot). Thus, EA occurs both with tissues that are soft and pliable,

such as pig muscle, as well as tissues that are hard and stiff, such as carrot (Figure 1.2B). In mammals, EA is strong for certain tissue types, such as arteries, intestines, and cornea across a range of species. Some common themes are identified: for instance, the higher the fraction of anionic polymers (proteins and/or polysaccharides) in the biological material, the higher the EA strength. Interestingly also, because tissues often have anisotropic structure, adhesion by EA can be strong in one tissue orientation, but weak or non-existent in the perpendicular one.

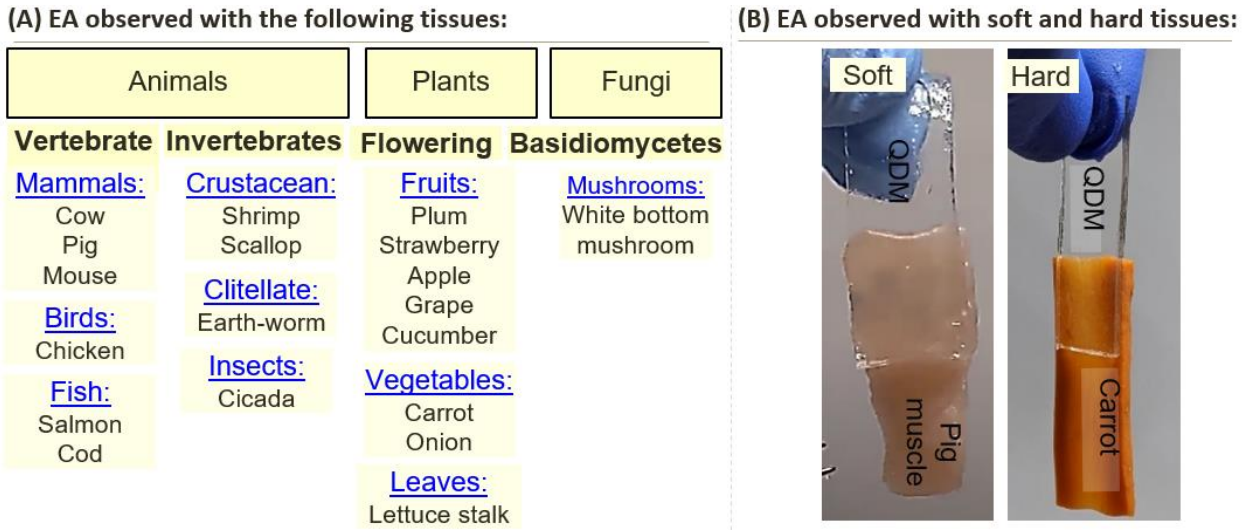

Figure 1.2. Diversity of biological materials to which cationic gels can be electroadhered. (A) A list of selected animals, plants and fungi that allow EA of a cationic (QDM) gel. (B) EA of a QDM gel can be done both to soft tissues (e.g., pig muscle) as well as hard tissues (e.g., carrot).

1.2.3 Mechanism for Electroadhesion

Finally, in Chapter 5, we delve into the mechanism behind EA. The EA strength between a cationic gel and an anionic material (gel or tissue) can be systematically enhanced in several ways. These include increasing the polymer concentration in the cationic gel as well as the cationic charge density. We also conduct experiments to unravel the contributions to EA from the charged

polymer chains and the counterions. At a high voltage of ~ 100 V, the gels undergo "zipping", i.e., they rapidly lock into adhesion due to electrostatic interactions in a manner that resembles the closing of a zip (Figure 1.3). This suggests that cationic and anionic chains form an electrostatic complex (ESC), that underpins the EA. We postulate that the ESC is the key to why the adhesion remains strong and can even be permanent.

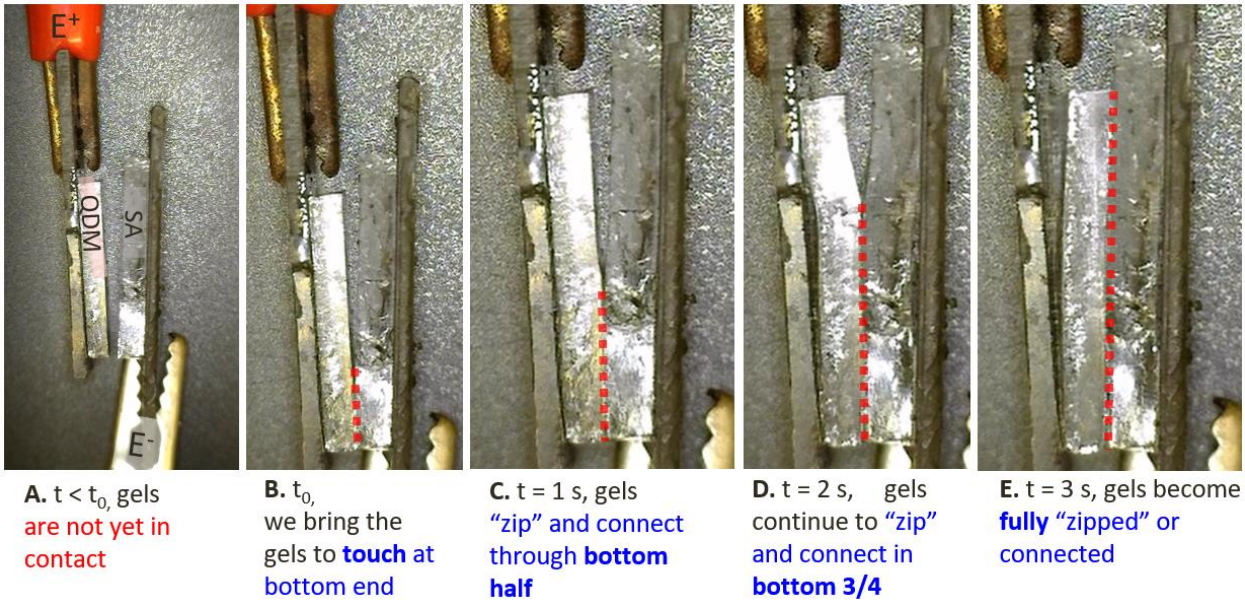

Figure 1.3. Zipping experiment showing the electrostatic attraction of cationic and anionic gels. (A) Gels of QDM (cationic, left) and SA (anionic, right) are placed in the EA orientation and are contacted at their bottom end at $t = 0$. A high DC field (100 V) is applied. (B-E) The gels instantly lock together, and the closure of the gel-gel interface resembles the closure of a zip; hence the term "zipping". These findings provide evidence for an electrostatic complex (ESC) being formed at the gel-gel interface, which we postulate is the key to EA.

1.3 Significance of This Work

The significance of this work is first and foremost in the application of electroadhesion to tissue repair. Currently, if a tissue is torn, sutures or staples are needed to rejoin the torn pieces and thereby allow the tear to repair naturally over time. This suturing is a surgical operation that requires considerable skill on the part of a surgeon, and this often implies a difficult and expensive

procedure. Surgical adhesives have been explored as alternatives to sutures,[6,25-31] but have many limitations.[26,28] In this dissertation, we report a new way to repair tissues, using a cationic gel as a patch and by applying a modest electric field across the gel and tissue.[19] The resulting EA can be strong enough to eliminate the need for sutures altogether. No separate adhesive is necessary! Our discovery opens up new possibilities for tissue repair that could be effective, simple, and less expensive. Future work will investigate the applicability of EA towards surgeries, first in animals, and then potentially in humans.

The work performed in this dissertation sets the stage for future surgical applications. The broader impacts from our studies in Chapters 3-5 include:

- In Chapter 3, we present the first example of gel-tissue electroadhesion with different bovine tissues. We also show that the use of gel-patches to seal leaks from holes or cuts in tissue is feasible in an *in vitro* setting.

- In Chapter 4, we show that EA can occur with a variety of animals and plants, suggesting that it should also work with human tissues for surgical repairs.

- Lastly, in Chapter 5, we present a new mechanism for EA and thereby explain how we can enhance the strength of adhesion induced by EA. This understanding will help in fine-tuning EA for surgical applications.

Chapter 2

Background

In this Chapter, we will discuss the properties of hydrogels, the fundamentals of adhesion, the classes of adhesives, and the methods to characterize the adhesive strength between two soft materials. All the above will be background for the work done in Chapters 3-5.

2.1 Polymer Hydrogels

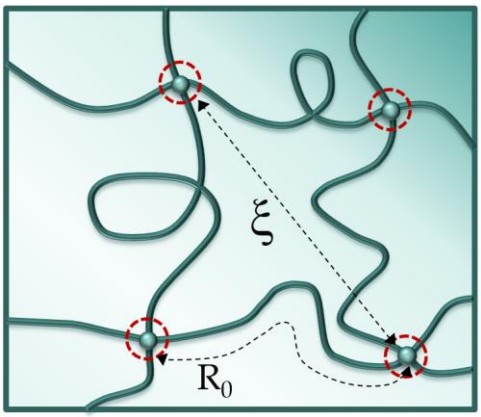

Figure 2.1. Schematic of a hydrogel network. Polymer chains are crosslinked into a network by physical or chemical bonds, and this network is swollen with water. The network has a characteristic mesh or pore size ξ. The average length of polymer chain between adjacent crosslinks is denoted by R_0.

Polymer hydrogels are three-dimensional (3-D) networks of polymer chains, crosslinked by chemical (covalent) or physical bonds (Figure 2.1). [32-37] The matrix of the hydrogel is swollen with water, which makes up most the hydrogel's weight.[32-35] The polymer network can be composed of natural polymer chains such as alginate (a polysaccharide) or gelatin (a protein)[37,38], or of synthetic polymers such as acrylamide, acrylate or polyethylene glycols (PEGs).[32,36] Jell-O

is the popular name for gelatin hydrogels, and it is formed by physical bonding between the gelatin chains.[39] Contact lenses, which are usually gels of an acrylate derivative, are an example of a chemical hydrogel crosslinked by covalent interactions.[39,40] A gel network that is swollen in water will have a pore or mesh size ξ associated with it. This size can be decreased by increasing the density of crosslinks in the network.[32-37] The gel will swell in water due to the favorable entropy of mixing between the polymer and solvent.[41] This swelling will be opposed by the decrease in entropy as chain segments become stretched.[36,37,42] The mixing contribution depends on the polymer's affinity for the solvent,[43] which is enhanced when the polymer chains are charged.[44]

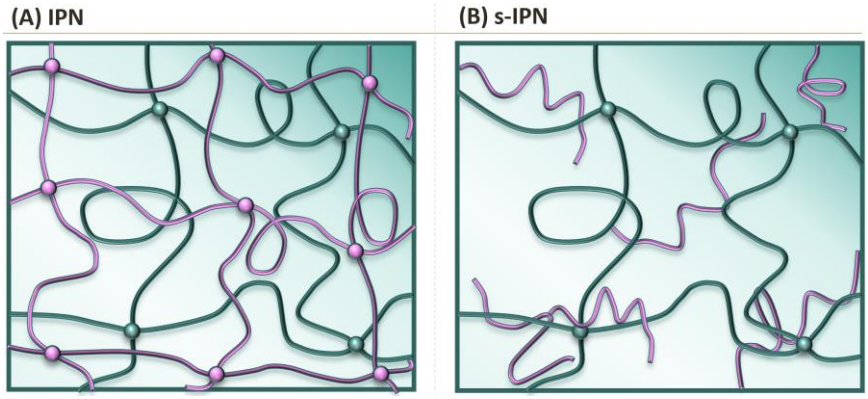

Figure 2.2. Interpenetrating networks (IPNs) and semi-interpenetrating networks (s-IPNs). (A) An IPN is a gel with two distinct crosslinked polymer networks unconnected to each other (shown in green and pink). (B) A s-IPN is a gel in which one polymer (green) is crosslinked into a network while the other polymer (pink) exists as linear chains entangled with the first polymer.

Chemical gels can be categorized based on their network structure. Interpenetrating networks (IPNs) are gels in which two or more unconnected networks co-exist (Figure 2.2A). For example, one network could be formed by physical bonds (e.g., a gel of gelatin), and thereafter, a monomer could be polymerized in the gel by free-radical polymerization to form a covalently-linked second network.[45,46] Another closely related term to IPN is a "double network", which has

a similar connotation as IPN, but is used specifically to denote a subclass of tough IPNs.[36,46,47] The term semi-IPN (or s-IPN) is used for a gel in which one polymer forms a network whereas the second polymer simply exists as linear chains within the first network (Figure 2.2B).[18,45,46] That is, chains of the second polymer will simply be entangled with those of the first.

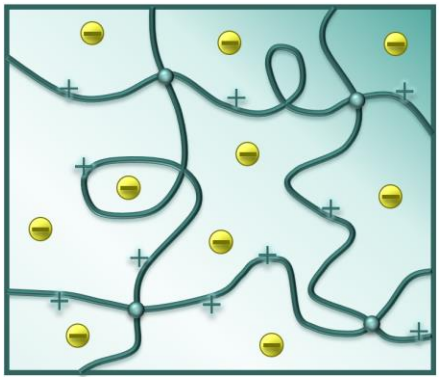

Figure 2.3. Schematic of a polyelectrolyte (cationic) hydrogel. The chains in the gel have ionizable groups, and in water at ambient pH, these groups ionize and acquire a positive charge. Correspondingly, negatively charged counterions, shown in yellow, are released into the water.

Polyelectrolyte (ionic) gels can be made from cationic or anionic monomers.[48-51] The polymer chains in these networks will be positively or negatively charged, i.e., they will be ionized in water at ambient pH (Figure 2.3).[48,49] The charges on the chains will be associated with counterions, which will be released into the water.[52-54] For example, in the case of the cationic gel shown in Figure 2.3, the charges on the chains could come from quaternary ammonium salts (–$N(CH_3)_3^+$), and correspondingly, the counterions will be anions such as Cl^-.[53,54] The backbone charge and the counterions dictate many of the properties of the gels.[52] For example, ionic gels swell much more in water compared to nonionic gels due to repulsions between the charges and the higher osmotic pressure due to the counterions.[55]

2.3 Adhesion and its Classification

Adhesion is the tendency of two materials to remain joined to each other.[2,3,56] Typically, to adhere two solid materials ("substrates"), an adhesive is spread or placed at the interface between the substrates and then these substrates are pressed together.[2,3] Bonds between the substrate and the adhesive join the two materials, and cohesive forces within the adhesive provide internal strength to prevent failure.[2,56] Adhesion can arise as a result of very different interactions (bonds), ranging from weak physical bonds[15,17,57] to strong chemical bonds.[7,58] One example is the adhesion of animals like lizards or geckos to a vertical wall. The adhesion of gecko feet to the wall does not require an adhesive – rather it relies on van der Waals (vdW) interactions that set in at close proximity (~ 1 nm) between the gecko feet tips and the wall.[57] Conversely, when an epoxy glue is used to join two metal objects, the glue forms covalent bonds with both objects.[58]

Specific challenges arise when we attempt to adhere two soft materials, such as two tissues. For example, if the adhesive is much stiffer than the soft materials to be adhered, the adhesion may not hold up and failure (delamination along with a thin layer of substrate) may occur.[59,60] An example is the use of cyanoacrylate glues to join soft tissues.[61] Another source of complexity in the context of adhesion is in adhering two wet materials, such as an implant and a tissue in the body.[62] Using adhesives on wet surfaces is not an easy task. This is because water molecules interfere with hydrogen-bonding, which play a role in the adhesion. Specialized adhesives exist for wet environments,[63] for example by utilizing catechol chemical groups.[12,64-66] Underwater creatures like mussels adhere to rocks in the ocean or to boat surfaces by using catechol-bearing polymers that are secreted in the form of threads.[64-66]

2.4 Adhesives for Tissue

We will now discuss the adhesives that have been developed specifically for tissues.[25-28,31,67] These adhesives have been optimized for the body's biological setting, i.e., the presence of water as well as salt. Typically, when a tissue has a defect (cut or tear), sutures or staples are used to repair it. However, there are instances where adhesives are used instead. In the clinic, adhesives without sutures are used only on very small tissue defects (< 1 mm) and adhesives completely fail to repair defects larger than 3 mm.[26,28] In some surgeries, adhesives can be used in conjunction with sutures.[29,63] Adhesives hold tissue together during wound healing until tissue regains mechanical strength, while sealants prevent leakages and bleeding.[28]

Surgical adhesives can be divided into two classes depending on whether the source from which they are derived is natural or synthetic. Examples of **naturally derived adhesives** are those based on fibrin, collagen or gelatin.[26,28] Tisseel and Hemaseel are fibrin-based glues and are used in the clinic to stop bleeding, i.e., as hemostatic agents.[26,28] They have also been shown to adhere tissues together but are not typically used for this purpose.[68] Note that fibrin is a key protein involved in the blood-clotting cascade.[69] FloSeal is a gelatin-based adhesive that is also used in the clinic as a hemostatic agent.[26,28] Note that gelatin is a denatured form of the protein collagen.

Examples of **synthetically derived adhesives** include those based on cyanoacrylates, polyethylene glycol (PEG), or polyurethanes (PU).[26,28] Dermabond is a cyanoacrylate glue that is used in the clinic for closing small lacerations and skin grafting.[27] Note that the 'Super Glue' that is commonly used in homes is also a cyanoacrylate glue. Duraseal and Focalseal are PEG derived

adhesives used to stop spinal fluid and air leaks from punctures in the body.[26,28] Finally, TissuGlu is a PU-based spray-on adhesive used for cosmetic procedures.[26,28]

All of the adhesives named above are approved by the FDA for use in humans.[26,28] However, they all have limitations.[26,28] Fibrin-based glues tend to be weak cohesively and can be used only on very small injuries (< 1 mm). Gelatin-based materials are also weak cohesively (partly because gelatin gels convert into sols when heated to ~ 40°C).[70] Additional crosslinking is needed to strengthen gelatin-based materials.[71] Collagen-based materials generally have weak adhesion. Cyanoacrylates offer strong adhesion and mechanical strength; however, the body reacts adversely to these materials, and hence they are limited to external use such as on the skin. PEG-based materials have high adhesion strength; however, they tend to swell appreciably, which can cause discomfort and pressure build-up on surrounding tissues. PU-based adhesives have long curing times and generate toxic byproducts, thereby limiting their usefulness. These limitations provide the motivation behind further research and development into tissue adhesives. For an adhesive to potentially replace sutures, it will need to have strong cohesive properties, strong adhesion, favorable immune response, low swelling and a short application time.[26,28]

2.5 Methods for Characterizing Adhesion Strength

Different methods exist for measuring adhesion strength between soft materials.[72,73] Some of the common methods are discussed in this section, including: (1) the lap-shear test,[74] (2) the pull-off test,[75] and (3) the peel test.[76,77]

2.5.1 Lap-Shear Test

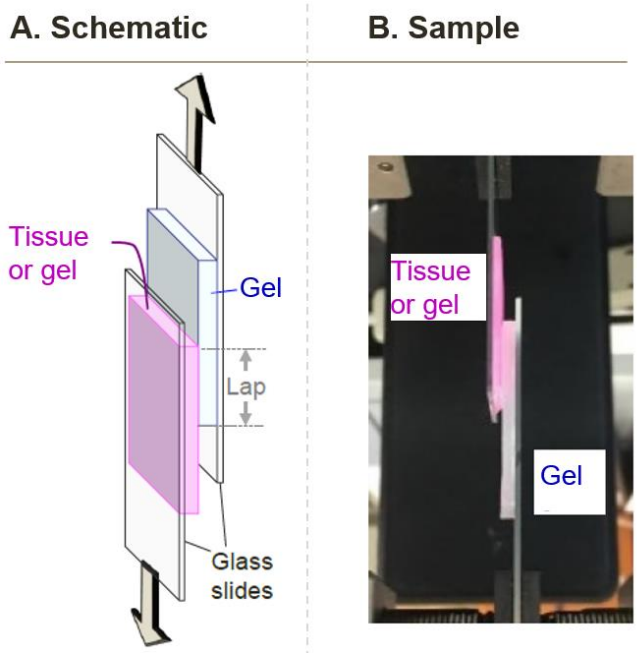

Figure 2.4. Schematic of the protocol for a lap-shear test (A) and a photo of a test in progress (B). Samples are anchored to glass slides, which are gripped and pulled axially. The lap area between the two test materials experiences the shear.

In lap-shear testing, two samples are adhered over an area called the lap (Figure 2.4) and are then pulled axially until they detach.[74] Typically, if the samples are soft and deformable, they are adhered on their opposite sides to hard non-deformable materials such as glass slides. This allows all the stresses to go to the lap area (adhesion zone), where the samples experience a shear deformation. For each type of sample, it is important to follow the protocol for lap-shear testing

established by the American Society for Testing and Materials (ASTM).[78] The protocol includes recommendations on the sample size (length and width) as well as the lap size. If the samples are stuck using an adhesive, then the thickness of the adhesive between the samples must also be carefully controlled.[79] Also, the rate at which the samples are deformed (i.e., the rate at which the two samples in Figure 2.4 are pulled) must be chosen depending on the sample type.

2.5.2 Pull-Off Test

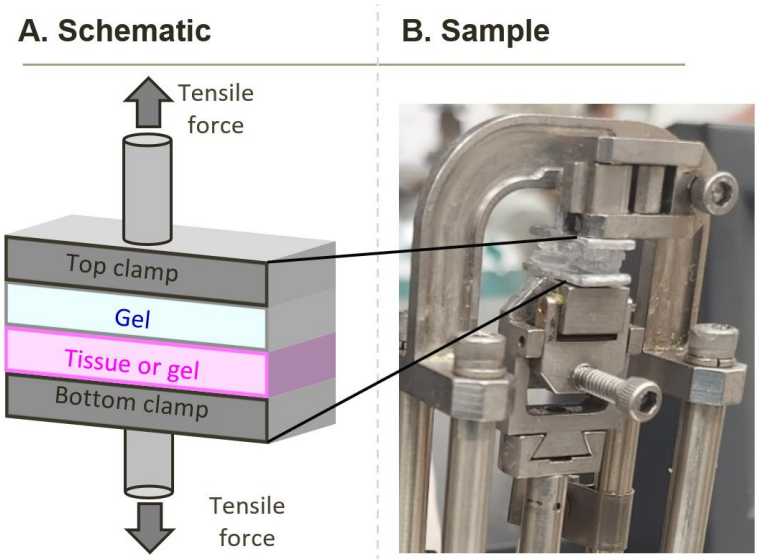

Figure 2.5. Schematic of the protocol for a pull-off test (A) and a photo of a test in progress (B). Samples are anchored to the top and bottom clamp (e.g., using superglue) and then adhered to each other. The clamps are then moved apart axially at a specified rate until the samples detach from each other.

In pull-off testing, two samples are adhered to each other and then their reverse side is anchored to clamps using a strong adhesive (e.g., superglue, which is based on cyanoacrylates). The clamps are then moved apart axially at a fixed rate (Figure 2.5).[75] Note that the clamps move in a direction normal to the adhesive interface. Here too, ASTM protocols should be used for the sample size as well as the rate of deformation.

2.5.3 Peel Tests

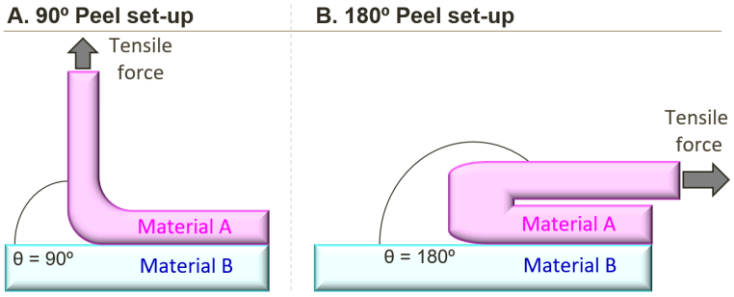

Figure 2.6. Schematics of peel tests done at 90° (A) and 180° (B). The leading edge of material A is extended beyond Material B and pulled either at (A) 90° or (B) 180° angles.

In peel tests (Figure 2.6), two samples are adhered over a zone, but the leading edge of one sample is left free. A tensile force is applied to that leading edge such that it is peeled off from the bottom sample. The peeling typically would take place either at 90° or at 180°.[76,77] Typically, when two soft materials adhere, fibrils will form at the leading edge, which elongate as the two materials are detached. Eventually these fibrils break and the leading-edge advances.[80] Note that, for peel testing, at least one of the materials has to be flexible enough such that it will not rupture when deformed to the angles required in the testing protocol.

2.6 Failure Modes During Adhesion Tests

In the above tests, the samples being adhered will eventually fail, i.e., de-bond, under the applied deformation. When failure occurs (i.e., the materials are no longer stuck together), it can arise in different zones and these correspond to different "failure modes". Figure 2.7 shows an adhesive (in red) being used to adhere two strips of the same material (substrate, in blue). In the case of *adhesive failure* (Figure 8A), the adhesive is weakly bonded to the substrate, and so it detaches from the substrate.[2,81] In the case of *substrate failure* (Figure 8B), failure can occur due

to defects in the substrate material, such as cracks that propagate due to the applied deformation. Lastly, failure within the adhesive itself is referred to as *cohesive failure*. Here the internal strength of the adhesive is weak, so the deformation causes the adhesive to break apart.[2,81] As a result, patches of adhesive can be seen on both substrates.

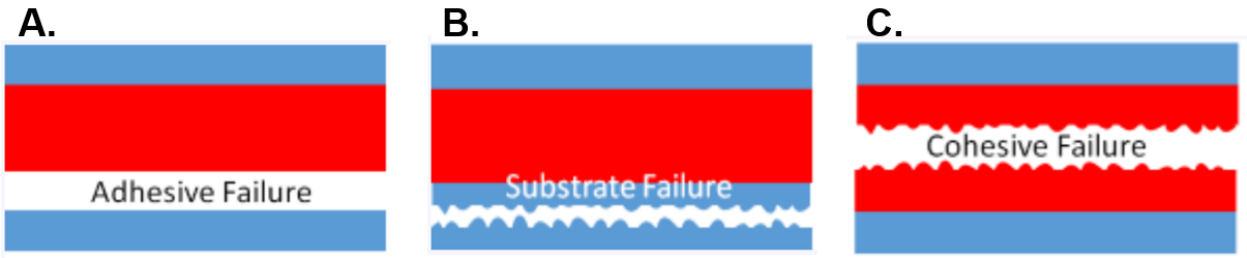

Figure 2.7. Schematics of failure modes during adhesion testing. (A) Adhesive failure; (B) Substrate failure; (C) Cohesive failure. Adapted from Ref. 2.[2]

Chapter 3

Electroadhesion of Gels to Tissues: A New Way to Seal Cuts and Tears

---

The results presented in this chapter have been published in the following journal article: L. K. Borden, A. Gargava, and S. R. Raghavan, "Reversible electroadhesion of hydrogels to animal tissues for sutureless repair of cuts or tears." *Nature Communications* (12), 4419 (**2021**)

3.1 Introduction

The phenomenon of 'electroadhesion' involving two oppositely charged polyelectrolyte hydrogels was first reported about ten years ago.[18] The starting point is to take two solid gels (slabs or strips), each formed by chemical crosslinking of monomers, with one gel having a cationic backbone and the other an anionic backbone. The two gels are contacted with each other along one face and electrodes are placed along either side. Thereafter a DC voltage is applied in a specific orientation. Within seconds, the two gels become strongly adhered. The same gels will not adhere if contacted in the absence of the field. Thus, the adhesion is induced by the electric field, and hence the term 'electroadhesion' for this phenomenon.[18,20,22-24,82-84] If the polarity of the field is reversed, the gels lose their adhesion and can be detached. The mechanism for electroadhesion is still not completely understood, but it is believed to involve molecular rearrangement of both polymer chains and counterions at the gel-gel interface.[18,20,22-24,82-84] Thus far, there have been only a few applications of electroadhesion, such as to assemble gels into 3-D structures.[20,23,84] On the whole, however, electroadhesion has remained an oddity that has attracted only moderate interest in the scientific community.

In this study, we hypothesized that electroadhesion could be induced between hydrogels and other kinds of soft matter. In testing this hypothesis, we have discovered that gels could indeed

be electroadhered to animal (bovine) tissues. This result is surprising because, while some tissues can be soft and gel-like, they are structurally very different from conventional polymer gels.[85,86] We show that gel-tissue electroadhesion only works between certain types of gels and tissues, and the reasons for the same are discussed. Our work significantly enlarges the landscape of materials that can be electroadhered, and thereby the utility of this phenomenon.

One obvious application is as an adhesive to reseal damaged tissues. Currently, if a tissue is torn, sutures or staples are needed to rejoin the torn pieces and thereby allow the tear to repair naturally over time. This suturing is a surgical operation that requires considerable skill on the part of a surgeon,[87] and this often implies a difficult and expensive procedure. Adhesives have been explored as alternatives to sutures during surgery.[26,29,30,67,87-90] Several polymeric adhesives are available for surgical use, including those based on cyanoacrylates, fibrin, and polyethylene glycol (PEG) derivatives.[26] Most of these materials are intrinsically sticky and cling upon contact with tissue. Such adhesives have many limitations: in particular, they are usually not strong enough to hold two cut pieces of tissue together. As a result, adhesives usually cannot replace sutures, but are sometimes used along with sutures (e.g., instead of ten sutures, a combination of two sutures and an adhesive may be used).[29,90] Also, if the adhesive forms a solid film (immediately after application, or after a period of drying), this could result in a physical barrier that hinders the supply of nutrients to the underlying tissue.[27] In comparison, adhesives in hydrogel form are preferable due to their soft nature and their permeability to water and nutrients.[26,67,87-89] For a gel-adhesive to provide a viable alternative to sutures, it should stick strongly to tissues. Even better would be to have a non-adhesive gel that can develop adhesion on command, and moreover, for this adhesive to be reversible (removable) in case of error.

To test the hypothesis that electroadhered gels could potentially enable an alternative mode of surgery, we describe a series of *in vitro* studies in this paper. First, we describe model systems of oppositely charged polymer gels, one in the form of rectangular strips and the other as hollow tubes. In an initial case, a hole is made in the tube wall and a small gel strip is electroadhered over the hole. We show that water can be flowed through the patched tube (with no leaks through the sealed hole) at pressures that exceed normal blood-pressure. Next, in a more extreme case, the tube is cut into two and we attempt to join the segments by adhering a sleeve of gel around the cut segments. For this, a long gel strip that is robust and flexible is fabricated, and by electroadhesion, we are able to effectively 'suture' the cut segments of the tube. We then describe similar experiments on the use of electroadhered gels to seal holes in a tubular animal tissue, i.e., a section of bovine aorta. By applying a DC field of 10 V for a short time (10–20 s), strong adhesion between gel and tissue is achieved. This adhesion can be reversed at a later time by reversing the polarity of the field. Our studies collectively demonstrate the potential utility of electroadhesion in biomedical applications.

3.2 Experimental Section

Materials. The following chemicals were from Sigma-Aldrich: the monomers acrylamide (AAm) and N,N′-methylenebis(acrylamide) (BIS), the initiator ammonium persulfate (APS), calcium chloride dihydrate ($CaCl_2$) salt, tannic acid, sodium hydroxide, phosphate buffered saline (PBS) tablets, and the dye rhodamine B. The accelerant N,N,N′,N′-tetramethylethylene-diamine (TEMED) was from TCI America. The monomer N,N′-dimethylaminoethyl meth-acrylate, quaternary ammonium salt (QDM) was from MPD Chemicals. Two biopolymers were purchased from Sigma-Aldrich: alginate (Alg) (from brown algae, medium viscosity) and agarose (Type 1-A, low EEO, melting temperature ~88°C). Laponite XLG nanoparticles (LAP) were a gift from Southern Clay Products. Cyanoacrylate-based glues (Gorilla Glue gel and Krazy Glue) and Rust-Oleum hydrophobic coating were purchased from The Home Depot. Deionized (DI) water was used in all experiments.

Synthesis of Alginate Tubes. Alginate tubes were prepared by a variation of the method described by Gargava *et al.*[91] First, a template of cylindrical agarose gel containing Ca^{2+} ions was prepared. For this, 2.5 wt% of agarose and 5 wt% of $CaCl_2$ were added to DI water and heated above 80°C until the agarose completely dissolved. The hot solution was then poured into a tube that was capped at one end. Upon cooling to room temperature, a solid (gel) cylinder of agarose was obtained. This cylinder was then placed in a solution of 2 wt% Alg for 12 min. During this time, Ca^{2+} ions diffuse out of the agarose, leading to an Alg gel around the cylindrical core. The final step was to dip this material in a 3 wt% $CaCl_2$ solution for 20 min and then cut off the edges. The tube of Alg could then be slid off the agarose core. Alg tubes can be prepared over a range of dimensions using this method. For our purposes, we prepared the tubes in two typical dimensions

by using agarose cores of different diameters and lengths: (a) 1 cm diameter and 10 cm length; and (b) 2 mm diameter and 60 cm length. Tubes were stored in a 1 wt% $CaCl_2$ solution and dyed with 0.1 mM rhodamine B for contrast purposes. Typically, tubes were used within 24 h of preparation.

Synthesis of QDM gels. Cationic QDM gels were prepared using the following protocol. First, DI water was degassed by bubbling nitrogen gas for 30 min. To assist with easy removal of the gels, Petri dishes used in gel preparation were coated with a spray of Rust-Oleum hydrophobic coating, then allowed to sit for 10 min, and thereafter wiped dry. Two variations of QDM gels were prepared: with and without LAP. For synthesis of QDM gel without LAP the following were combined: 1 M (1.4 g) AAm, 0.16 M (809 μL) of QDM solution, 0.019 M (0.06 g) BIS, 0.0088 M (0.04 g) APS and 0.01 M (30 μL) TEMED in 20 mL of degassed DI water. Next, the above monomer mixture was poured into a pre-coated Petri dish and maintained in a nitrogen environment for 3 h, whereupon the gel became fully polymerized. For synthesis of QDM gel with LAP, the first step was to add 1 wt% (0.2 g) of LAP particles to 20 mL degassed water and to stir until the particles were well-suspended (as ascertained by the sample appearing clear and homogeneous). Thereafter, the pH of the solution was lowered to 4.5 using 1 M HCl. Next, 0.16 M (809 μL) QDM was added dropwise to the LAP mixture followed by 1 M (1.4 g) AAm, 0.0095 M (0.03 g) BIS, 0.0088 M (0.04 g) APS and 0.01 M (30 μL) TEMED. When the pH was below 5, QDM was able to dissolve in the LAP suspension (without clumping). TEMED increased the pH back up to around 8.5. The above solution was placed in a pre-coated Petri dish and polymerized as before. After polymerization, gels were stored in a fridge and typically used within 24 h of preparation.

Synthesis of SA gels. Anionic SA gels were prepared by a similar procedure as described above for QDM gels. In this case, the monomer solution contained 1.4 M (2 g) AAm, 0.11 M (0.2 g) SA, 0.019 M (0.06 g) BIS, 0.0088M (0.04 g) APS and 0.01 M (30 μL) TEMED in 20 mL of degassed DI water. The above solution was poured into a pre-coated Petri dish and maintained in a nitrogen environment for 2 h. After polymerization, gels were stored in a fridge and typically used within 24 h of preparation.

Tissue Preparation Protocol. All tissues were obtained ethically, immediately after slaughter from a local butcher. All experiments on tissues were conducted within 24 h of tissue harvest. When the tissues were first received, organs were typically encased in fat and other matrix material. For example, the aorta was surrounded with fat and connected to parts of the heart and lungs (see Figure 3.6). Thus, for experiments with the aorta, it had to be harvested and cleaned from the surrounding parts. The harvested aorta was then further segmented into smaller pieces for the electroadhesion experiments, as shown in Figure 3.6. For many experiments, segments of tissue were sliced to a thickness of 0.3 ± 0.1 mm. The exceptions were in the cases of tissues that were naturally thin, such as the cornea.

Adhesion Experiments. A DC power source (Agilent, model E3612A) with a range of 0–60 V, 0–0.5 A was used for the electroadhesion experiments. The voltage was set to 10 V for most experiments. For the gel-tissue experiments reported in Table 3.1, the following procedure was used. From a given batch obtained from the butcher, tissues of interest were harvested, and for a given tissue type, at least three tissue samples were prepared as described above. Three QDM gel strips were then prepared. First gel-tissue contact adhesion was measured, and then their

electroadhesion. Two observers were used to independently rank the adhesion strength in each experiment on a scale of 0–4, where 0 = negligible, 1 = weak, 2 = moderate, 3 = strong, and 4 = very strong adhesion (this scale is also indicated at the bottom of Table 3.1). The average of both observers' rankings was recorded for that experiment. Whenever in question, the second observer was blinded to the sample type so that their assessment was not biased. After three such trials with a tissue, the average of the readings was determined, and this is the one shown in Table 3.1.

Pressure Testing. The test setup is shown schematically in Figure 3.3A. A peristaltic pump (Pharmacia-LKB-pump P-1) was used to pump a 0.1% $FeCl_3$ solution through the Alg tube at a flow rate 5 mL/min. The tube was placed in a basin with a length of 15 cm, width of 5 cm and height of 5 cm. Openings were made on both sides to allow passage of the tube. The basin was filled with 0.1% tannic acid solution up to a height of 2 cm and the Alg tube (60 cm in length) was placed such that its middle portion was submerged in this solution (see Figure 3.3A). Clamps were fixed at the bottom of the basin to control the path and location of the Alg tube in the basin. A pressure gauge (PRTemp 1000, from Madge Tech) was placed upstream of the Alg tube and the pressure was recorded in real-time (every 2 s) on a computer using the Madge Tech software. Pressure readings were obtained during flow in the tube before puncture, during puncture and following puncture repair by electroadhesion of a QDM gel patch. Burst pressures (for a patched tube) were determined by clamping shut the far end of the Alg tube and continuing flow into the tube, leading to pressure build up within the tube. The highest pressure recorded before the patch became dislodged was designated as the burst pressure.

Lap-Shear Testing. Lap-shear tests were conducted using an Instron Model 5565 instrument. Tests were done according to protocols recommended by the American Society for Testing and Materials (ASTM) which have been used in previous studies.[64,78,92] Gels and tissues were cut into rectangular segments with dimensions of 1.5 × 4 cm. The QDM gel segment was 3 mm thick, the Alg segment was 1 mm thick and tissue segments were 2.5 ± 1 mm thick. Gel-gel and gel-tissue samples were electroadhered over a lap height of ~ 1.5 cm (see Figure 3.9A). Following electroadhesion, the dangling ends of the gel and tissue were stuck securely to glass slides using cyanoacrylate glue. For securing the QDM and Alg gels to the glass slides, Krazy Glue was found to be the best and a 1 h cure time was used. For securing tissue to the same slides, Gorilla Glue was the best and a 2 h cure time was used (during this time, the tissue face exposed to air was covered by a piece of gauze soaked with PBS solution). The glass slides provided a hard and non-elastic backbone for the Instron to grip onto, which ensured that shear was applied on the lap area alone. The Instron was then used to elongate the sample at a rate of 10 mm/min, and the stress was recorded during this process. At least three samples were tested for each of the categories in Figure 3.9C and the statistics were analyzed using the Student's T-test.

3.3 Results and Discussion

3.3.1 Gel-Gel Electroadhesion

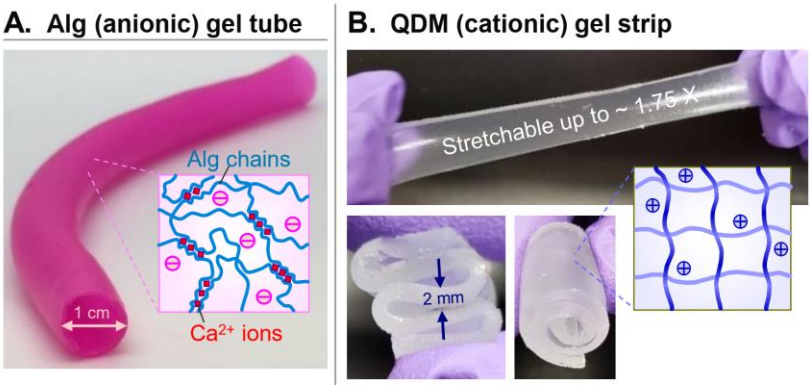

Figure 3.1. Gels used in our electroadhesion studies. (A) Anionic gel of alginate (Alg), crosslinked by divalent Ca^{2+} cations. The gel is made in the form of a hollow tube. (B) Cationic QDM gel strip, made by polymerization of acrylamide derivatives. The photos show that the gel is elastic, stretchable, and flexible. Schematics of the gel structure are shown as insets.

Our initial studies were conducted with a combination of gels, one cationic and the other anionic. To mimic tubular tissues, we fabricated the anionic gel in the form of a tube. The gel in this case is composed of the anionic polysaccharide sodium alginate crosslinked into a network by divalent Ca^{2+} cations. The procedure for creating tubes with a wall of alginate (Alg) gel was described in an earlier study from our lab[91] and is adapted here (see Experimental Section for details). Through this procedure, we can control all the dimensions of the tube, including the length, inner diameter, and wall thickness. Figure 3.1A shows a 10-cm long tube with an inner diameter of 1 cm and a wall thickness ~ 1 mm. The inset illustrates the structure of the gel wall, which consists of Alg chains connected at zones by Ca^{2+} ions. The tube has a pink color due to a trace amount of rhodamine B (RB) dye added during the synthesis.

The counterpart to this tube is a cationic gel, made in the form of a rectangular strip. This gel is synthesized by polymerizing a mixture containing acrylamide (AAm, a nonionic monomer),

quaternized dimethyl aminoethyl methacrylate (QDM, a cationic monomer), bis(acrylamide) (BIS, a nonionic crosslinker) and laponite (LAP) nanoparticles. The molar ratio of QDM relative to all the monomers dictates the level of charge on the gel strands, and this is kept at 16 mol%. The ratio of BIS to all the monomers dictates the stiffness of the gel, and this is maintained at 1.6 mol%. If the BIS content is too high, the gel becomes brittle. We found that adding 0.1 wt% of LAP to the gelling mixture significantly improves the flexibility and stretchability of the final gel, consistent with previous studies from our lab.[93] The overall gel is denoted as QDM to signify its cationic nature. Figure 3.1B shows that the QDM gel strip is flexible enough to be twisted or rolled up. The strip can also be stretched up to ~ 1.75 times its original length without rupture.

We first confirmed that the cationic QDM gel-strips could be stuck by electroadhesion (EA) to the anionic Alg gel-tubes. Our setup for EA involves two graphite electrodes and a DC power supply. The electrodes have to be placed in contact with the above gels in a particular orientation, as shown by Figure 3.2A. That is, the strip and tube are brought into contact, and then the positive electrode (E^+) is made to contact the cationic gel strip (G^+), while the negative electrode (E^-) is contacted with the anionic gel tube (G^-). With this orientation (denoted from now on by $E^+G^+G^-E^-$), a DC voltage of 10 V is applied for ~ 10 s. When the voltage is switched off, the QDM strip is found to be strongly adhered to the alginate tube (Figure 3.2B), and this adhesion persists thereafter. If the reverse electrode orientation ($E^+G^-G^+E^-$) is used at the start, the two gels will not stick. Conversely, if electroadhered gels are reconnected to the field in the above reverse orientation, and a 10 V field is applied for ~ 10 s, the gels lose their adhesion and can be easily detached. To our knowledge, this is the first demonstration of EA between a covalently crosslinked

gel and a physically crosslinked one. In previous reports of EA,[18,23] the gels were all covalently crosslinked.

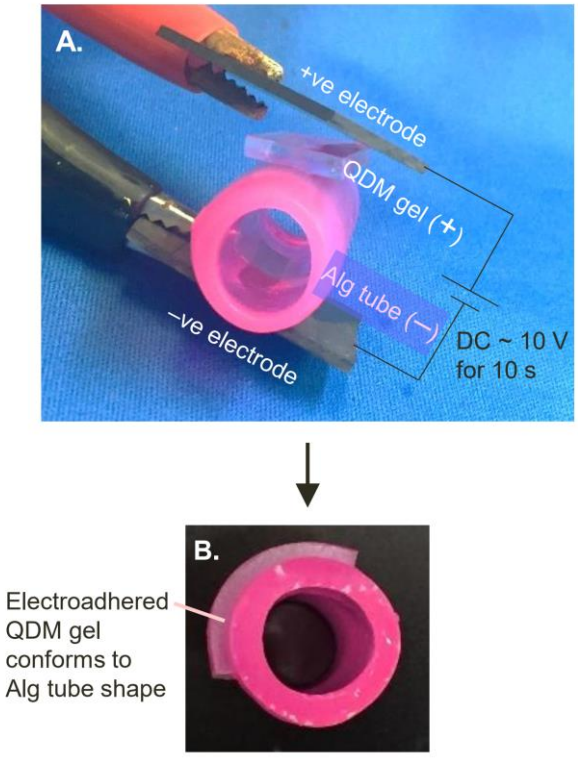

Figure 3.2. Electroadhesion of QDM gel-strip to Alg tube. (A) The gel and tube are contacted with graphite electrodes, with the positive electrode touching the cationic QDM gel and the negative electrode touching the anionic Alg tube. (B) Upon applying 10 V of DC for 10 s, the gel gets tightly adhered to the tube and conforms to the tube shape. In cases where a puncture is made in the tube wall, adhesion of the gel over the puncture location serves to patch up the puncture (see Figure 3.5).

3.3.2 Electroadhesion for Repairing Cut or Broken Gel-Tubes

In our first set of experiments, we introduced a cut in the wall of an alginate tube and stuck a QDM gel over the cut. The cut was made with a needle or razor blade and its size could be varied. We then made rectangular patches of the QDM gel (15 mm long, 8 mm wide and 2 mm in

thickness). Using the EA procedure described above, we affixed the QDM gel patch so as to cover the cut in the tube wall. Note that the patch adheres tightly to the tube and it conforms to the tube's curvature (Figure 3.2B).

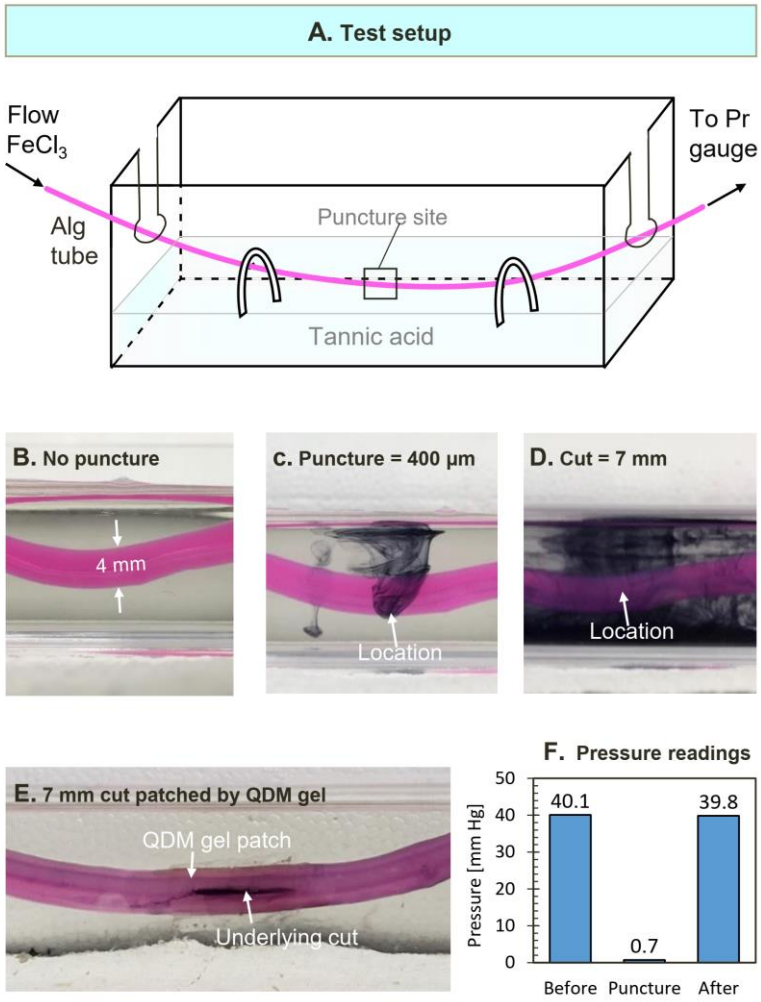

Figure 3.3. Electroadhesion of QDM gel to patch a cut in the Alg tube wall. (A) Schematic of test setup. An aqueous solution of 0.1 wt% $FeCl_3$ is pumped through the lumen of the Alg tube, which is submerged in an aqueous bath of 0.1 wt% tannic acid. If the $FeCl_3$ leaks out of the tube, it reacts with the tannic acid and a black precipitate is formed immediately in the bath. (B) When the tube is intact, there is no leakage, and the bath is clear. (C) Tube is punctured with a needle to create a hole of 400 µm diameter. (D) Tube is cut to a length of 7 mm with a blade. In (C) and (D), as the fluid in the tube leaks out, the black precipitate can be seen in the bath. (E) The tube from (D) is patched by a QDM gel, and when flow is resumed through the tube, no leakage can be seen. (F) A pressure gauge placed upstream of the tube records the pressure in the tube. The pressure drops to near-zero in the case of a cut in the tube (similar to D) as the fluid leaks out. When the tube is patched up (similar to E), the pressure is restored to its original value.

To test the strength of the patch-tube adhesion, we introduced a flow of fluid through the patched tube. If the patch was not affixed, fluid would leak out of the cut in the tube. The question then is whether the patch could completely seal the leak and moreover if it could withstand the pressure exerted by the fluid. We developed a protocol for leakage tests that involves submerging the Alg tube in a water bath containing 0.1% of tannic acid (Figure 3.3A, B). A 0.1 wt% solution of iron chloride ($FeCl_3$) in water is then flowed through the lumen of the tube using a peristaltic pump. When $FeCl_3$ contacts tannic acid, a black precipitate of ferric tannate is instantly formed.[94] Even if a small puncture (400 μm) is made in the tube wall using a needle, the leakage of fluid from the puncture can be readily detected by the eye due to the formation of the black precipitate (Figure 3.3C). This leakage is much greater when a large cut (7 mm in length) is made in the tube wall with a blade (Figure 3.3D). Figure 3.3E shows the alginate tube with the above large cut patched by a QDM gel using EA. In this case, there is stable flow of fluid through the tube with no leak whatsoever.

To quantify the above experiment, we installed a pressure gauge to the tube upstream of the puncture site. This measures the pressure *P* exerted by the fluid flow on the tube wall. When some of the fluid leaks out through the cut, *P* drops relative to its initial value (which corresponds to stable flow with no leak). If the leak is considerable, then *P* drops to nearly zero. For example, the bar graph in Figure 3.3F shows that the initial *P* is 40.1 mm-Hg as fluid is flowed through the tube at a flow rate of 5 mL/min. When a cut of 7 mm length is made in the tube wall and flow is resumed at the above flow rate, *P* drops to 0.7 mm-Hg. Next, the cut is patched with a QDM gel using EA and the experiment is repeated – *P* then increases to 39.8 mm-Hg, which is nearly the

same as the initial pressure. These data show that the electroadhered patch holds up well to the above flow conditions.

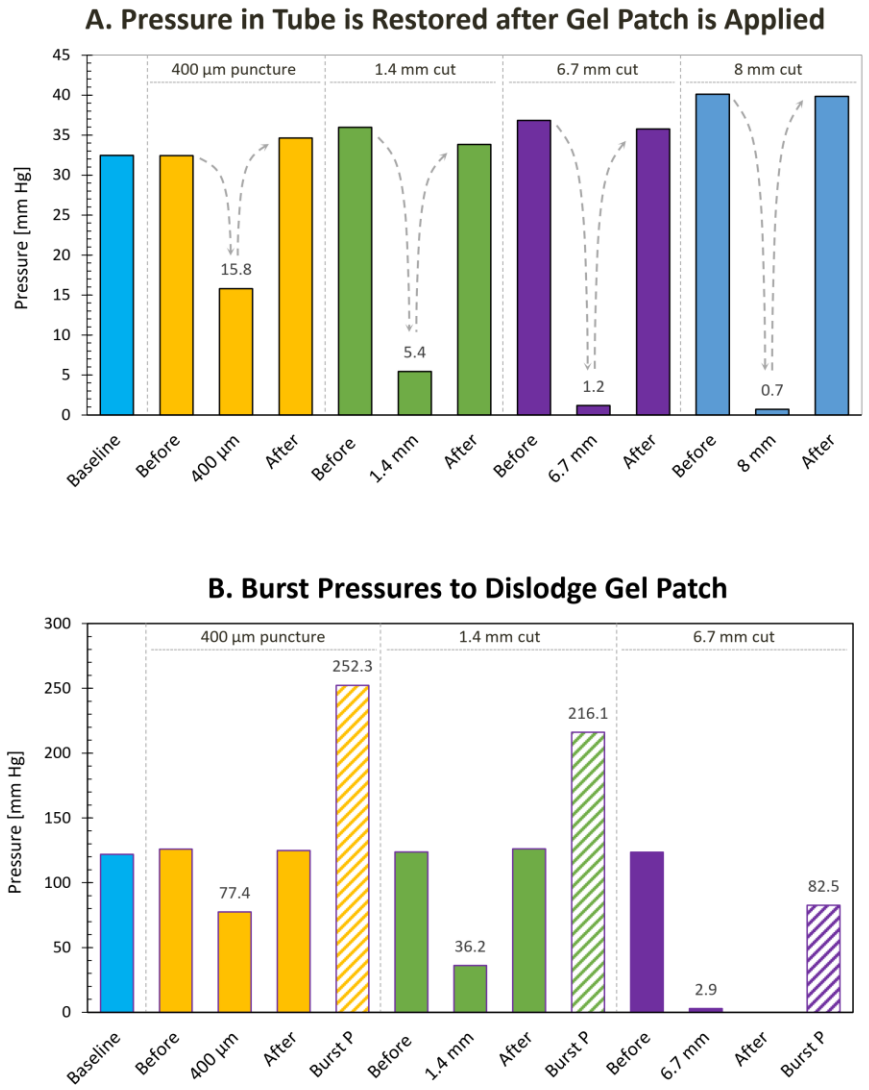

Figure 3.4. Pressure changes in tube before and after applying a gel patch by electroadhesion. (A) Pressure readings before a puncture/cut is made in the wall of an alginate (Alg) tube and after the cut is sealed by electroadhesion of a QDM gel patch. Data are shown for different cut sizes, and for each case, the three bars are the readings for flow (i) before cut (baseline); (ii) when cut is made and not sealed; and (iii) after cut is sealed. In all cases, the pressure drops as fluid leaks out through the cut but returns to baseline values once the cut is sealed. (B) For different cut sizes, data are further shown for the burst pressure required to dislodge the QDM gel patch from the tube wall. For these experiments, the baseline pressures are higher than in (A). Note that the burst pressure far exceeds the baseline pressure for small cut sizes.

The pressure readings above depend on both the flow conditions and the size of the cut in the tube.[95] If the flow rate is increased above a critical value, the pressure exerted by the fluid is able to dislodge the electroadhered patch and the fluid then leaks into the surrounding bath. We define the pressure at this point of failure as the burst pressure P_{burst}, and it represents a limit for the conditions studied. Figure 3.4 shows pressure readings for various puncture/cut sizes. P_{burst} is 252 mm-Hg for a small (0.4 mm) puncture, 216 mm-Hg for a medium (1.4 mm) puncture, and 82 mm-Hg for a large (7 mm) cut. These P_{burst} values indicate robust sealing capability under typical blood-flow conditions (normal systolic blood pressure being 120 mm-Hg in healthy humans).[96] Note that P_{burst} can be easily increased by either using a larger gel-patch around the cut or by introducing a second gel-patch over the first in a cross-geometry.

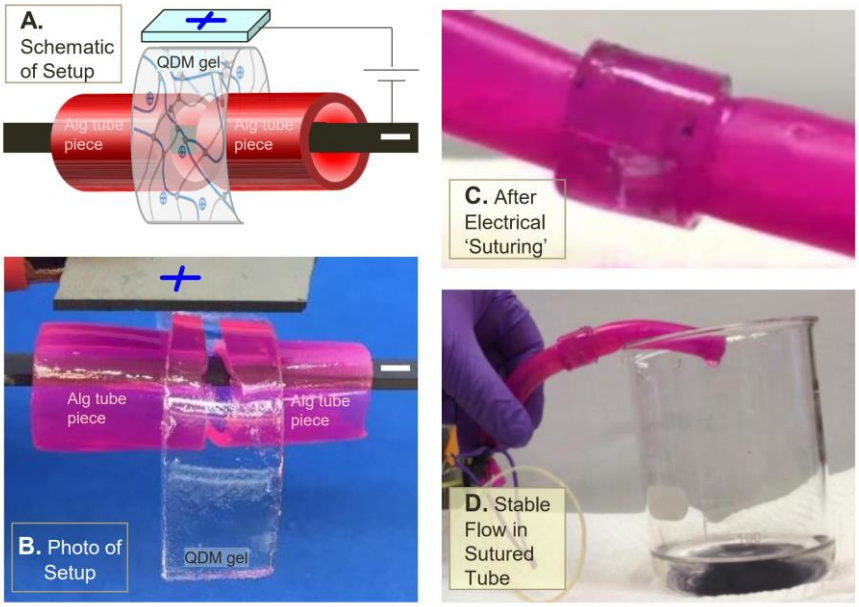

Figure 3.5. Electrical 'suturing' of two severed segments of a tube. A long QDM gel-strip is used as a sleeve around the two pieces of the Alg tube. The electrode orientation is as indicated. Schematic of the process is shown in (A) and a photo in (B). (C) Following this process, the Alg tube segments are found to be 'sutured' (joined) by the gel sleeve. (D) Stable flow occurs through the repaired tube to the waste beaker.

Next, we examined if electroadhesion could repair a much more extreme 'injury' compared to a cut in the tube wall. In this case, we severed the alginate tube in half and attempted to join the two pieces using a QDM gel-strip. First, a long and flexible gel-strip (15 mm long, 8 mm wide and 2.5 mm in thickness) was made. The two pieces of the tube were contacted laterally and the QDM gel-strip was wrapped around the tube segments (Figure 3.5A). During electro-adhesion, the negative electrode was kept in contact with the tube at all times, while the positive electrode was rotated along the exterior of the gel-strip (Figure 3.5B). The net result is that the QDM gel functions as a sleeve that wraps around the cut pieces (Figure 3.5C). Note that the length of the gel strip was chosen to match the perimeter of the sleeve so that there is no gap between the ends of the strip. Thus, the patched tube behaves like a single entity. We can flow fluid through the patched tube without leaks (Figure 3.5D).

3.3.3 Gel-Tissue Electroadhesion

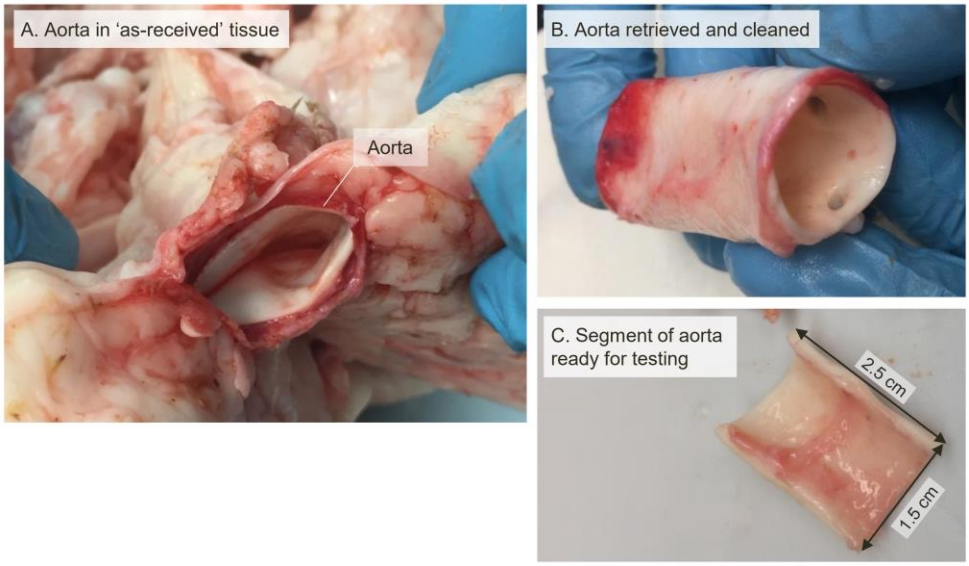

Figure 3.6. Preparation of a sample of bovine aorta for electroadhesion experiments. (A) As received, in the "raw" state, the aorta is encased in fat, and connected to other tissues. (B) The aorta is removed from the surrounding tissues and the fat encasings. (C) A segment of the aorta is cut to the desired size, comparable to the size of a gel segment. This is used for the electroadhesion experiments.

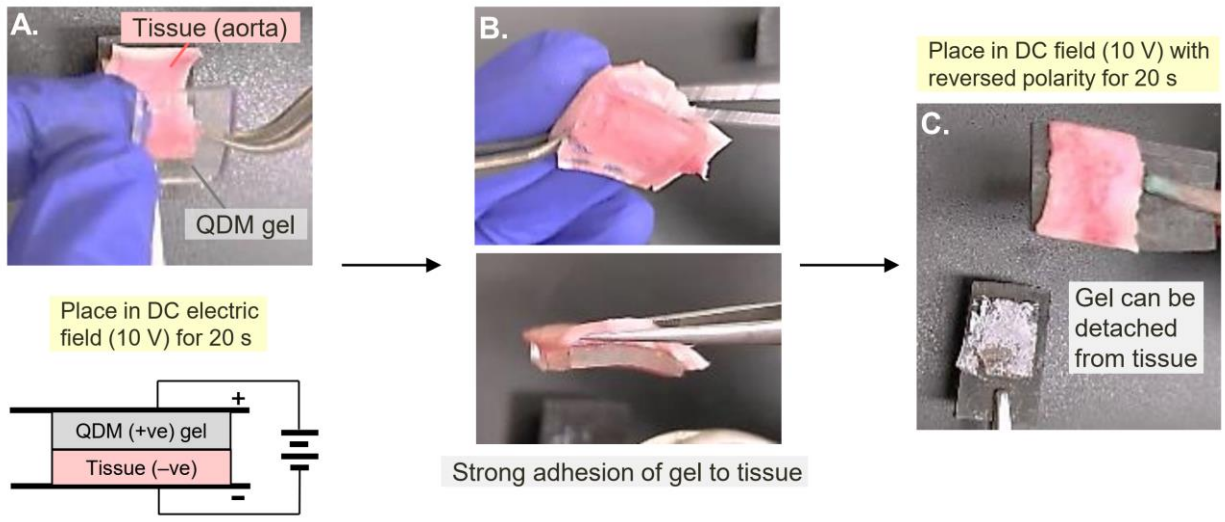

Figure 3.7. Electroadhesion of QDM gel to bovine tissue. (A) Strips of bovine aorta and QDM gel are contacted in a ($E^+G^+T\,E^-$) configuration, with the gel touching the positive and the tissue the negative electrode. (B) 10 V of DC is then applied for 20 s, whereupon the gel becomes strongly adhered to the tissue. (C) When the gel-tissue pair is stretched on both sides, the gel breaks, but a portion of the gel remains adhered to the tissue. This indicates that the adhesion is significant.

We then set out to determine whether EA could be extended to soft materials other than gels. Specifically, could gels be electroadhered to animal tissues? For these studies, we worked with bovine tissues, obtained from a local butcher. Tissues were cleaned and prepared for our studies, as exemplified in Figure 3.6. Tissue samples were then tested along with the same QDM gels as above. First, we tested a piece of bovine aorta, which is one of the largest arteries in an animal.[96] A rectangular strip (1.5 x 2.5 cm^2) of the aorta was used along with a similar strip of the QDM gel. As shown in Figure 3.7A, the gel and tissue are contacted with electrodes in the same orientation as before ($E^+G^+G^-E^-$), with the cationic QDM gel (G^+) connected to the positive electrode and the tissue (T) to the negative electrode. A DC voltage of 10 V is then applied for ~ 20 s, whereupon the gel becomes strongly adhered to the tissue (Figure 3.7B). This suggests that the tissue behaves like an anionic gel, and hence we notate it as T^-. No adhesion is observed if the reverse orientation ($E^+T^-G^+E^-$) of the field is used. Also, if the

electroadhered gel-tissue pair is placed in the reverse orientation and the field is applied, the gel-tissue adhesion is lost and the two can be easily separated, as in the gel-gel case (Figure 3.7C). We conclude that the QDM gel can be reversibly electroadhered to the aorta.

Regarding the strength of EA between gel and tissue, a few points need to be clarified. First, when the QDM gel is contacted with the aorta in the absence of the field, we do find a weak adhesion, which we term 'contact adhesion'. This adhesion is weak enough that the gel can be peeled off intact from the tissue by hand without much force. In contrast, when the gel is electroadhered to the aorta, the gel cannot be peeled off by hand or scraped off from the aorta by using a scalpel. In Figure 3.7B, the gel-tissue pair is pulled on two sides by applying a tensile force to the overhanging portions. When the tension exceeds a certain limit, the QDM gel breaks into two pieces, but the portion of the gel that is adhered to the tissue does not detach. We thereby conclude that strong adhesion of the gel to the tissue is induced by the field and that this adhesion is much stronger than the contact adhesion between the two. We will quantify the strength of EA later in this paper.

Once EA of the QDM gel to the aorta was confirmed, we proceeded to test the same phenomenon with other classes of bovine tissue. In all cases, we cut a strip of tissue similar to that in Figure 3.7 and tested it against a similar strip of QDM gel. First, we examined if there was 'contact adhesion' when the strips of gel and tissue were pressed together without a field. The extent of adhesion (or lack thereof) was assessed using a subjective scale for adhesion strength (see Table 3.1). For this purpose, we attempted to detach the gel from the tissue and noted the ease with which this could be done. The results were then classified into: 0 =

negligible, 1 = weak, 2 = moderate, 3 = strong, and 4 = very strong adhesion. For a given gel-tissue pair, the results for 'contact adhesion' provided the baseline. Next, we attempted to induce EA of the same gel-tissue pair using the same protocol as in Figure 3.7 (i.e., using 10 V of DC, applied for 20 s). After the field was switched off, we again assessed the adhesion strength using the above 0–4 scale and compared the results to the baseline. The results for all types of tissue are presented in Table 3.1.

Adhesion			**No Adhesion**		
Tissue (Bovine)	**Adhesion Strength** Following Electroadhesion	**Adhesion Strength** Following Contact Adhesion	Tissue (Bovine)	**Adhesion Strength** Following Electroadhesion	**Adhesion Strength** Following Contact Adhesion
Aorta (descending thoracic)	**3**	1-2	**Heart**	0-1	0
Cornea (inner layer)	**3-4**	0	**Brain**	0-1	0
Lung	**2**	0	**Spleen**	0-1	0
Cartilage (articular)	**2**	0	**Fat**	0	0
			Thymus	1-2	1
Tendon (transverse section)	**3-4**	0	**Tendon** (longitudinal section)	1-2	0
Skeletal muscle (neck, transverse section)	**2-3**	0	**Skeletal muscle** (neck, longitudinal section)	1	0
Skeletal muscle (cheek, transverse section)	**2**	0	**Skeletal muscle** (cheek, longitudinal section)	1-2	0

N = 3 for all samples. All electroadhesion tests done with 10 V DC, applied for 20 s.
Numerical scores represent strength of adhesion assessed on a scale of 0-4: 0 - Negligible; 1 - Weak; 2-Moderate; 3 - Strong; 4 - Very strong.

Table 3.1. Results of electroadhesion tests done with QDM gels and various bovine tissues. Electroadhesion was significant relative to contact adhesion only for the tissues listed in the left half of the table.

Table 3.1 (left half) indicates several tissues for which the strength of EA is much higher than the baseline case of contact adhesion. The largest contrast is in the case of the cornea from the eye and tendon (transverse section), where the QDM gel shows negligible contact adhesion (0 on the scale), but very strong EA (~ 4 on the scale). Other tissues for which

EA is clearly stronger and distinct relative to the baseline include the lung, the cartilage, and certain types of skeletal muscle. The case of the aorta, which was depicted above in Figure 3.7 is one in which contact adhesion is not zero, but EA is clearly much stronger. Conversely, the right half of Table 3.1 lists the tissues for which EA is not significant under the conditions studied. In the case of the heart, the brain, the spleen, and fat tissue, there is no significant adhesion, either on contact or due to the field. In the case of the thymus, weak adhesion is observed due to the field, but this is not sufficiently distinguishable from contact adhesion. Tissues can be structurally complex, and the complexity is especially evident in our studies with tendon and skeletal muscle (bottom three entries in Table 3.1). If these tissues are cut in a longitudinal section, the samples do not exhibit significant EA; however, if the same tissues are cut in a transverse section, EA is appreciable. Thus, there is significant anisotropy in the tissue structure, which also affects the results here. All in all, we conclude from Table 3.1 that cationic QDM gels can be electroadhered to some types of animal tissue.

Why does EA work with tissues? And why does it work only with some tissue types and not others? We made anionic counterparts to the QDM gel by copolymerizing AAm with an anionic monomer like sodium acrylate (SA). However, this gel could not be electroadhered to any tissues. Thus, in all the successful cases of EA we have found, the gel was cationic (i.e., QDM), which then implies that the tissue must be anionic. Animal tissues are expected to have a microstructure consisting of cells (either discrete or close-packed into clusters) embedded in a network of polymer chains, i.e., the extracellular matrix (ECM).[85,86] The ECM tends to have different composition in different tissues. Two key proteins in the ECM are collagen and elastin. We attempted to find the percentage of each of these proteins in the tissues studied

here.[97-101] These numbers are shown in Table 3.2, which is divided into two halves similar to Table 3.1, with the tissues that exhibit EA on the left and those that do not on the right. In addition to the proteins, the water content in each tissue is also shown.

Adhesion				No Adhesion			
Tissue (Bovine)	Percent Collagen	Percent Elastin	Percent Water	Tissue (Bovine)	Percent Collagen	Percent Elastin	Percent Water
Aorta	23	40	84-87	Heart	3	0	74
Cornea	70		78	Brain	0.2	0	73
Lung	11	5	84	Spleen	3	5	79
Cartilage	58		80	Fat		9	50
				Thymus			
Tendon (transverse section)	85	5	55-70	Tendon (longitudinal section)	85	5	55-70
Skeletal muscle (transverse section)	2-7	0	80	Skeletal muscle (longitudinal section)	2-7	0	80

Values correspond to bovine tissue unless otherwise noted below. Values rounded to nearest integer.

Table 3.2. Collagen, elastin, and water content of tissues that do and do not exhibit electroadhesion. Notes: (a) Aorta: Collagen and elastin compositions of aorta,[97] water content.[101] (b) Cornea: collagen composition,[100] elastin percent values not given,[102] water content.[103] (c) Lung: collagen and elastin composition in rat lung,[97] water content.[104] (d) Cartilage: collagen composition of human cartilage,[101] elastin percent values not given,[105] water content.[106] (e) Tendon: collagen and elastin composition of tendon,[97] water content.[107] (f) Skeletal muscle: collagen and elastin compositions of skeletal muscle,[98] water content.[104] (g) Heart: collagen and elastin compositions of heart,[97] water content.[104] (h) Brain: collagen and elastin compositions of rat brain,[97] water content.[104] (i) Spleen: collagen and elastin compositions of spleen,[97] water content.[104] (j) Fat: collagen percent not given,[108] elastin composition of human adipose (fat) tissues,[109] water content.[104] (k) Thymus: collagen percent not given,[110] no data on elstin and water content available in literature.

One observation from Table 3.2 is that many (but not all) the tissues in the left half have a high collagen content. Collagen itself is a protein that has a net neutral charge at ambient pH,[111,112] and on its own would not impart anionic character to the tissue. However, collagen-rich tissues often are associated with protein-sugar hybrid polymers called

glycosaminoglycans (GAGs), which are known to be strongly anionic.[101,113] The GAGs anchor cells to the ECM by attaching simultaneously to proteins on the cell surface as well as to the collagen fibers in the ECM.[113] GAGs such as heparan sulfate have high affinity to collagen type I and III,[113] which are the main types of collagen in the aorta. Another observation from Table 3.2 is that some types of collagen-rich ECMs also have high concentrations of elastin. Elastin is reported to be cationic at ambient pH, which allows it to bind to GAGs via electrostatic interactions. Collectively, in a tissue that contains collagen, GAGs, elastin, and other polymers, the overall composition of charged polymers will dictate the net charge of the tissue. It is possible that only tissues with a net anionic character will have a propensity to undergo EA (to cationic gels like QDM). Another factor could be the water content in the tissue; if this is too low (such as in the case of fat or brain tissue), the tissue may not exhibit EA.

An additional factor to consider is the ionic strength of the (fluid in the) tissue. Interactions between cationic and anionic polymers will be impacted by the ionic strength. In this regard, we have soaked the QDM gel and a representative tissue (aorta) in different fluids of biological relevance and then examined their adhesion. All these fluids are expected to have an ionic strength around 0.15 M. If soaked in whole blood (bovine), the gel and tissue electroadhere just as in their native state. When soaked in blood plasma (bovine) or in phosphate-buffered saline (PBS), the gel-tissue adhesion was initially weaker, but built up thereafter. By increasing the time over which the field was applied from 20 s to 60 s, we were able to obtain significant adhesion between the gel and tissue in all cases.

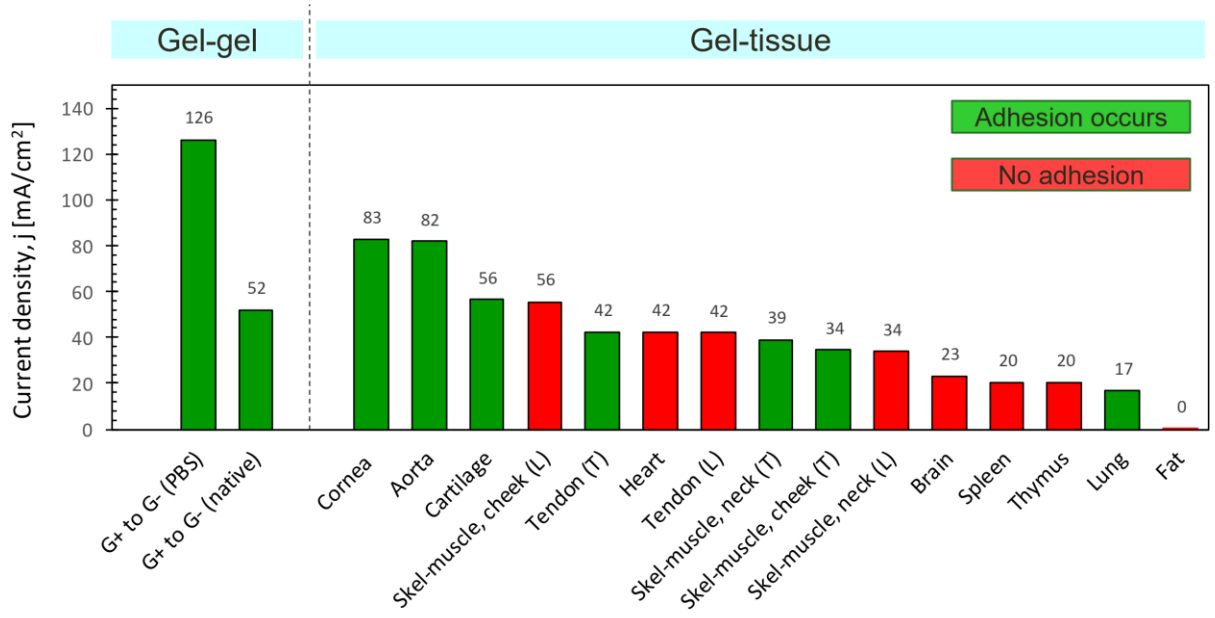

Figure 3.8. Current density during electroadhesion experiments on gel-gel and gel-tissue pairs. All pairs were placed in an electric field of 10 V DC that was applied for 20 s. In the gel-gel cases, a cationic QDM gel (G^+) was contacted with an anionic SA gel (G^-). In the gel-tissue cases, the cationic QDM gel (G^+) was contacted with various tissues. In all experiments, the current *I* starts high and decreases with time. The highest recorded current is used to calculate the current densities j shown in the plot (note: $j = I$ / area of contact). The area of contact ranged between 1.6 and 2.4 cm^2 for the various tissues. No obvious correlation is seen between *j* and the occurrence of electroadhesion (refer to Table 3.1 in the text). The data for gel-gel pairs in their native state (i.e., as prepared in deionized water) or after soaking in PBS demonstrate that *j* mainly depends on the ionic strength of the fluid.

We have also recorded the current *I* during EA experiments, which is reported for various pairs in Figure 3.8. Data in this figure are shown for the current density *j* (i.e., *I*/area of contact). We note that *j* seems to depend mainly on the ionic strength of the gel and tissue: for example, *j* is 52 mA/cm^2 when two gels (G^+ and G^-) are electroadhered in their native state (i.e., after preparation with deionized water) but increases to 126 mA/cm^2 when the same gels are soaked in PBS. Similar currents were observed even if gels of the same charge (e.g., two G^+) were contacted, which would be a case of no adhesion. In the case of gel-tissue experiments, *j* for various tissues are shown in Figure 3.8. For tissues that electroadhere, *j*

varies from a low of 17 mA/cm^2 for the lung to around 80 mA/cm^2 for the aorta and cornea. For tissues that do not electroadhere, j is nearly zero for fat tissue, whereas it is 42 mA/cm^2 for heart tissue. From these numbers, no clear relationship can be discerned between j and adhesion (or lack thereof). It should be mentioned that the *j* values we report correspond to the highest current recorded, which is near the start of the experiment. With time, the current drops to a steady-state that is 20-30% of the above values.

Next, we attempted to measure the gel-tissue adhesion strength and compare it to that for the gel-gel case. The measurements were done using the lap-shear test protocol, which is described in more detail in the Experimental Section.[64,78,92] In this test, two rectangular samples are adhered to each other over a portion of their area, which is called the 'lap' (Figure 3.9A). The outer surfaces of the two samples are then stuck to glass slides using cyanoacrylate glue. The setup is then placed in the testing instrument, with each glass slide being gripped on its end by the jaws of the instrument. A tensile stress is then applied until failure occurs, and the magnitude of the stress-at-break is a measure of the adhesion strength. Stress vs. strain curves are presented in Figure 3.9B for two sets of samples: a QDM gel adhered to an Alg gel, and the same QDM gel adhered to bovine aorta. For both cases, we ran the test first under 'contact adhesion', where the samples are pressed together without a field. Next, the two samples are electroadhered and the test is repeated. In both the gel-gel and the gel-tissue cases, the stress-strain curves for EA extend up to much higher stresses compared to contact adhesion (Figure 3.9B), indicating the strong adhesion imparted by the electric field.

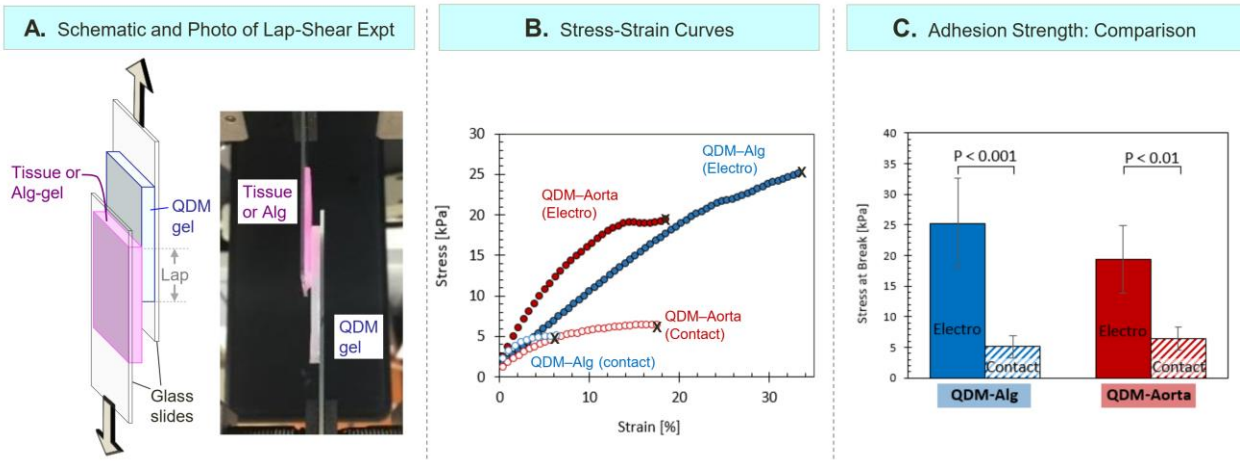

Figure 3.9. Adhesion strength measurements using the lap-shear protocol. (A) Schematic of the lap-shear experiment and a photo of an experiment in progress. Samples are first adhered over a lap region and then affixed to glass slides on their reverse sides using cyanoacrylate glue. Tension is then applied to the ends of the slides. (B) Stress vs. strain curves from lap-shear experiments for two sets of samples: gel-gel (QDM-Alg) and gel-tissue (QDM-aorta). Data are shown for the cases of electroadhesion and contact adhesion (control). The samples delaminate at the end of each curve, marked by an X. The stress at this point is a measure of the adhesion strength. (C) Adhesion strengths from the curves in (B) for the QDM-Alg and QDM-Aorta samples and for the two cases of electro- and contact adhesion.

The adhesion strengths determined from the above curves are plotted in Figure 3.9C. The strength of gel-gel (QDM-Alg) electro-adhesion is found to be ~ 25 kPa. For comparison, Asoh and Kikuchi measured the adhesion strength (using the same lap-shear technique) for a pair of cationic and anionic acrylamide-based gels and reported values around 10 kPa.[22] For the electroadhered gel-tissue pair (QDM-aorta), the adhesion strength is about 20 kPa, which is comparable to that for the gel-gel case. In both cases, the strength of contact adhesion is much lower (~ 5 kPa). These measurements confirm our findings from earlier in the paper that, for both the gel-gel and gel-tissue cases, EA is substantially strong. One difference we noted was regarding the failure mechanism in the lap-shear experiment. In the gel-gel case, when failure occurred, it was generally a cohesive failure, [64,78,92] i.e., pieces of each gel were found

to remain on the other. In the gel-tissue case, failure was generally an adhesive failure,[64,78,92] with the gel delaminating from the tissue. This difference could be because the tissue tested (aorta) was generally much stiffer than the QDM and Alg gels.

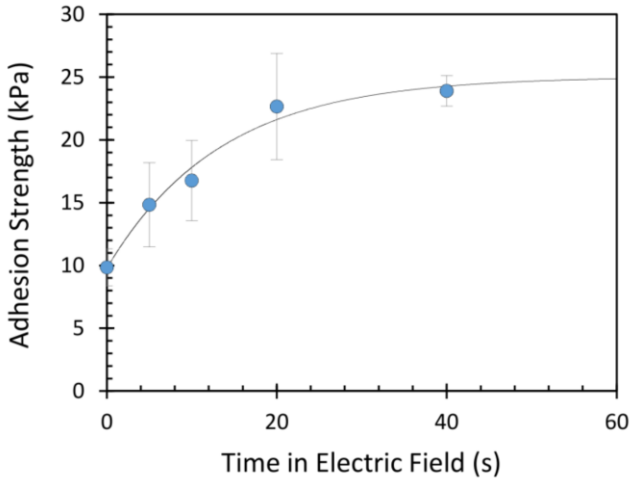

Figure 3.10. Gel-tissue adhesion strength as a function of time in the electric field. Adhesion between QDM gels and aorta strips were measured after different durations of exposure to the field (10 V DC). The lap-shear technique was used and the stress-at-break was used to quantify the adhesion strength. The plot shows that electroadhesion develops within ~ 10 s in the field and the adhesion strength saturates by about 20 s. The data shown are averages (across at least three samples) and the error bars correspond to standard deviations. The line through the data is a guide to the eye.

We also studied the adhesion strength as a function of time under the electric field, and the corresponding data are shown in Figure 3.10 These data are for QDM gels crosslinked with BIS (but not containing LAP nanoparticles) in contact with bovine aorta. The same lap-shear protocol as in Figure 3.9 was used and the stress-at-break was used as a measure of adhesion strength. Gel-tissue pairs were placed for different times in an electric field generated by 10 V DC. The data reveal that sufficient electroadhesion (i.e., much higher than contact adhesion) develops within 10 s in the field. Subsequently, the adhesion strength tapers off to a constant

value by about 20 s, and similar values are obtained with higher contact times (40 s). Thus, a time of 20 s in the field seems to be more than adequate to induce appreciable electroadhesion between gel and tissue. Similar data for adhesion strength as a function of contact time has been reported previously for gel-gel adhesion.[24]

3.3.4 Electroadhesion for Repairing Cut or Damaged Tissue

Finally, we explored whether an electroadhered gel patch could seal cuts on a tissue, effectively mimicking a surgical procedure. These studies are similar to those we had previously demonstrated with the anionic gel tube in Figure 3.5, where cuts were sealed by a QDM gel patch. We again chose the cationic QDM gel, but this time the experiment involved a segment from the descending thoracic aorta of a cow, which was about 15 cm long and 2 to 2.5 cm in diameter (Figure 3.11A). For the purposes of our experiment, we exploited the fact that the aorta has pairs of holes along its length (marked by arrows in Figure 3.11A). These holes correspond to arterioles, which are small branches from the aorta that transport blood to various organs.[96] If the aorta is used as a tube, fluid will leak out through the arterioles. This is shown by Figure 3.11B, where we have replicated the test protocol from Figure 3.5. A solution of 0.1% $FeCl_3$ is pumped through the lumen of the aorta. The fluid leaks out through the arterioles and drips into the bath containing 0.1% tannic acid, whereupon a black precipitate of ferric tannate is instantly formed. (Note that the aorta was not submerged in the bath to avoid any reaction of the tissue with the tannic acid.)

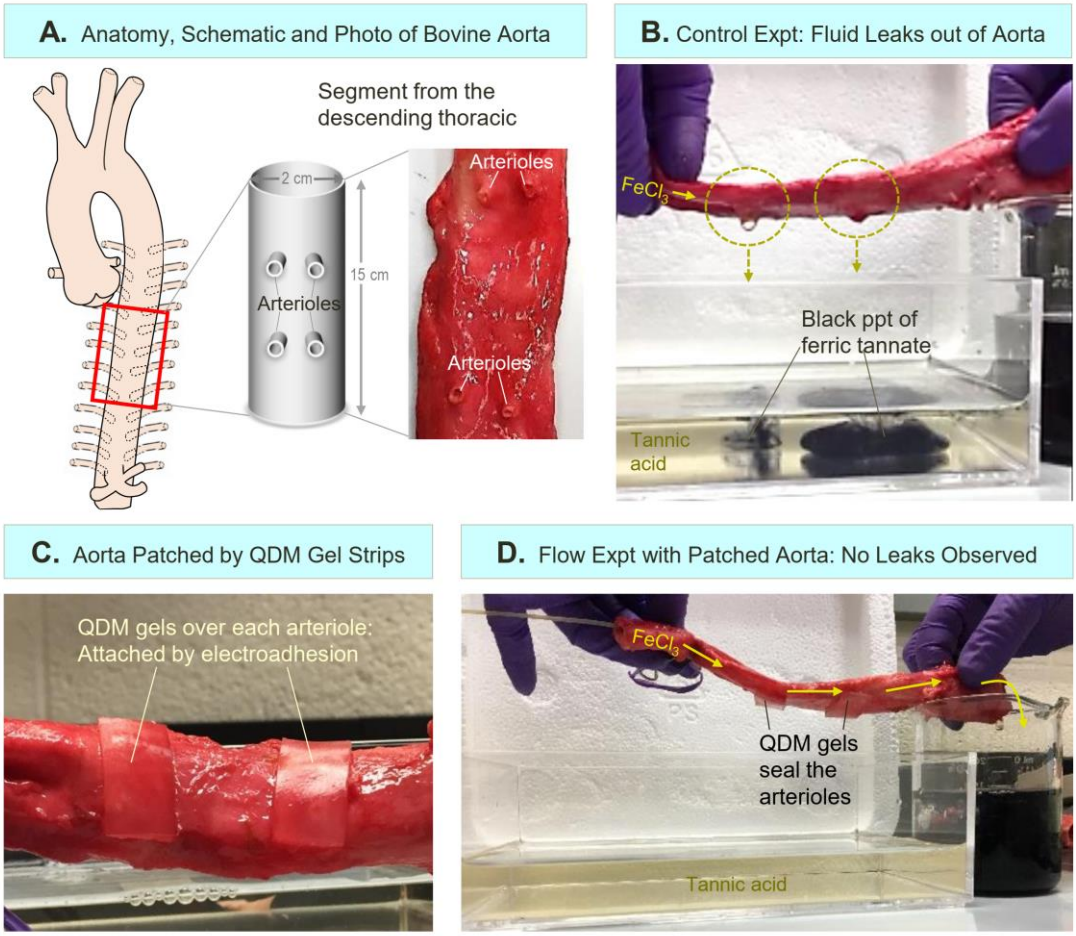

Figure 3.11. Electroadhesion of QDM gels to patch openings in the aorta. (A) The anatomy of the aorta, which is a large artery, is depicted on the left. A 15-cm long segment from the descending thoracic region of the aorta is used in the study. The segment is a hollow tube that has holes on its surface corresponding to arterioles (side branches), as shown both in the schematic and the photo. (B) When an aqueous solution of 0.1 wt% $FeCl_3$ is pumped through the aorta, the fluid leaks out of the arterioles and falls into the bath containing tannic acid, whereupon a black precipitate of ferric tannate is formed. (C) Two QDM gel strips are electroadhered to the aorta so as to cover the arterioles. (D). When the $FeCl_3$ solution is pumped through the patched aorta, no leaks are observed (the bath stays clear), and the fluid flows steadily into the beaker on the right.

Next, we made two rectangular patches of the QDM gel for the two pairs of arterioles in the aorta segment under study. We affixed the gel patches over the arterioles (one patch covers two adjacent arterioles) using electroadhesion (10 V, 20 s). The gels adhered tightly to the tissue, as can be seen in Figure 3.11C. Thereafter, the flow of $FeCl_3$ solution through the aorta was restarted. Figure 3.11D shows that there are no leaks through the arterioles, i.e., the holes remain

sealed, allowing fluid to flow right through the aorta. The fluid is collected in a beaker containing 0.1% tannic acid at the end of the aorta. The black precipitate of ferric tannate is seen in the beaker but not in the water bath, thus confirming that there are no leaks through the tissue during the flow process.

3.3.5 Prospects for Biomedical Applications

Our results indicate the potential for EA to be useful in biomedical scenarios: it could enable surgeries in the future to be performed without the need for any sutures. Compared to current surgical adhesives, [26,29,30,67,87-90] an electroadhered gel patch provides a very robust seal that persists. Also, the unique feature of EA is that it develops on external command when an stimulus is applied. In case of a mistake, the adhesion can be reversed, and the gel patch can be readily detached from the tissue. Subsequently, the patch can be reapplied on command. Many challenges will have to be addressed for this technique to be translated to the clinic. First and foremost, a better understanding of the adhesion mechanism is needed. Ideally, we should have the ability to electroadhere gels to any type of tissue, provided the gel is chosen carefully. The gels should also be biocompatible and not cause an adverse immune response in the body. Moreover, for many types of surgeries, it will be important for the gel to be biodegraded into benign products within a set number of days after surgery. We believe biocompatibility and biodegradability are tractable problems because, in principle, QDM could be replaced with many other kinds of cationic gels.

Lastly, there is a question about applying electric fields and whether that would be safe in regard to a live animal. The voltage used here is 10 V DC, which on its own is not especially high.[114-116] Moreover, the field has to be turned on only for 20 s, which is a short enough time to

avoid any adverse reaction. Incidentally, with regard to the voltage, we have found that EA of gels to tissues can be achieved even with voltages as low as 3 V but applied for a longer duration (~ 60–120 s). No adhesion was seen for voltages below 3 V for both gel-tissue and gel-gel systems. Previous studies of gel-gel adhesion have reported weak adhesion even below a voltage of 3 V.[24] Conversely, with some of the tissues in Table 3.1 for which EA was unsuccessful, a longer application time (> 20 s) and/or a different voltage could change the results. Thus, altering these parameters as well as the chemistry of the gel could well lead to strong EA with more of the tissue types listed in the table. These are aspects that will need to be studied carefully in the future.

3.4 Conclusions

In this study, we demonstrated that the phenomenon of EA could be applied to new materials and geometries. We utilized cationic (QDM) gels and animal (bovine) tissues. Gel and tissue were brought into contact with each other and with electrodes in a $E^+G^+T^-E^-$ orientation (i.e., with the cationic gel G^+ touching the positive electrode E^+ and the tissue T^- the negative electrode E^-). A DC voltage of 10 V was then applied for 20 s, whereupon the gel became strongly adhered to the tissue, with the adhesion persisting after the field was turned off. The strength of adhesion between QDM gel and bovine aorta, measured by lap-shear testing, was ~ 20 kPa. In addition to the aorta, EA also worked with the cornea, the lung, cartilage, and certain types of skeletal muscle and tendon. Only cationic gels could be electroadhered to tissues, which suggested that the tissues had anionic character. Also, if the electroadhered gel-tissue pair was placed in a field with reversed polarity, the adhesion was lost and the two could be separated.

We then explored the possibility of using electroadhesion to seal cuts or tears in tubes. Initial experiments in this regard were done with tubes of anionic Alg gel as a model system. As an extreme case, two severed pieces of an Alg tube were joined using an electroadhered QDM gel strip that was flexible enough to encircle the tube while spanning the cut segments. In a similar manner, in the case of bovine aorta, QDM gels were electroadhered over openings in the tissue (corresponding to arterioles). In both cases, the electroadhered patches provided a robust and durable seal, allowing fluid to flow right through the lumen of the tubes. These studies raise the possibility of using electroadhesion to perform surgical repairs in the future. The use of strongly adhered gel patches could obviate the need for sutures or staples in many surgical procedures. The ability to achieve adhesion on command with an electric field, and moreover the ability to reverse the adhesion in case of an error, could enable surgeries to be done in a rapid, durable, and precise manner. Future work will address the challenges mentioned in the previous section before this technique could be used in clinical applications (such as gel biocompatibility and immune tolerance).

Chapter 4

Electroadhesion of Gels to Various Animal and Plant Tissues

4.1 Introduction

In Chapter 3, we reported the first examples of electroadhesion (EA) between cationic hydrogels and biological tissues, specifically bovine tissues. Only cationic gels could be adhered by EA to tissues, not anionic or nonionic gels. The adhesion of cationic gels was strong to some tissues (such as the cornea and blood vessels), but weak or non-existent to others (such as the brain and adipose tissues). [19] Our studies raise numerous questions regarding the phenomenon of EA. What causes EA? Why are there differences in EA between various tissues? Prior to our work, EA had been shown to arise between cationic gels (denoted by G^+) and anionic gels (denoted by G^-).[18,21,23,24] In our studies, we substituted the anionic gels with tissues. Mammalian tissues are generally known to have anionic character (and hence will be denoted by T^-). By extension, could EA arise between a cationic gel and *any* anionic soft material? There is also the question of structure at the micro or nano scale. Gels that undergo EA are networks of chains with ionic backbones. Do biological tissues always have a network structure similar to hydrogels? If not, what kind of structure is needed for a material to undergo EA?

In this Chapter, we attempt to address many of the above questions by examining a wide range of biological tissues and testing their adhesion to cationic gels (G^+) via EA. Soft tissues from a variety of animals (mammals, birds, fish, reptiles, insects) are studied. In addition, we also examine a range of plant-derived materials, including vegetables and fruits. All in all, we have tried to cover biological species across the domains of life, and many of these species have tissues

or organs (composed of biological cells) that allow EA of cationic gels. Soft materials, regardless of their origin, have elastic moduli in the range of 10^3 to 10^7 Pa.[117-122] In addition to cell-bearing soft materials, we have also examined some soft everyday materials such as foods (e.g., cheese and tofu), which have biologically derived polymers (proteins and polysaccharides) in them.

Our studies allow us to identify several themes or hallmarks of EA across the various systems. EA is induced in all cases by a low DC field (5 to 10 V; field strength 1 to 4 V/mm), applied for a short time (10 to 60 s). The adhesion induced by EA persists after the field is switched off. However, if at a later time, the field is re-applied with a reversed polarity, the adhesion can be reversed. We have used pull-off tests to characterize the adhesion strength achieved by EA. Consistent trends are found with regard to tissue type: for example, muscles in many different animals (cow, chicken, fish) can be adhered to gels by EA with an adhesion strength around 15 kPa. Also, tissues with anisotropic structure adhere strongly to gels in one orientation (transverse) but not in the perpendicular one (longitudinal). Somewhat surprisingly, we find that gels can be adhered by EA not only to soft tissues like muscles but also to stiff ones like the carrot. The results from our study are promising because they suggest that EA has wide applicability to biological materials, including potentially to human tissues.

4.2 Experimental Section

Materials. The following chemicals were from Sigma-Aldrich: the monomers acrylamide (AAm) and N,N′-methylenebis(acrylamide) (BIS), sodium acrylate monomer (SA), phosphate buffered saline (PBS) tablets and the initiator ammonium persulfate (APS). The accelerant N,N,N′,N′-tetramethylethylene-diamine (TEMED) was from TCI America. The monomer N,N′-dimethylaminoethyl meth-acrylate, quaternary ammonium salt (QDM) was from MPD Chemicals. Cyanoacrylate-based glues (Krazy Glue) and Rust-Oleum hydrophobic coating were purchased from The Home Depot. Deionized (DI) water was used in all experiments.

Synthesis of QDM gels. Cationic QDM gels were prepared using a modified protocol from our previous publication.[19] First, DI water was degassed by bubbling nitrogen gas through it for 20 minutes. For synthesis of QDM gel the following were combined: 1 M (1.4 g) AAm, 0.16 M (809 μL) of QDM solution, 0.019 M (0.06 g) BIS, 0.0088 M (0.04 g) APS and 0.01 M (30 μL) TEMED were mixed in 20 mL of degassed DI water. Next, the above monomer mixture was poured into a Petri dish. To assist with easy removal of the gels, Petri dishes used in gel preparation were coated with a spray of Rust-Oleum hydrophobic coating, then allowed to sit for 1 min, and thereafter wiped dry. The petri dish with the monomer solution was then placed in a nitrogen environment for 1.5 h, whereupon the gel became fully polymerized. After polymerization, the gels were stored in a fridge and typically used within 24 h of preparation.

Synthesis of SA gels. Anionic SA gels were prepared by a similar procedure as described above for QDM gels.[19] In this case, the monomer solution contained 1.4 M (2 g) AAm, 0.11 M (0.2 g) SA, 0.019 M (0.06 g) BIS, 0.0088M (0.04 g) APS and 0.01 M (30 μL) TEMED in 20 mL of

degassed DI water. The above solution was poured into a pre-coated Petri dish and maintained in a nitrogen environment for 2 h. After polymerization, gels were stored in a fridge and typically used within 24 h of preparation.

Tissue Preparation Protocol. Cow, pig, and chicken tissues were obtained ethically, immediately after slaughter from a local butcher or farm. C57 black mouse tissue was obtained from an alternative animal study, IACUC number 30703 at Children's National Hospital in Washington DC. Fish (both salmon and cod), shrimp and scallop were purchased fresh (never frozen) from Whole Foods. Earthworms and cicada were found in nature. All experiments on tissues were conducted within 24 h of tissue harvest. The tissues were kept refrigerated from harvest point until the experiment but brought to room temperature before any experiment was performed. When the tissues were first received, organs were typically encased in fat and other matrix material. For example, the salmon muscle in Figure 4.1 and the chicken muscle for pull-off tests performed in Figures 4.3 were covered in scales/skin and an epithelial layer. Thus, for experiments with muscle, it had to be harvested and cleaned from the surrounding parts. The muscle was either used in the transverse orientation or in the longitudinal orientation (more on this in the body of text). The tissues were cut into smaller pieces for experiments with the focus on cutting segment of tissue muscle without an epithelial layer. For experiments in Figures 4.1 and 4.4 the tissue was segmented into slices of 1.5 x 3.5 x 0.3 ± 0.1 cm. For pull-off tests in Figures 4.3 and 4.6 the slices of muscle were segmented into slices of 1.3 x 0.7 x 0.3 ± 0.1 cm. Tissues were always covered in gauze soaked in PBS solution after sectioning and before use.

Adhesion Experiments. A DC power source (Agilent, model E3612A) with a range of 0–60 V, 0–0.5 A was used for the electroadhesion experiments. The voltage of 10 V was used for all experiments, unless indicated otherwise. Depending on the pair of material adhered (gel-gel, gel-animal tissue, or gel-plant tissue) a different electric field application times were required. For gel-gel pairs we applied the field for 10 s, for gel-animal tissue pairs - 30 s, for gel-plant tissue pairs- 60 s, unless otherwise specified. EA orientation was always ($E^+G^+M^-E^-$), meaning the cationic gel (G^+) was placed in contact with the positive electrode (E^+), while the anionic material: gel (G^-), animal tissue (T^-), plant tissue (P^-) or fungi tissue (F^-) was placed in contact with the negative electrode. For reversal of adhesion the electrode and materials orientation were always ($E^+M^-G^+E^-$). Note, M^- stands for anionic material and is a place holder for anionic gel, animal, plant, or fungi tissues.

Pull-off Mechanical Testing Protocol. Pull-apart adhesion testing was performed on a TA Instruments DMA Q800. Gel-gel and gel-tissue samples were prepared with dimensions of 0.7 x 1.3 x 0.6 cm (each gel is 0.3 cm in thickness). These pairs were either electroadhered or brought together by contact. Each pair was superglued to the dynamic mechanical analyzer (DMA) clamp. Contact adhesion control samples were compressed at 1 N for 1 min, and following this compression period, pulled apart via a controlled force ramp at a rate of 0.1 N/min until failure. Electroadhered samples were run as-is with a controlled force ramp at a rate of 0.1 N/min until failure.[75] Stress at failure was recorded. Each sample was replicated 5 times (n = 5). In the gel-tissue samples, the tissue layer was secured to the top (fixed) clamp and the gel layer to the bottom (movable) clamp. Contact and EA samples were run under same conditions as the gel-gel samples.

Rheological Studies. Rheological experiments reported were conducted using an AR2000 stress-controlled rheometer (TA Instruments) at 25°C, set to 0.1% strain. A flat plate geometry (20 mm diameter) was used to perform steady-shear rheology on various types of tissues. Tissues were segmented to thickness of 1-2 mm.

Electroadhesion of Multi-System Soft Material Chain. Samples were cut using a punch biopsy with diameter of 5 mm. Gel thickness was 2 – 3 mm while chicken tissue and SB tissue thickness was 2 – 5 mm. In line with our previous study, we used wired graphite as the electrodes. The electrodes were placed across the adhering pair alone. Once the materials achieved adhesion, another layer was added. The electrodes never crossed the already-adhered interface, rather were placed on the last link in the chain and the new sample slice. See our previous study for more elaborate and schematic details.

4.3 Results and Discussion

4.3.1 Electroadhesion Exhibits Common Features Across Different Pairs of Materials

In this Chapter, we will demonstrate electroadhesion (EA) between various pairs of soft materials. In a pair of materials that undergo EA, one has to be cationic, while the other anionic. In our experiments, the cationic material is fixed to be a hydrogel denoted as QDM. This gel is made by free-radical polymerization of a mixture containing the cationic monomer quaternized dimethylaminoethyl methacrylate (QDM). The three panels of Figure 4.1 show that QDM gels (G^+) can be adhered by EA to a variety of anionic materials, including anionic gels (top panel), animal tissues (middle panel), and plant tissues (bottom panel). The anionic gel (G^-) is made by polymerizing a mixture containing the anionic monomer sodium acrylate (SA).[19] As an example of an animal tissue (T^-), we use a slice from a species of fish, i.e., salmon. This slice corresponds to the muscle, and it exhibits a vivid orange color. As an example of plant tissue (P^-), we have selected a slice of strawberry. Both the animal and plant tissue slices are from their inner portions, not their exterior. The anionic nature of tissues will be discussed in a later section.

All these materials are cut into thin strips, with a thickness ~ 2 - 5 mm and a long dimension of ~ 2 cm. They are all soft solids with sufficient dimensional integrity such that they can be lifted up and held vertically between one's fingers. Prior to performing an EA experiment, as a first step, we test the three pairs of materials (G^+/G^-, G^+/T^-, G^+/P^-) for contact adhesion. That is, we press each pair together by hand and observe if the materials remain strongly adhered (Figure 4.1A). In all cases, the contact adhesion is negligible or weak, and so the materials can be easily separated. The lack of contact adhesion underscores the fact that the subsequent EA is due to the electric field.

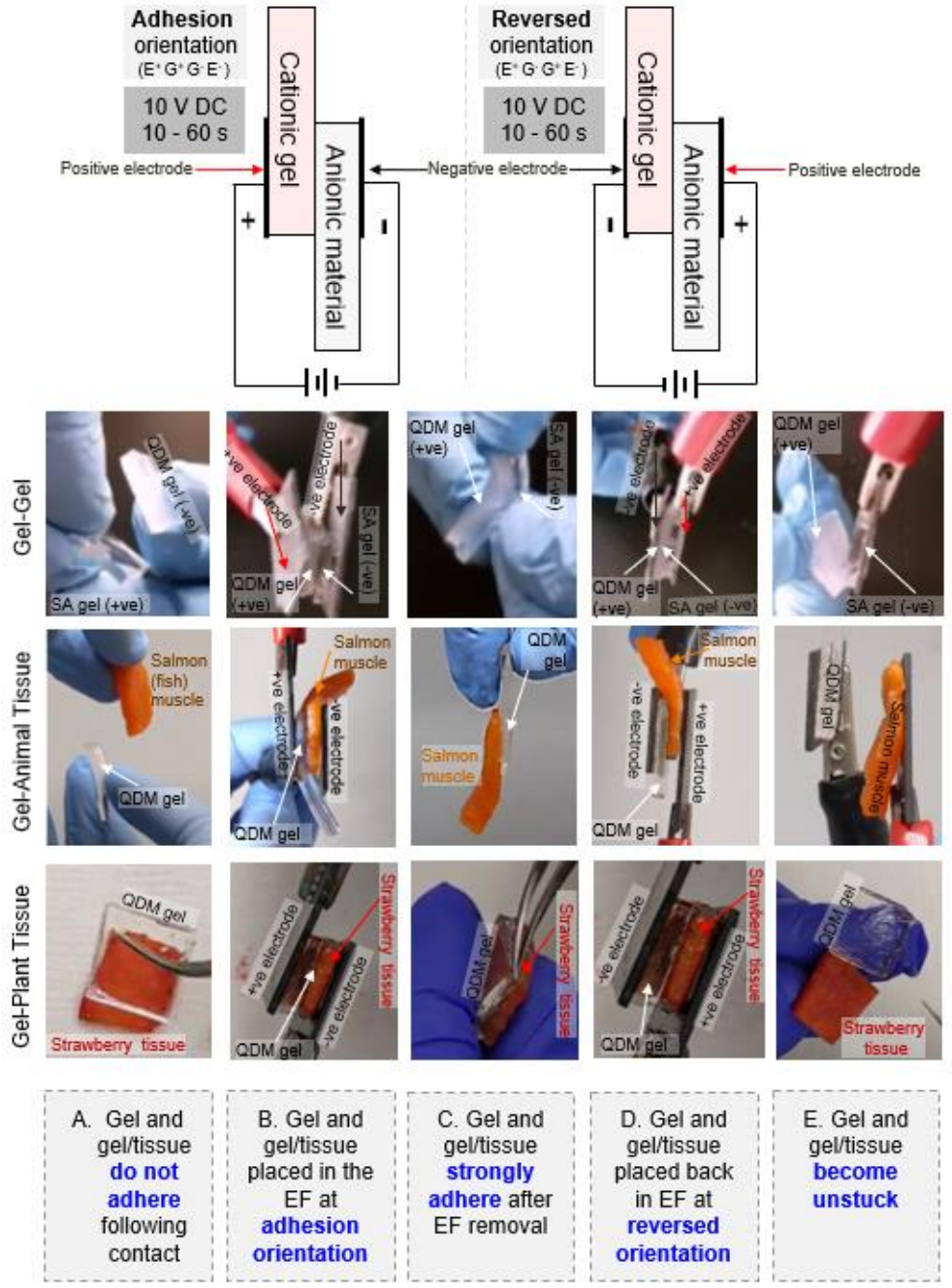

Figure 4.1. Common features in the electroadhesion (EA) of three diverse material pairs. EA requires a cationic and an anionic material. Here, the cationic material is kept the same and is a QDM gel (G^+). The anionic material is either an anionic gel (G^-), an animal tissue (T^-) (muscle from salmon), or a plant tissue (P^-) (slice of strawberry). (A) The material pairs exhibit no adhesion on contact in the absence of the field. (B) DC field of 10 V is turned on for 30 s in the EA orientation ($E^+G^+T^-E^-$). (C) Upon removal from the field, the materials are found to be strongly adhered, and this adhesion persists indefinitely. (D) The adhered pair is placed in the same DC field with the orientation reversed ($E^+T^-G^+E^-$) and the field is switched on for 30 s. Upon removal from the field, the materials have lost their adhesion and can be detached.

Next, we connect the materials to a DC power source in the adhesion orientation (Figure 4.1B). In this orientation, the cationic gel (G^+) contacts the positive electrode (E^+) and the anionic material (e.g., T^-) the negative electrode (E^-). While in this $E^+G^+T^-E^-$ orientation, we apply a low DC voltage (typically 10 V) for a short time (10 to 60 s). During this time, the material pairs develop a strong adhesion, i.e., EA. This adhesion develops within 10 s for the G^+/G^- pair, while it takes around 30 s for the G^+/T^- pair and around 60 s for the G^+/P^- case. The field is then turned off and each pair is found to be strongly adhered (Figure 4.1C) – the pairs are held vertically to show their adhesion. Importantly, the EA persists indefinitely thereafter. Next, we show that the adhesion is reversible. The adhered pairs are placed back in the DC electric field, but the orientation is reversed (Figure 4.1D): the cationic gel (G^+) now contacts the negative electrode (E^-) and the anionic material (e.g., T^-) the positive electrode (E^+). While in this $E^+T^-G^+E^-$ orientation, we apply the same 10 V DC again for a short time (10 to 60 s). When the field is turned off, the pair are found to have lost their adhesion and can be easily detached.

To summarize, we reiterate some of the common features of EA across the range of materials in Figure 4.1. First, adhesion is induced by applying a *low DC electric field* (~ 10 V potential) in a specific "adhesion" orientation ($E^+G^+T^-E^-$) for just a *short time* (~ 10 to 60 s). This adhesion *persists after the field is turned off*. Lastly, this *adhesion can be reversed* by applying the same DC potential in the "reverse" orientation ($E^+T^-G^+E^-$). All these features are observed in every case of EA documented in this paper. In the literature, other instances of electrically triggered adhesion are described, but they either require much higher voltages, or an AC field, or the field may need to be applied over much longer times.[83,123-127] Moreover, in all these cases, the adhesion *does not persist* long after the field is removed.[128,129]

4.3.2 Gels Can be Electroadhered to Tissues from All Classes of Animals

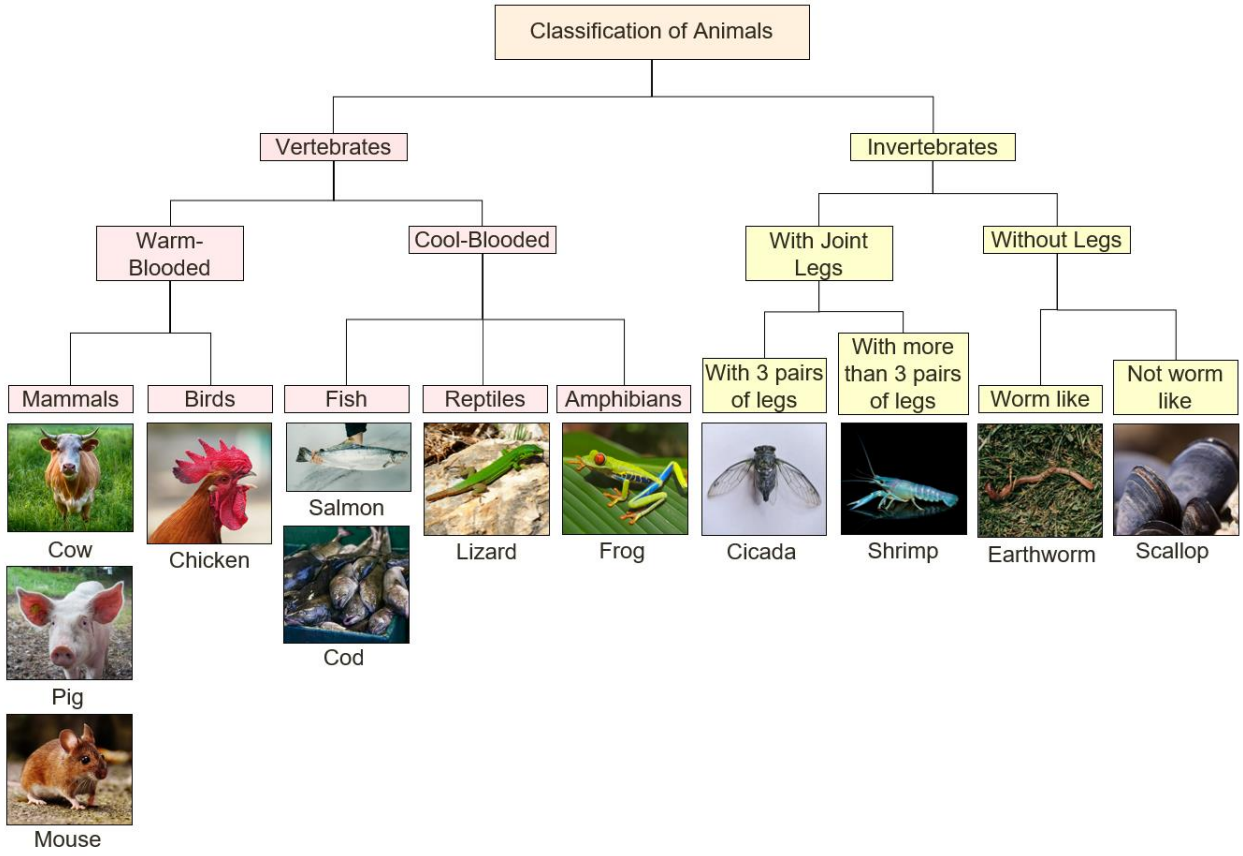

Figure 4.2. Animal species whose tissues can be adhered to gels by EA. QDM gels (G^+) can be adhered by EA to tissues from all the above animals, with each animal placed in its appropriate phylum and class. All EA experiments were done using 10 V DC applied for 30 s.

We now will discuss EA of cationic (G^+) gels to various animal tissues. In previous work, we had shown that these gels could be adhered by EA to bovine (cow) tissues. In the present work, we have tested tissues from animal species extending across the various phyla and classes. All the animals in Figure 4.2 show evidence of EA to at least one of their tissues, indicating that the phenomenon of gel-tissue adhesion is universal and extends across biology. Note that all animal tissues were sourced ethically (see Experimental Section for details). EA was done using the same conditions discussed under Figure 4.1: a DC field of 10 V was applied across the gel-tissue pair

for 30 s. The field was then switched off and the gel-tissue pair was assessed visually. If strong adhesion occurred, the pair could be held vertically as shown in Figure 4.1C and the materials would not fall off. Moreover, when adhesion was strong, attempts to dislodge the gel from the tissue using tweezers would be unsuccessful and the gel would break in the process. In selected cases, we also measured the strength of adhesion using pull-off testing. Thus, we confirmed that our visual assessments were consistent with specific cutoffs for adhesion strength (see below for discussion). We also confirmed that: (a) the adhesion induced by EA was much stronger than contact adhesion; and (b) the adhesion could be reversed by reversing the polarity of the field.

We now discuss the various animals in the chart (Figure 4.1). Among warm-blooded vertebrate animals,[96] we found EA to tissues of mammals (cow, pig, mouse) as well as birds (chicken) – these results are further classified by tissue type and discussed below. Among cold-blooded vertebrates, we found EA to tissues of fish (salmon and cod), amphibians (frog), and reptiles (lizard). EA also occurs with selected tissues in invertebrates that are land-based (insects like cicada and worms like earthworm) or aquatic (crustaceans like shrimp and mollusks like scallop). Note that in animals with a hard shell, the tissue tested for EA was from the soft interior. Conversely, in the case of frogs and earthworms alone, EA could be achieved to the outer skin of these animals. Lastly, it is worth noting that *every animal* we tested had a tissue to which EA could be done. There were no animals that proved an exception to this rule.

4.3.3 Gels Can be Electroadhered to Tissues from Plants and Fungi

In addition to the animal kingdom, tissues from other kingdoms, specifically plants and fungi, were also tested for EA. Successful EA of cationic (G^+) gels was accomplished with species

from both these kingdoms. The conditions were the same as for animals (10 V DC for 30-60 s). Figure 4.3 presents examples of gels adhered by EA to plant-based materials. The examples include root vegetables (carrot), leaf vegetables (lettuce), bulb vegetables (onion), vegetables and fruits that grow on vines (cucumber, grape), fruit that grow on trees (plums), and fruit from herbs (strawberries).

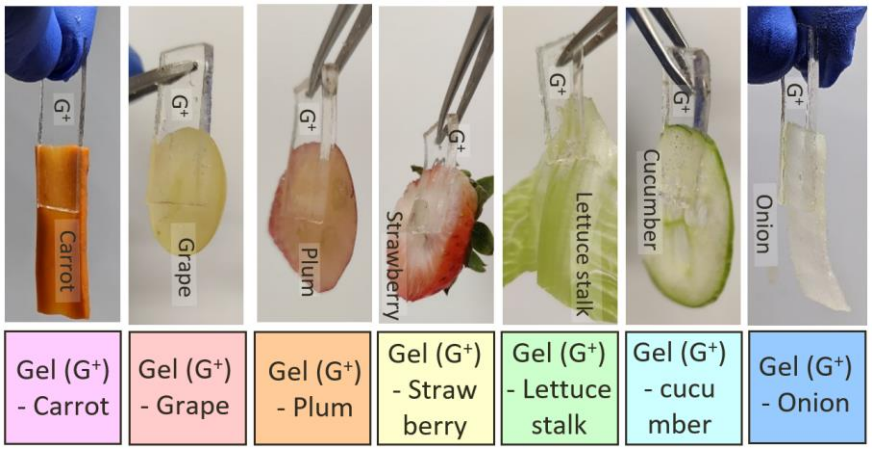

Figure 4.3. Plant tissues that can be adhered to gels by EA. Photos are shown of QDM gels (G^+) adhered by EA to various plant-based materials. All EA experiments were done using 10 V DC applied for 30 to 60 s.

Note from the photos in Figure 4.3 that the gel is adhered to the inner portion of the vegetable or fruit and not its outer skin (the skin is generally a hydrophobic layer).[130] In the case of lettuce, EA only occurred with the stalk and not the leaves. We did try EA to many plant leaves and also flower petals – with no success. Again, a hydrophobic coating is expected to be present on the surfaces of leaves or flowers. There was also no EA in the case of some fruit (pineapple, peach, melon) and vegetables (tomato, radish). Thus, unlike the case of animals, we do have several plant-based materials that are not amenable to EA, at least under the conditions studied

here. In addition to plants, we also tried fungi, i.e., common mushrooms. Gels could indeed by adhered by EA to mushrooms.

4.3.4 Electroadhesion Varies with Animal Tissue Type in a Fairly Consistent Way

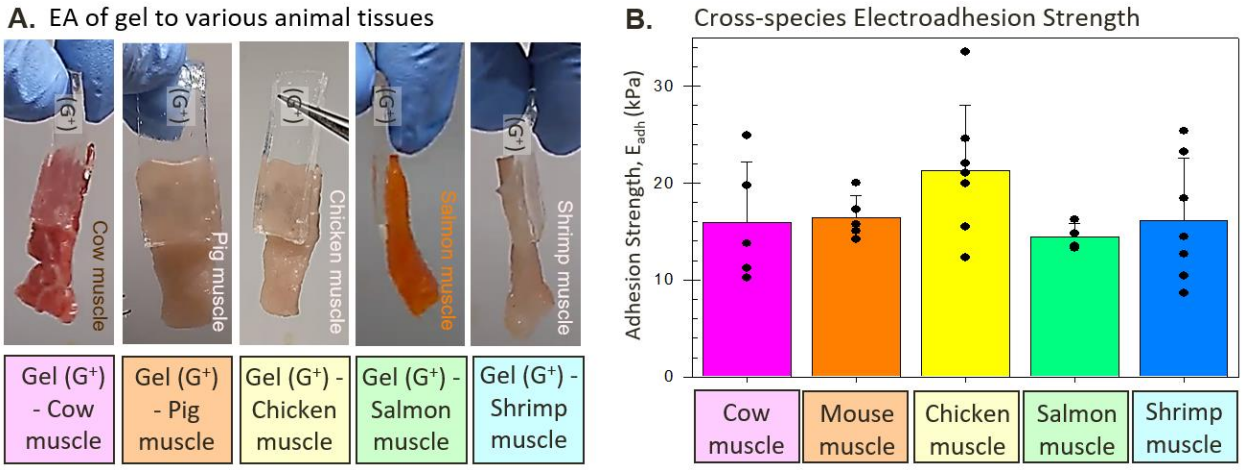

Figure 4.4. Comparison across species of EA to skeletal muscle tissues. (A) Photos of QDM gels (G^+) adhered by EA to skeletal muscle (transverse segments) from various animals. All EA experiments were done using 10 V DC applied for 30 s. (B) Adhesion strength E_{adh} from pull-off tests for the various pairs in (A). For each pair, $n \geq 5$ measurements were done, and the error bars correspond to the standard deviations.

We return to animals and compare results across a range of animals. One tissue type that exists in mammals, birds, fish, and even invertebrates like crustaceans is the muscle.[131] We adhered QDM gels to muscles from several species using EA under the typical conditions. The species tested included mammals (cow, pig/mouse), birds (chicken), fish (salmon), and crustaceans (shrimp). In all cases, the muscle chosen was a skeletal muscle and the segment selected was in the transverse orientation (this will become important later). All pairs show strong adhesion, which is evident from the photos in Figure 4.4A. This adhesion is further quantified using pull-off tests – the adhesion strength E_{adh} plotted in Figure 4.4B is the stress required to pull one sample off the other. The values of E_{adh} for the various gel-tissue pairs are all around 17 kPa. Thus, the data

confirm that gels can be strongly adhered to muscle tissue regardless of the species from which the muscle is taken. Also, in each of the above cases, we confirmed that the E_{adh} induced by EA was much higher than the E_{adh} for contact between gel and tissue. Wet materials often show weak adhesion on contact due to capillary forces arising from a thin layer of water between the surfaces.[132] From the literature, the strength of this contact adhesion is expected to be ~ 5 kPa.

E_{adh} > 16 kPa - Strong	
Artery (aorta)	(Cow, pig, chicken, mouse)
Cornea	(Cow
Trachea	(Chicken)
Dermis	(Mouse)
Fascia	(Mouse)
Skeletal Muscle (T)	(Cow, pig, mouse, chicken)
Tendon (T)	(Cow)
8 kPa < E_{adh} < 16 kPa - Moderate	
Intestine	(Chicken), (Mouse bowel - strong)
Cartilage	(Cow)
Skeletal Muscle (L)	(cow, mouse, chicken)
E_{adh} < 8 kPa - Weak or No-Adhesion	
Heart	(Cow, pig, mouse), (Chicken heart - moderate)
Lung	(Pig, mouse, chicken), (Cow lung - moderate)
Fat	(Cow, mouse, chicken)
Brain	(Cow, mouse, chicken)
Spleen	(Cow, mouse, chicken)
Liver	(Pig mouse, chicken)
Kidney	(Cow, mouse, chicken)
Tendon (L)	(Cow)

Table 4.1. Classification of tissues with regard to their ability to adhere to gels by EA. The classification is based on the adhesion strength E_{adh} of the tissues to QDM gels (G^+) following EA (10 V DC for 30 s). For each tissue type, the tissues were sourced from different animal species (three mammals and one bird), which are named in brackets. Outliers in each category are indicated separately.

Next, we turn our attention to tissue types relevant to mammals. We have been able to obtain various tissues from three mammalian (cow, pig, mouse) and one bird species (chicken). In

some cases, such as skeletal muscle and arteries, we have data from several animals. Thus, we can identify similarities across species, and this is shown in a semi-quantitative manner in Table 4.1. Here, tissues are divided into three categories based on their adhesion to gels induced by EA. Tissues that exhibit *strong adhesion* to gels have adhesion strengths E_{adh} (from pull-off tests) > 16 kPa. On the other extreme, tissues with *weak or no adhesion* have E_{adh} < 8 kPa; note that these values are indistinguishable from contact adhesion. Between these two extremes, we have the category of moderate adhesion (8 kPa < E_{adh} < 16 kPa).

Table 4.1 shows several tissues that exhibit strong adhesion due to EA. These include arteries (aorta) and skeletal muscle (transverse segments) which we were able to access from all four animals under study. Strong adhesion to tendons and cornea from cows was previously reported in our earlier paper. Some other tissues such as trachea and fascia show strong adhesion, but we have data only for one animal. In the case of intestines, we found moderate adhesion in the case of chicken intestines, but strong adhesion in the case of intestines from mice. In the category of weak/no adhesion, we have several tissues that show consistent trends, including adipose (fat), brain, spleen, liver, and kidney. Heart and lung are inconsistent across species. For example, adhesion to cow and pig hearts was weak, but adhesion to mouse and chicken hearts was moderate.

Another way to show the patterns existing across animal species is presented in Figure 4.5. Here we refer to both the strong and moderate cases as “adhesion” (green), whereas the other cases are marked as “weak or no adhesion” (in red). Moreover, we show only those tissues for which we have multiple data points across species. Patterns emerge showing adhesion in some tissues (e.g., arteries, muscles, intestines) and no adhesion in others (brain, adipose, spleen).

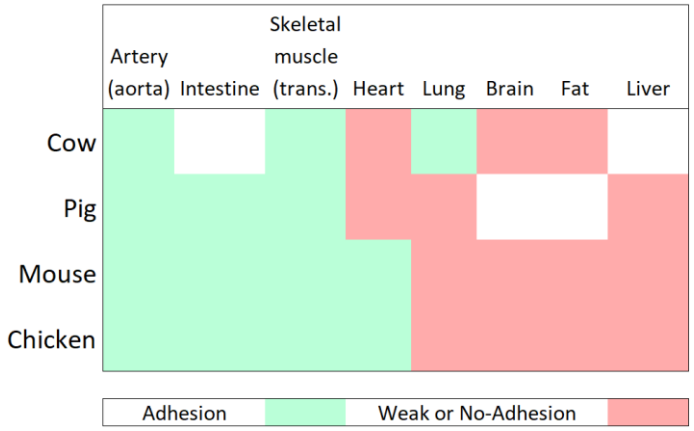

Figure 4.5. Cross-species similarities in EA across cow, pig, mouse and chicken tissues. For each tissue from a given animal, the result is classified as adhesion (in green) if the EA is strong or moderate (as per Table 4.1) and no adhesion (in red) for the other cases.

4.3.6 Anionic Biopolymers in Tissues Hold the Key to Electroadhesion

Why do some tissues show EA to gels while others do not? This is a complex question, but as a first step to understanding these differences, we must discuss the microstructure of biological tissues. All living creatures are composed of cells, but in higher organisms such as animals and plants, cells (microscale containers) are collected and organized into tissues,[96] i.e., into soft, macroscale solids with dimensional stability. In terms of structure, we can classify tissues into two kinds, and we show schematics for each kind in Figure 4.6: (1) Cells along with a polymer matrix (Figure 4.6A, B); and (2) Cells close-packed and connected into a solid, with very little external matrix (Figure 4.6C, D).[85,86]

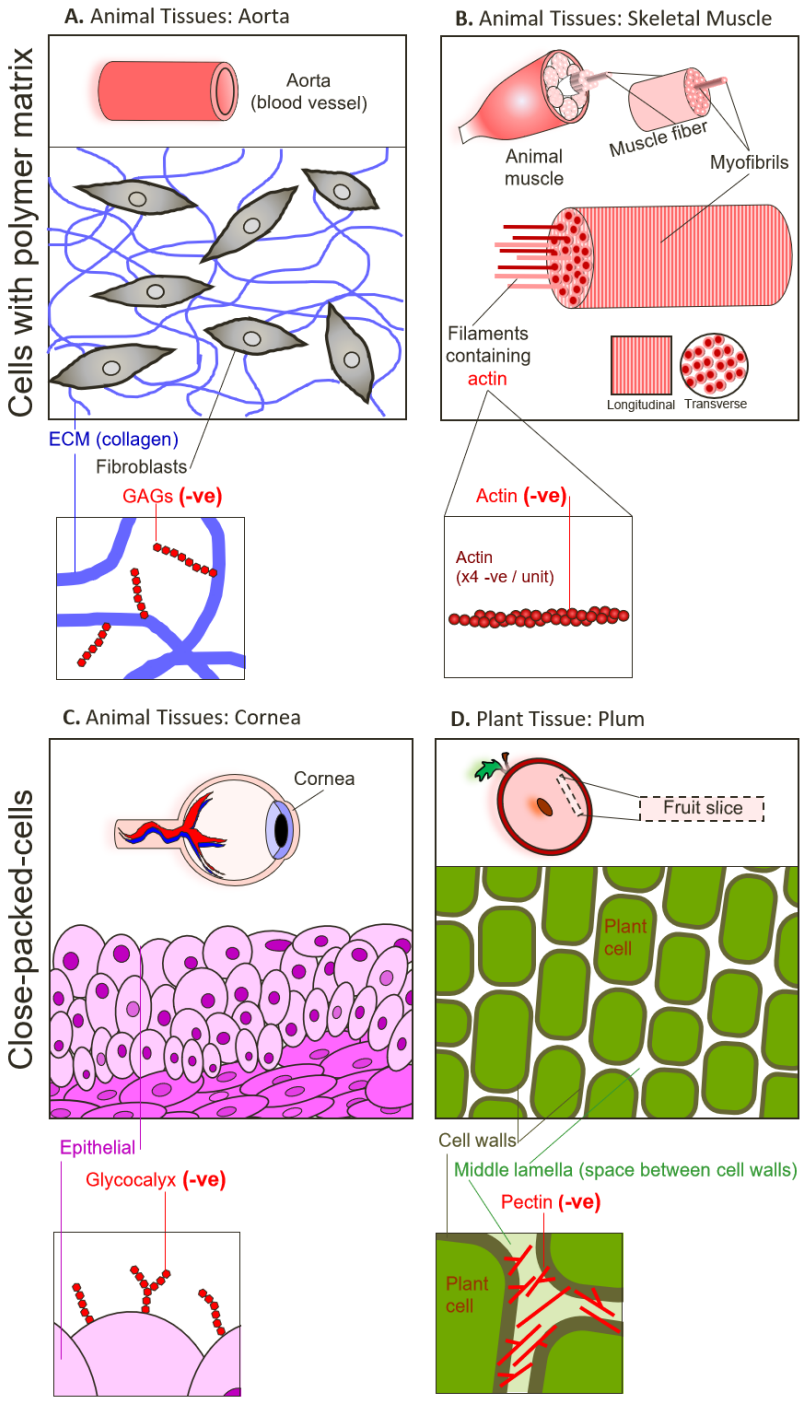

Figure 4.6. Structures of animal and plant tissues to which EA of gels is observed. In all cases, anionic biopolymers in the tissue are expected to underlie the EA. (A) The aorta has cells embedded in an ECM, which has anionic GAGs. (B) Muscles are composed of fiber bundles, made of the anionic protein actin. A transverse cut through the muscle exposes fiber ends, which are absent in a longitudinal cut. (C) The cornea has close-packed epithelial cells that each have an anionic outer layer (glycocalyx). (D) Plant tissues are made of close-packed cells attached at their cell walls, which have the anionic polysaccharide pectin.

In the first category of tissue, an example is the aorta (Figure 4.6A). This is a connective tissue in which the outer layer (tunica externa) consists of cells (fibroblasts) embedded in an extracellular matrix (ECM).[133] The ECM is a fibrous mesh akin to the polymer network in a hydrogel like QDM. It is formed by collagen fibers, which are associated with anionic polymers called glycosaminoglycans (GAGs) (see inset to the figure).[101,113] In the case of muscle (Figure 4.6B), instead of a random mesh, fibers are arranged in aligned bundles, and these are formed from the proteins actin and myosin.[134] Note that actin is anionic. The figure also points out that a transverse cut of the muscle exposes fiber ends whereas a longitudinal cut is parallel to the fibers.[134] This will become important in discussing the results in Figure 4.7.

In the second category of tissues (formed by close-packed-cells), the first example is the cornea (Figure 4.6C). This has an outer layer of epithelial cells, with each cell membrane having an outer glycocalyx.[135,136] The glycocalyx (see inset) is a thin layer of anionic glycoproteins and glycolipids.[137] In the case of plant tissue (Figure 4.6D), such as fruit like plums or strawberries, the cells each have a cell wall, formed by polysaccharides like cellulose and pectin.[138,139] In particular, pectin is an anionic polysaccharide and in the cell wall it is often complexed with calcium (Ca^{2+}) ions.[140] To summarize, in both the common types of structures that underlie tissues, anionic biopolymers (proteins, glycoproteins, or polysaccharides) are likely to be present. The density of anionic charge is likely to be the first key factor in explaining the differences in EA across tissues. That is, we hypothesize that strong adhesion arises when a high density of anionic polymers is exposed at the tissue surface (i.e., at the interface with the gel). Conversely, a low density of such polymers at the surface may explain the weak to no adhesion observed with other tissues.

4.3.7 For a Given Tissue Type, Electroadhesion May Vary with Tissue Orientation

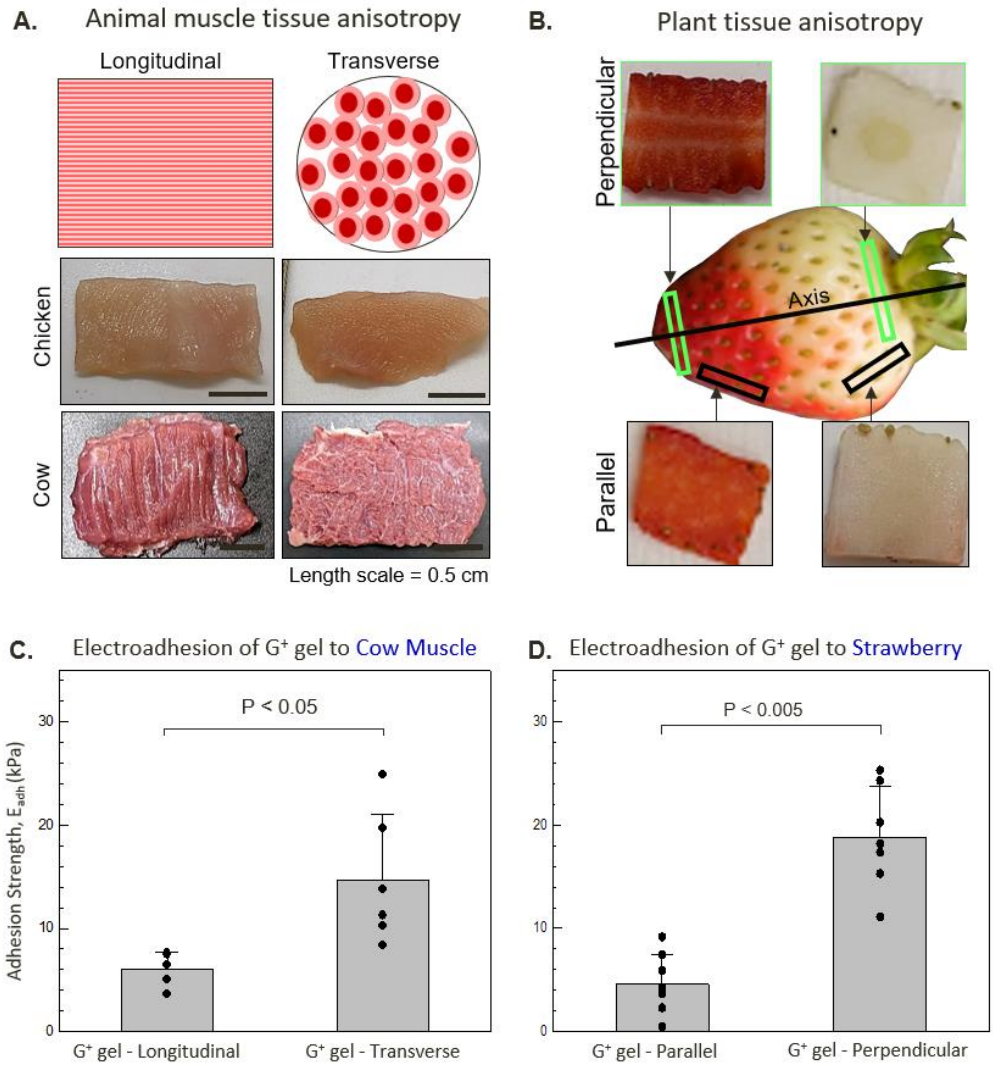

Figure 4.7. Tissue anisotropy and its effects on adhesion to gels by EA. (A) In the case of animal muscle, a transverse cut through the muscle exposes fiber ends, which are absent in a longitudinal cut. The differences between the two can be seen even at the macroscale in the cases of cow and chicken muscle. (B) In the case of plant tissues (strawberry), slices perpendicular to the axis of the fruit (marked in green), are distinct from slices parallel to the axis (marked in black). (C) Muscle tissues are adhered to QDM gels (G^+) by EA (10 V, 30 s) and compared: the adhesion strength E_{adh} is much higher for the transverse segments. (D) Strawberry tissues are likewise adhered by EA to QDM gels and E_{adh} is much higher for the perpendicular slices.

As briefly mentioned earlier under Table 4.1, the EA results for gel-muscle adhesion are markedly different for transverse or longitudinal segments. We believe these differences are related to the anisotropy of muscle tissues, which was indicated in Figure 4.6B. Figure 4.7

discusses tissue anisotropy in more detail, and we see its effects in both animal and plant tissues. In the case of animal muscle, the differences between the longitudinal and transverse orientations can be seen in both cow and chicken muscle at the macroscale (Figure 4.7A). The longitudinal slice is cut parallel to the fiber bundles whereas the transverse segment is cut perpendicular to the bundles, thereby exposing the fiber tips.[141,142] These segments are adhered to QDM gels (G^+) by EA (10 V, 30 s) and compared using pull-off tests. Figure 4.7C shows that the adhesion strength E_{adh} is ~ 15 kPa in the case of the transverse segments, which is much higher than the E_{adh} of ~ 6 kPa for the longitudinal segments. We believe this is because, in the transverse segments, due to the exposed fiber tips, a higher density of anionic proteins (i.e., actin) are available at the interface with the gel.

Anisotropy in plant tissues is illustrated in Figure 4.7B in the case of a strawberry. A slice of strawberry can be cut either perpendicular to its axis (green rectangles) or roughly parallel to its axis (black rectangles). Adhesion tests to QDM gels (G^+) by EA show that the former exhibit much higher E_{adh} (~ 20 kPa) than the latter (~ 4 kPa) (Figure 4.7D). These differences are quite surprising – and it does not matter if the strawberry is ripe (red colored) or raw (white colored), as can be seen from Figure 4.7B. But in fact, the anisotropy of plant tissues has a known origin. For plant tissues to grow, the cell wall has to disintegrate,[143] and the anionic pectin in the cell wall is the key for this. Cell growth occurs typically in one direction by an enzymatic process that converts the carboxylate in pectin to an ester. The esterified pectin loses its charge and thus cannot crosslink with Ca^{2+}; in turn, the cell wall is weakened and the tissue grows in that direction.[143] In other words, plant tissues will typically have a high fraction of anionic pectin in one orientation whereas in the perpendicular orientation, there will be a high fraction of esterified pectin (nonionic). Thus,

the two orientations of the strawberry that we examined may correspond to different extents of anionic polymers, much like in the case of animal muscle.

4.3.8 Electroadhesion is Observed with both Soft and Stiff Tissues

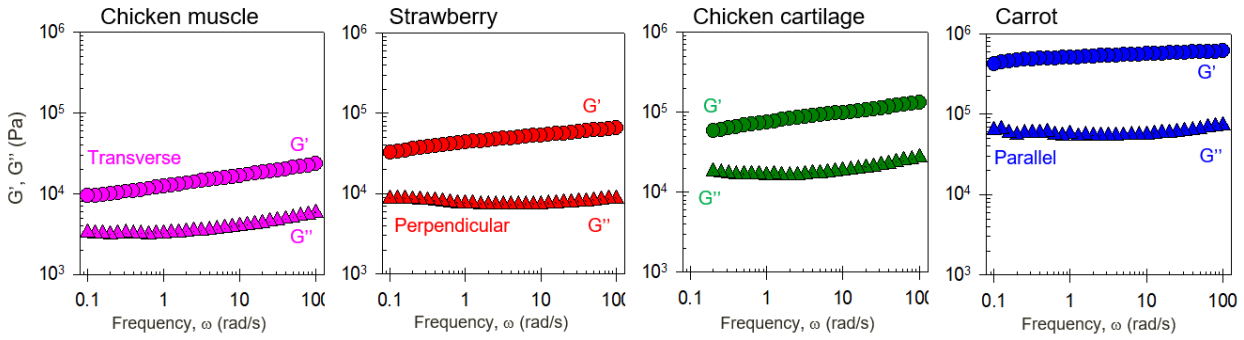

Figure 4.8. Rheology of selected animal and plant tissues that can be adhered by EA to gels. Plots of the elastic (G') and viscous (G'') moduli as functions of angular frequency ω are shown for (A) chicken muscle; (B) strawberry; (C) chicken cartilage; and (D) carrot. All these tissues show strong adhesion by EA to QDM gels (G^+).

Having found EA to many animal and plant tissues, we wondered if there were any systematic trends in the rheology of the tissues. Figure 4.8 shows the dynamic rheology of four different tissues, two from animals (chicken) and two from plants, arranged in order from soft to stiff. The plots are of the elastic (G') and viscous (G'') moduli as functions of angular frequency ω. All tissues exhibit a mostly elastic response, as expected, with $G' > G''$ over the range of ω. The value of the elastic modulus G' (at a fixed frequency around 0.1 rad/s) is a convenient measure of the tissue stiffness. From the data, G' is ~ 9 kPa for chicken muscle; 34 kPa for a slice of strawberry; 58 kPa for chicken cartilage; and 420 kPa for a slice of carrot. Thus, the stiffness varies by 50-fold across this range of tissues. All the tissues in Figure 4.8 exhibit strong adhesion by EA to QDM gels (G^+), with the adhesion strength E_{adh} exceeding 16 kPa. This means that strong EA

is possible to both relatively soft tissues ($G' < 10$ kPa) as well as to rather stiff tissues ($G' > 400$ kPa).

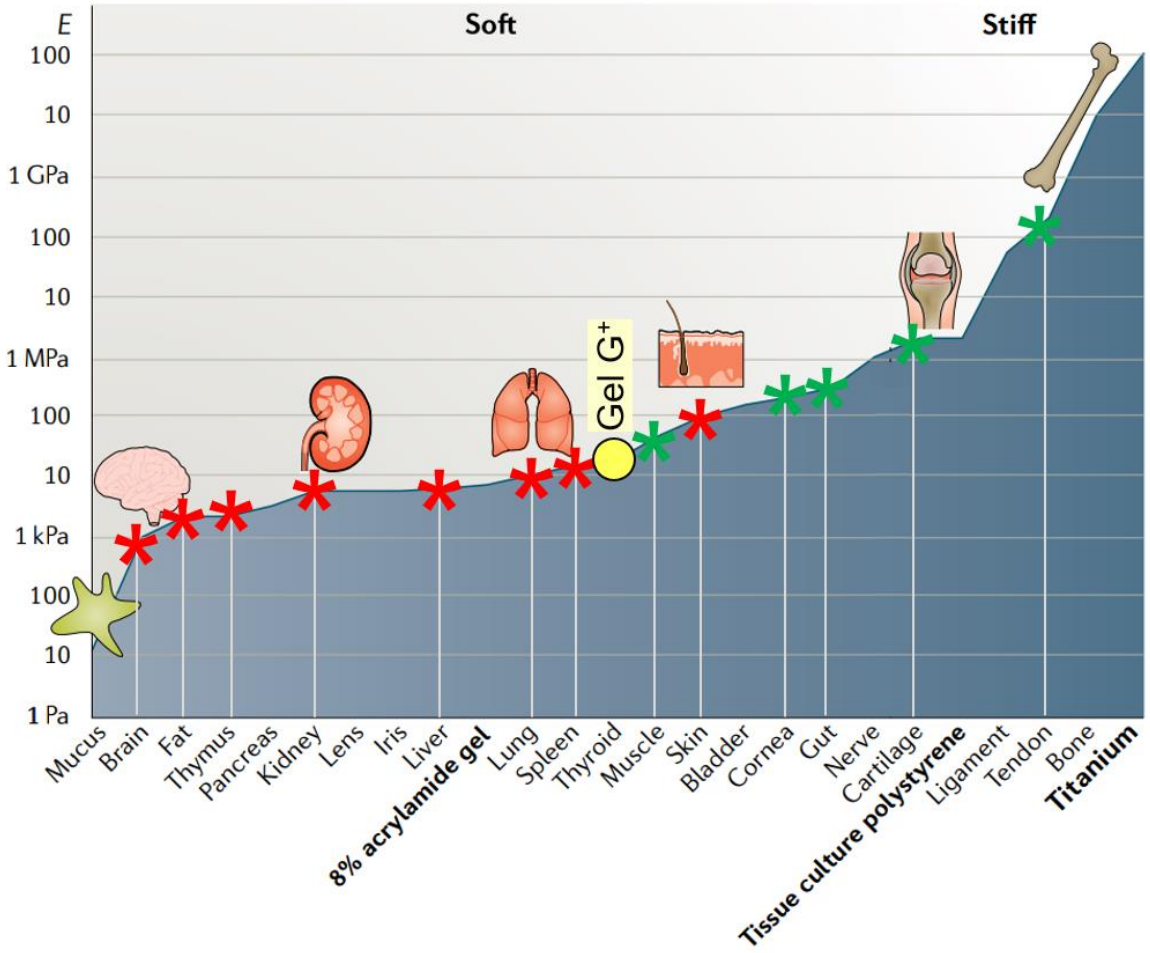

Figure 4.9. Stiffness of various tissues correlated with their ability to undergo EA to gels. A schematic plot of the elastic modulus (E) for different tissues is shown (adapted from Guimaraes)[119]. On this plot, data from Figure 4.5 for the success (green symbols) or failure (red symbols) of EA to QDM gels (G^+) is marked. A trend is seen where EA preferentially occurs to the stiffer tissues on this plot.

A further pattern regarding tissue rheology is shown by Figure 4.9. Here, we present a schematic plot first introduced by Guimaraes et al.[119] that shows the typical stiffness of various tissues in the body. On this plot, we have superposed our EA results from Figure 4.5 regarding the

observation of adhesion (green) or no adhesion (red) of QDM gels (G^+). The pattern that jumps out is that EA preferentially occurs with stiffer tissues. All the soft tissues we tested (such as the brain, fat, and kidney) showed weak or no adhesion. It is unlikely that tissue mechanics is the sole reason why these soft tissues gave no EA. For example, both brain and fat tissues have a high fraction of nonpolar substances and correspondingly a low content of water.[104] It is also unclear if these tissues have a significant fraction of anionic polymers in them. More work is required to answer these questions definitively.

4.4 Conclusions

In this chapter we described the phenomena of EA to go far beyond adhesion to bovine tissues. We have found EA of a cationic gel to tissues of various animals, including mammals (e.g., cow, pig, mouse); birds (e.g., chicken); fish (e.g., salmon, cod); reptiles (e.g., lizard), amphibian (e.g., from), as well as various invertebrates (e.g., shrimp, worms). In addition, gels can also be adhered to plant tissue, including fruits (e.g., plums) and vegetables (e.g.; carrot), and also to fungi (mushrooms). The results from our study are promising because they suggest that EA has wide applicability to biological materials, including potentially to human tissues.

In mammals, EA is strong for certain tissue types, such as arteries, intestines, and cornea across a range of species. Conversely, weak or no adhesion is observed with other mammalian tissues such as adipose and brain. These differences reveal some common themes in regard to EA: for instance, the higher the fraction of anionic polymers (proteins and/or polysaccharides) in the biological material, the higher the EA strength.

Interestingly also, because tissues often have anisotropic structure, adhesion by EA can be strong in one tissue orientation, but weak or non-existent in the perpendicular one. We see evidence for EA adhesion differences in both animal and plant tissues. Last, we see that EA occurs in soft and hard materials in animal and plant tissues. Further studies need to be done to fully understand why some tissues experience EA and others do not; is it abondance of anionic polymer, tissue orientation or other factors?

Chapter 5

Mechanism for Electroadhesion

5.1 Introduction

In this Chapter, we discuss the mechanism for the electroadhesion (EA) described in Chapters 3 and 4. We have previously shown that two soft materials of opposite charge can be induced to adhere permanently by applying a DC electric field of low voltage (~ 10 V) for a short time (10 to 20 s).[18,19] Typically, one of the two materials is a cationic hydrogel (denoted by G^+). The other can be an anionic hydrogel (G^-) or anionic tissue from animals (T^-) or plants (P^-). Importantly, after the field is removed, the material pair remains adhered permanently.[18,19] Due to these features, EA could be potentially useful in the surgical repair of tissues. Because the same features of EA arise in pairs of gel/gel (G^+/G^-), gel/animal tissue (G^+/T^-) and gel/plant tissue (G^+/P^-), a common mechanism is expected to underlie all these systems, and we will attempt to decipher it. A deeper understanding of the EA mechanism will be particularly useful in optimizing the use of EA in surgical repair.

The term electroadhesion was originally used by Johnsen and Rahbek (JR) back in 1923 to describe a different kind of electrically induced adhesion.[144] The JR effect refers to adhesion between a metal and a semiconductor when a DC field (~ 440 V) is applied across the pair in contact.[144] The applied field polarizes the atoms at the interface, leading to an electrostatic attraction between the two solids. However, when the field is switched off, within seconds, the JR adhesion is eliminated, and the solids can be detached.[83,125,127,145-148] In recent studies, JR adhesion

has been extended to gel-like soft materials. Meyer et al. dried two anionic gels until their water content was reduced to ~ 10%. These dried gels were placed in contact and 500 V DC was applied, whereupon the materials adhered while in the field, but detached when the field was turned off.[129] Hayward et al. studied ionoelastomers, which are elastomeric (rubber-like) polymers with charged backbones, with the material itself being free of water. They sandwiched a cationic and an anionic ionoelastomer and applied a DC field of just 1 V. An adhesion developed instantly between the materials, but when the field was switched off, the adhesion ceased.[128]

Electroadhesion as it applies in our context was first discovered by Asoh and Kikuchi in 2010.[18] They showed that cationic and anionic hydrogels developed a strong adhesion when exposed to ~ 10 V DC for 10–20 s. This adhesion could also be reversed by applying the DC field with opposite polarity. In their original studies, the gels both had free ionic polymer chains (i.e., chains that were not crosslinked to the gel network). The authors hypothesized that the field induced *electrophoresis* of the free chains across the gel/gel interface (i.e., the cationic chains would migrate into the anionic side, and the anionic chains into the cationic side). Hence, they termed the ensuing adhesion as electrophoretic adhesion (EPA).[18,20-22,84] Under this hypothesis, the cationic and anionic chains would interpenetrate over an interfacial (nanoscale) zone, and the strong electrostatic bonds between the polyion complexes in this zone could explain why the adhesion persisted long after the field is removed.

Subsequently, Velev and co-workers showed that free ionic chains in the gels were not necessary for the field-induced adhesion. Instead, the cationic gel could simply be a crosslinked network of cationic chains and likewise the anionic gel a network of chains with anionic

backbones.[23] If so, when a DC field is applied, the only migration possible would be of chain *segments* between crosslinks in each gel. Still, strong and persistent adhesion between the gels is achieved after the field is removed. The gels investigated in our paper (G^+ and G^-) all have ionic backbones similar to those of Velev. Moreover, our recent studies have extended the range of adherent systems from gel/gel pairs (G^+/G^-) to gel/tissue pairs (G^+/T^- and G^+/P^-). Does electrophoresis of chain segments across the interface occur in *all* these systems? Is the interpenetration of cationic and anionic chains the key to why the adhesion persists after the field is removed? These are some of the questions we address in this Chapter. We will continue to use the more general term electroadhesion (EA) for the observed behavior rather than presuppose the need for electrophoresis.

In this Chapter, we will report a series of experiments on EA between cationic and anionic soft materials, including G^+/G^-, G^+/T^- and G^+/P^- systems. First, we will identify the essential hallmarks of EA in all these systems, including the key factors that increase or decrease adhesion strength. Thereafter, we will describe new experiments that yield insight into the adhesion mechanism. Specifically, when we apply a higher DC voltage (~ 90 V) across a gel/gel pair for just a few seconds, the gels "spring" into an adhesive state almost instantly, and this adhesion persists indefinitely after the field is removed. We refer to this phenomenon as "zipping" because the closure of the gel-gel interface mimics the closing of a zipper. The zipping experiments suggest that EA begins due to electrostatic attractions between polarized molecules on either side of the interface. Once they adhere, the materials remain pinned to each other, which may be *via* a combination of interfacial events as well as the interpenetration/entangling of charged polymers across the interface. Thus, our final mechanistic picture clarifies how the EA we observe is both

similar and distinct from the JR effect. In JR, materials get polarized by the field and hence adhere electrostatically, but there is no pinning, and therefore the adhesion dissipates as soon as the field is turned off. To distinguish the EA effect in G^+/G^-, G^+/T^- and G^+/P^- systems, we suggest naming it as EA_{RAPID}, where RAPID stands for Robust Adhesion Permanently Induced by a DC field.

5.2 Experimental Section

Materials. The following chemicals were from Sigma-Aldrich: the monomers acrylamide (AAm) and N,N′-methylenebis(acrylamide) (BIS), the initiator ammonium persulfate (APS), the monomer sodium acrylate (SA), the dye methylene blue (MB^+) and the dye orange (II) sodium salt (O_{II}^-). The accelerant N,N,N′,N′-tetramethylethylene-diamine (TEMED) was from TCI America. The monomer N,N′-dimethylaminoethyl meth-acrylate, quaternary ammonium salt (QDM) was from MPD Chemicals. Cyanoacrylate-based glues (Krazy Glue) and Rust-Oleum hydrophobic coating were purchased from The Home Depot. Deionized (DI) water was used in all experiments.

Synthesis of QDM gels. Cationic QDM gels were prepared using a modified protocol from our previous publication.[19] First, DI water was degassed by bubbling nitrogen gas for 20 min. For synthesis of regular QDM gel (Reg QDM) the following were combined: 1 M (1.4 g) AAm, 0.16 M (809 μL) of QDM solution, 0.019 M (0.06 g) BIS, 0.0088 M (0.04 g) APS and 0.01 M (30 μL) TEMED in 20 mL of degassed DI water. For the increased and decreased monomer gels and for increased and decreased charge gels we used a similar procedure as above, however we changed to the amounts of AAm, QDM and BIS added. The various compositions are provided in Table 1. For QDM gels with change in monomer concentration, we kept both the ratio of QDM/AAm (16.4%) and the ratio of BIS/monomer (1.7%) constant. For the gels with change to charge

(increase or decrease QDM), we kept the overall monomer concentration (1.15 moles) constant. To assist with easy removal of the gels, Petri dishes used in gel preparation were coated with a spray of Rust-Oleum hydrophobic coating, then allowed to sit for 1 min, and thereafter wiped dry. The above monomer mixture was poured into a pre-coated Petri dish and maintained in a nitrogen environment for 1.5 h, whereupon the gel became fully polymerized. After polymerization, gels were stored in a fridge and typically used within 24 h of preparation.

Quantities used (unit):	Reg QDM	Increased monomer by 50% *	Decreased monomer by 50% *	Increased charge by 50% **	Decreased charge by 50% **
Aam (g)	1.4	2.1	0.7	1.29	1.51
QDM (µL)	808	1004	335	1004	335
BIS (g)	0.06	0.09	0.03	0.06	0.06
APS (g)	0.04	0.04	0.04	0.04	0.04
TEMED (µL)	30	30	30	30	30

* Ratio of (QDM/Aam) = const, ratio of (monomer/BIS) = const

** Overall monomer concentration = same as Reg QDM

Table 5.1. Chemical compositions of various QDM gels

Synthesis of SA gels. Anionic SA gels were prepared by a similar procedure as described above for QDM gels.[19] In this case, the monomer solution contained 1.4 M (2 g) AAm, 0.11 M (0.2 g) SA, 0.019 M (0.06 g) BIS, 0.0088M (0.04 g) APS and 0.01 M (30 µL) TEMED in 20 mL of degassed DI water. The above solution was poured into a pre-coated Petri dish and maintained in a nitrogen environment for 2 h. After polymerization, gels were stored in a fridge and typically used within 24 h of preparation. We refer to this gel as SA or Reg SA.

Tissue Preparation Protocol. All tissues were obtained ethically, immediately after slaughter from a local butcher or farm. All experiments on tissues were conducted within 24 h of tissue

harvest. When the tissues were first received, organs were typically encased in fat and other matrix material. For example, the salmon muscle in Figure 5.1 was covered in skin and an epithelial layer. Thus, for experiments with muscle, it had to be harvested and cleaned from the surrounding parts. The harvested muscle was then further segmented into smaller pieces for the electroadhesion experiments, with the focus on cutting segment of tissue muscle without an epithelial layer.

Adhesion Experiments. A DC power source (Agilent, model E3612A) with a range of 0–60 V, 0–0.5 A was used for the electroadhesion experiments. The voltage was set to 10 V for all experiments, unless otherwise indicated. Depending on the pair of material adhered (gel-gel, gel-animal tissue, or gel-plant tissue) a different time in the electric field was required. For gel-gel and gel-animal tissue pairs we kept the pair in the field for 30 s, for gel-plant tissue pairs - 60 s. EA orientation was always ($E^+G^+M^-E^-$), meaning the cationic gel (G^+) was placed in contact with the positive electrode (E^+), while the anionic material (M^-): gel (G^-), animal tissue (T^-) or plant tissue (P^-) was placed in contact with the negative electrode (E^-). For reversal of adhesion the electrode and materials orientation were always ($E^+ M^-G^+E^-$).

Pull-off Testing. In both gel-gel and gel-tissue testing, pull-apart adhesion testing was performed on a TA Instruments DMA Q800. Gel-gel samples were prepared with dimensions of 0.7 x 1.3 x 0.6 cm (each gel is 0.3 cm in thickness). The gel-gel and gel-tissue pairs were either electroadhered or brought together by contact. These pair were superglued to the clamps of the dynamic mechanical analyzer. Contact adhesion control samples were compressed at 1 N for 1 min, and following this compression period, pulled apart via a controlled force ramp at a rate of 0.1 N/min until failure. Electroadhered samples were run as-is with a controlled force ramp at a rate of 0.1

N/min until failure. Stress at failure was recorded. Each sample was replicated 5 times (n = 5). In the gel-tissue samples, the tissue layer was secured to the top (fixed) clamp and the gel layer to the bottom (movable) clamp. Contact and EA samples were run under same conditions as the gel-gel samples.

Rheological Studies. Rheological experiments reported in Figure 5.4A were conducted using an AR2000 stress-controlled rheometer (TA Instruments) at 25°C, set to 0.1% strain. A flat plate geometry (20 mm diameter) was used to perform steady-shear rheology on gels of various BIS concentration.

Swelling and Drying. Samples for swelling experiments were obtained from the SA and Reg QDM gels. Samples were segmented to slices of 1.3 x 0.7 x 0.3 cm. There were then each weighed following segmenting. The samples were incubated in DI for various timepoints: 2.5, 5, 10, 20, and 40 mins, 1.5 and 3 h. Following these timepoints, the samples were reweighed. An SA and QDM sample were then electroadhered in a 10 V DC field for 30 s. Sets of n = 5 per group were tested in pull-off and volume expansion, V_e was calculated. $V_e = V_f / V_i$. Samples for drying were prepared in a similar manner, however instead of swelling in DI water, the samples were placed uncovered on a benchtop and dried in ambient conditions for the following timepoints: 0.5, 1.5, 5, 11, 24 and 36 h. Samples were prepared in sets of n = 5 for pull-off testing, and similarly to the above, the samples weights were recorded before and after the various drying points. Volume loss, V_l was calculated. $V_l = V_f / V_i$

Dye Diffusion. SA and QDM gels were prepared per instruction above, but the volume and composition was multiplied x3. This resulted in gels with thickness of 0.8 – 1 cm depending on the diameter of the petri dish. Gel samples were cut out with dimensions of 2 x 2 cm. A concentrated dye solution of ~ 0.01M dye was prepared from MB^+ and O_{II}^- separately. A drop of the dye solution was dropped into a petri dish and a slice of gel was placed on top of the dye for 15 s. MB^+ (+ve charge) was used to dye SA, while O_{II}^- (-ve) was used to dye QDM. Following the dyeing, gel was removed from the dye solution and its peripheries were cut off, resulting in a thin layer of dye (counter-ion surrogates) of ~ 1 mm at the bottom of the gel. The SA and QDM gels were brought together with the dye layers at the interface between the gels. They were monitored for diffusion or placed into an electric field of 20V for observation of counter-ion mobility. Results are presented in Figure 5.6.

Zipping Experiments. Studies to observe electrostatic attraction between two materials were conducted. Gel samples were cut into segments of 0.5 x 3 x 0.3 mm, and carrot samples were sliced into segments of 0.5 x 3 x 0.08 cm. The samples were each placed on top of the graphite electrodes at the EA orientation. Voltage was turned on and set to 90V DC for gel-gel and 50V for gel-carrot. A single tip of the two materials was brought together. The samples' response were recorded using a Dino-Lite Digital Microscope Premier. All material responses were recorded.

5.3 Results and Discussion

5.3.1 Electroadhesion and its Hallmarks

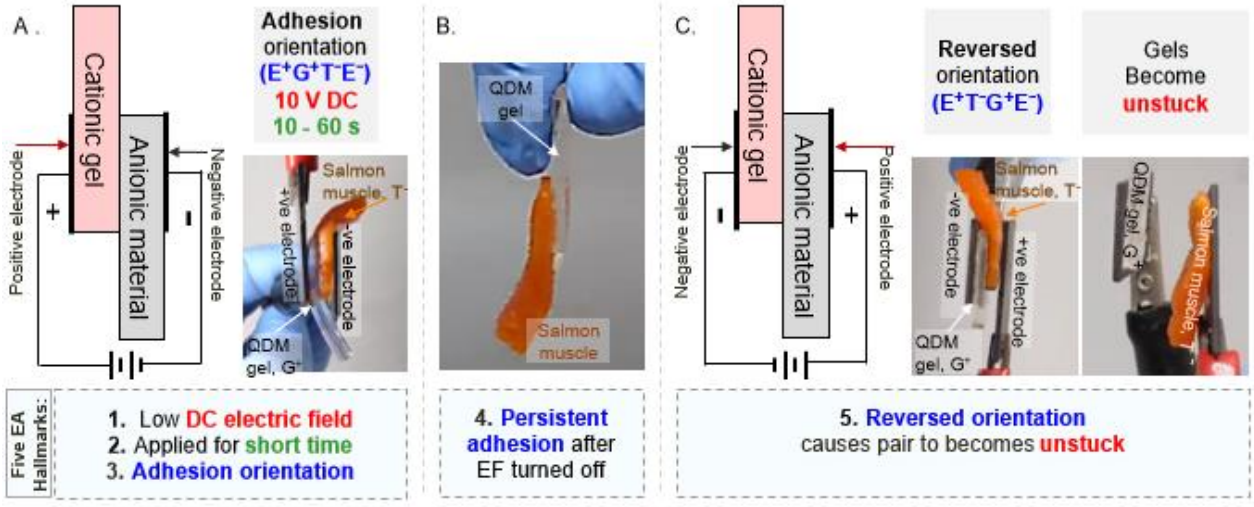

Figure 5.1. The hallmarks of electroadhesion (EA). EA arises between cationic and anionic soft materials. The examples shown here are a cationic gel (QDM) and a segment of anionic tissue (muscle from salmon). (A) Gel (G^+) is placed in contact with the positive electrode (E^+) and the tissue (T^-) in contact with the negative electrode (E^-). A low DC electric field (10 V) is turned on for 30 s in the $E^+G^+T^-E^-$ EA orientation. The low DC field is the first hallmark, a short time is the field is the second hallmark and the EA orientation is the third hallmark. (B) Upon removal from the field, the gel and tissue are found to be strongly adhered, and this adhesion persists indefinitely. Persistent adhesion after removal from the field is Hallmark 4. (C) The adhered pair is placed in the same DC field with the orientation reversed ($E^+T^-G^+E^-$) and the field is switched on for 60 s. Upon removal from the field, the materials have lost their adhesion and can be detached. The reversibility of the adhesion is Hallmark 5.

In the context of this Chapter, electroadhesion (EA) between two soft materials has the set of hallmarks outlined in Figure 5.1. In a pair of materials that undergo EA, one has to be cationic in nature, while the other has to be anionic.[18,19] In our experiments, the cationic material is fixed to be a hydrogel denoted as QDM. This gel is made by free-radical polymerization of a mixture containing the cationic monomer quaternized dimethylaminoethyl methacrylate (QDM). The QDM gel (G^+) is a transparent soft solid that can be held between one's fingers (Figure 5.1B). We

have shown that QDM gels can be electroadhered to a variety of anionic materials, including anionic gels and tissues.[19] The anionic gel used in most studies is made by polymerizing the anionic monomer sodium acrylate (SA) and is denoted as an SA gel (G^-). In Figure 5.1A, an animal tissue (T^-), i.e., salmon muscle, is chosen as an example of an anionic material, and this exhibits a vivid orange color.

First the gel and tissue are placed in contact and are shown to not adhere. This lack of contact adhesion is important because it emphasizes that the subsequent EA arises due to the electric field. Next, we connect the gel and tissue to a DC power source in the *adhesion orientation* (Figure 5.1A). In this orientation, the gel (G^+) contacts the positive electrode (E^+) and the tissue (T^-), the negative electrode (E^-). We apply a low DC voltage *(*Hallmark 1, typically 10 V) for a short time (Hallmark 2, 10 to 60 s), while in this $E^+G^+T^-E^-$ orientation (Hallmark 3). During this time, the gel and tissue develop a strong adhesion, i.e., EA. The field is then turned off and the pair are found to remain adhered (Figure 5.1B) – indeed, the EA persists indefinitely thereafter (Hallmark 4). Next, we show that the adhesion is reversible (Hallmark 5). The adhered gel-tissue pair is placed back in the DC electric field, but the orientation is reversed (Figure 5.1C): the gel (G^+) now contacts the negative electrode (E^-) and the tissue (T^-) the positive electrode (E^+). While in this $E^+T^-G^+E^-$ orientation, we apply the same 10 V DC again for a short time (10 to 60 s). When the field is turned off, the pair are found to have lost their adhesion and can be easily detached.

To summarize, the hallmarks of EA are the following:

(1) Adhesion induced by a **low DC electric field** (~ 10 V potential; field strength of ~ 2 V/mm).

(2) Adhesion induced by applying the field for a **short time** (~ 10 to 60 s).

(3) Adhesion induced by applying field in the **"adhesion" orientation** of electrodes ($E^+G^+T^-E^-$).

(4) Adhesion **persists after the field is turned off** (~ "permanent").

(5) Adhesion **reversed** by applying field in the "**reverse" orientation** of electrodes ($E^+T^-G^+E^-$).

Regarding the permanence of EA, we should note the following observations in the case of gel/gel (G^+/G^-) pairs. The adhesive strength of QDM/SA gels by EA was measured to be 23.5 kPa. This is sufficiently strong and durable to ensure that the adhesion is "permanent". With regard to aging studies, adhered gels seem to remain adhered as long as the gels are intact (i.e., the gels do not degrade or shrink). For example, we have gel/gel pairs of QDM/SA that underwent EA four years ago and were stored at room temperature in closed vials – the gels are still found to be strongly adhered four years later.

5.3.2 Electroadhesion Requires a Cationic and an Anionic Material

All instances of EA in soft materials (bearing the hallmarks outlined above) involve one *cationic* and a second *anionic* material. In initial EA studies, both the cationic and anionic materials were hydrogels.[18,20-22,84] In Chapters 3 and 4, we have extended EA to many new systems.[19] The cationic component is a gel such as QDM. We have shown that these cationic gels can be adhered to biological materials extending across the various kingdoms in nature, including tissues from various animals (mammals, fish, worms etc), as well as plant-based materials (fruit and vegetables), and also fungi (mushrooms). Biological tissues are known to have a net anionic character, but the tissue microstructure and the source of negative charge in the tissue can vary widely from one tissue to another.[113,133-135,138,140] This is illustrated by Figure 5.2.

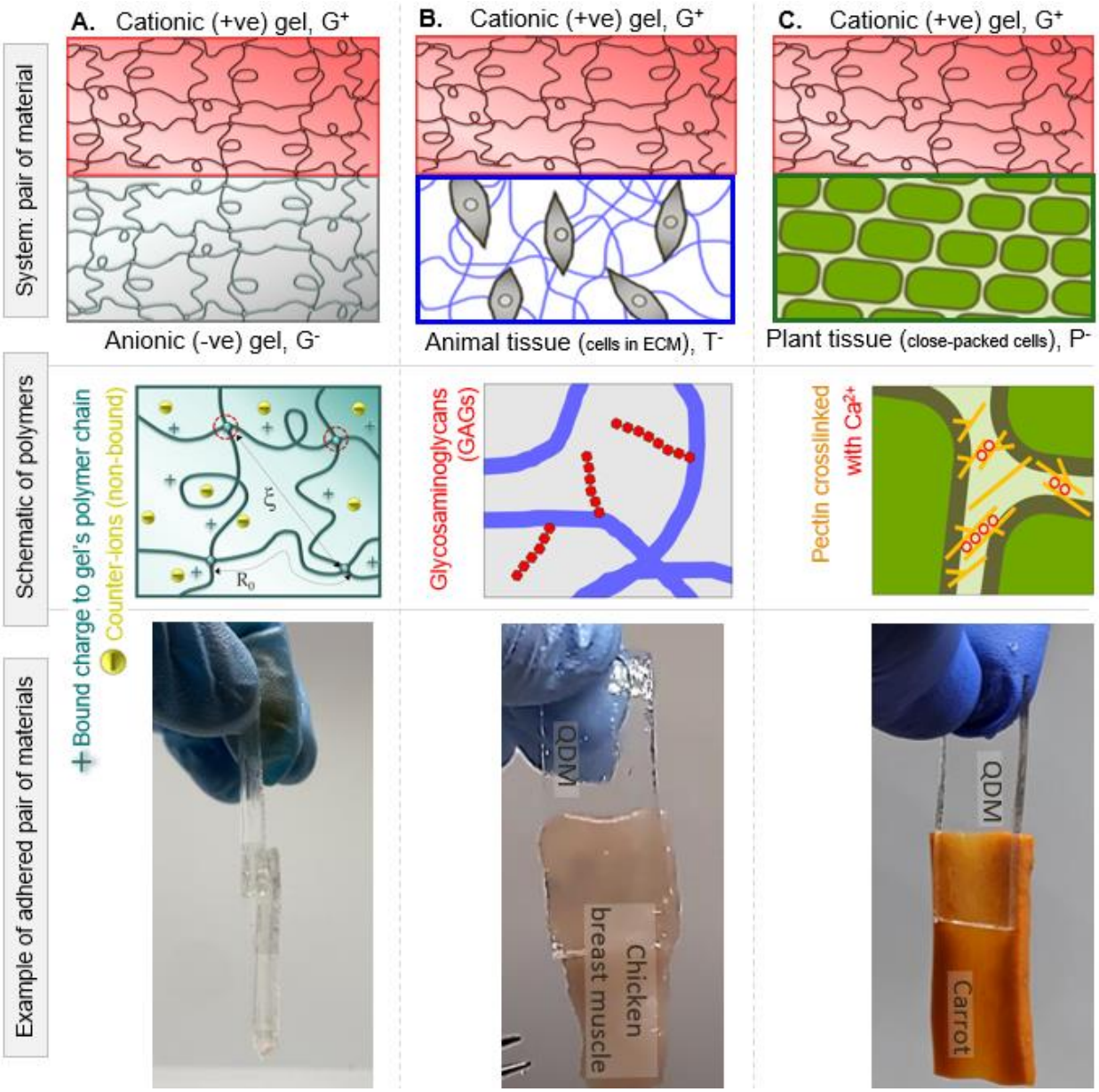

Figure 5.2. Cationic gels can be electroadhered to diverse materials. EA requires a cationic and an anionic material. As the cationic material, QDM gels (G^+) are consistently used in this work. As the anionic material, either gels or various biological tissues can be used, and these have varied structure. (A) EA of QDM to an SA gel (G^-). The gels are both crosslinked networks of polymer chains. The anionic nature of SA arises from COO^- groups along the chain backbone. (B) EA of QDM to a bovine aorta segment (T^-). The tissue is composed of cells surrounded by an extra-cellular matrix (ECM). The anionic nature comes from glycoproteins such as GAGs in the ECM. (C) EA of QDM to plant tissue (P^-), specifically a carrot slice. Many plant (as well as animal) tissues are formed by the close-packing of cells. In plants, the anionic nature arises from polysaccharides like pectin in the cell wall.

Figure 5.2 shows EA of QDM (G^+) gels to three different anionic materials. The photos show that the pairs are strongly adhered, which allows the combinations to be held vertically without detachment. Schematics of the microstructure in each of the materials is shown. Note that the QDM gel is a network of chains and the positive charge on the chains comes from amines (–$N(CH_3^+)$) along the chain backbones.[23] In Figure 5.2A, QDM is shown adhered by EA to an SA gel ($G^–$). The latter is also a crosslinked network, and its anionic nature comes from carboxylates (–$COO^–$) along the chain backbones.

Next in Figure 5.2B is an example of QDM adhered by EA to an animal tissue ($T^–$), in this case, a segment of a bovine aorta. Tissues mainly have two kinds of microstructure.[85,86] In one case, which is shown schematically in the figure, the cells are surrounded by an extra-cellular matrix (ECM).[149] The ECM can be envisioned as an entangled mesh of polymer chains or thicker fibers, some of which like the protein collagen are weakly charged, while others can be strongly anionic.[113] Anionic polymers in the ECM include various polysaccharides such as hyaluronic acid (having –$COO^–$) and the glycosaminoglycans (GAGs) such as heparan sulfate, chondroitin sulfate, and keratan sulfate (all having sulfates, i.e., –$SO_4^{2–}$ groups).[150] From a structural viewpoint, the ECM is similar to a hydrogel network in many ways, although the chains/fibers can be much thicker than in hydrogels.[151]

Animal tissues can have a second kind of microstructure, consisting of close-packed adherent cells.[135] In such tissues, cells bind to each other via junctions between their membranes, and there is little to no ECM around the cells.[96] Epithelial tissues, in particular, have this structure, and QDM can be adhered by EA to many such tissues.[152] The close-packed structure is also present

in many plant tissues (P^-), including fruits and vegetables.[138-140,143] Figure 5.2C shows an example of QDM stuck by EA to a slice of carrot. The schematic shows that most of the volume is occupied by cells, and in the case of plants, each cell is enclosed by an outer cell wall. The anionic character then comes from polysaccharides such as pectin (with $–COO^-$ groups) present within the cell wall.[138,143]

The three cases presented in Figure 5.2 (G^+/G^-, G^+/T^- and G^+/P^-) all show every one of the hallmarks of EA discussed in Section 5.3.1. Therefore, it is very likely that they all occur by the same mechanism. However, given the different microstructures of gels, animal tissues, and plant tissues, can we expect electrophoresis (under a DC field) to underlie the EA in all three cases? In gel/gel systems, there are no "free chains" as they are all connected by covalent bonds at crosslink junctions. Hence, only the *chain segments between adjacent junctions* can migrate by electrophoresis. In gel/tissue systems where there is an ECM, there may well be free chains, but the "chains" are actually thick and stiff fibers, which may not migrate easily in an electric field. In gel/tissue systems where the cells are close-packed, it is unlikely for a whole cell or a cell membrane or cell wall to deform and migrate across an interface. The charged polymers in this case are bound to the membrane or deep within the wall – and so it is unclear if these polymers can be "pulled off" the wall and transported across the interface.

So, what exactly is the mechanism for EA? Does electrophoresis have a role to play? To get to the bottom of this, we will first discuss experimental findings that inform us about the strength of adhesion achieved by EA. That is, what systematic "handles" do we have to increase

or decrease the EA adhesion strength? Most of these studies have been done on gel/gel systems for convenience, but the results broadly apply also to gel/tissue systems.

5.3.3 The Higher the Charge Density, the Stronger the Electroadhesion

First, we reiterate the requirement of *cationic* and *anionic* pairs for EA. In gel/gel pairs, we typically use QDM as the cationic (G^+) gel and SA as the anionic (G^-) gel. No EA occurs with two G^+ gels (e.g., two strips of QDM) or with two G^- gels (e.g., two strips of SA). Also, if we use a *nonionic* gel like acrylamide (AAm), no EA occurs with either QDM (G^+) or SA (G^-). In some of these cases, a weak adhesion may arise while the gels are in the DC field in the EA orientation (this is discussed more in Section 5.3.8), but when the field is switched off, this adhesion vanishes within ~ 60 s at most.

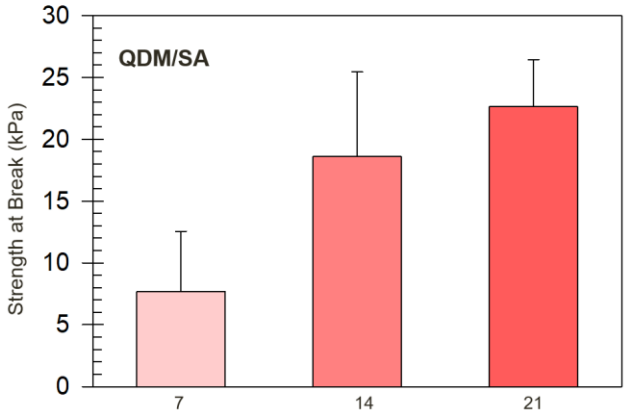

Figure 5.3. Effect of charge density on electroadhesion strength. QDM gels (G^+) with varying mol% of charged (QDM) monomer were prepared and these were stuck to identical SA gels (G^-) by EA (10 V, 30 s). Adhesion strength for these pairs from pull-off tests is shown to increase with increased QDM mol%. Error bars correspond to standard deviations from $n \geq 4$ measurements.

The charge requirement is further underscored by our studies with gels of varying ionic character. For strong electroadhesion between a cationic and an anionic gel, the cationic gel must

be *highly cationic*, and the anionic gel must be *highly anionic*.[54] For example, Figure 5.3 shows data for G^+/G^- pairs in which we fixed the anionic SA and varied the charge density on the cationic QDM. Charge density can be easily increased by increasing the molar ratio of QDM among the monomers used to make the gel. We then induced EA between the G^+/G^- pairs (using 10 V DC for 30 s) and then measured the adhesion strength using pull-off tests. Figure 5.3 shows that the pull-off adhesion strength increases monotonically with the cation fraction in the G^+ gel.

5.3.4 The Higher the Crosslink Density, the Weaker the Electroadhesion

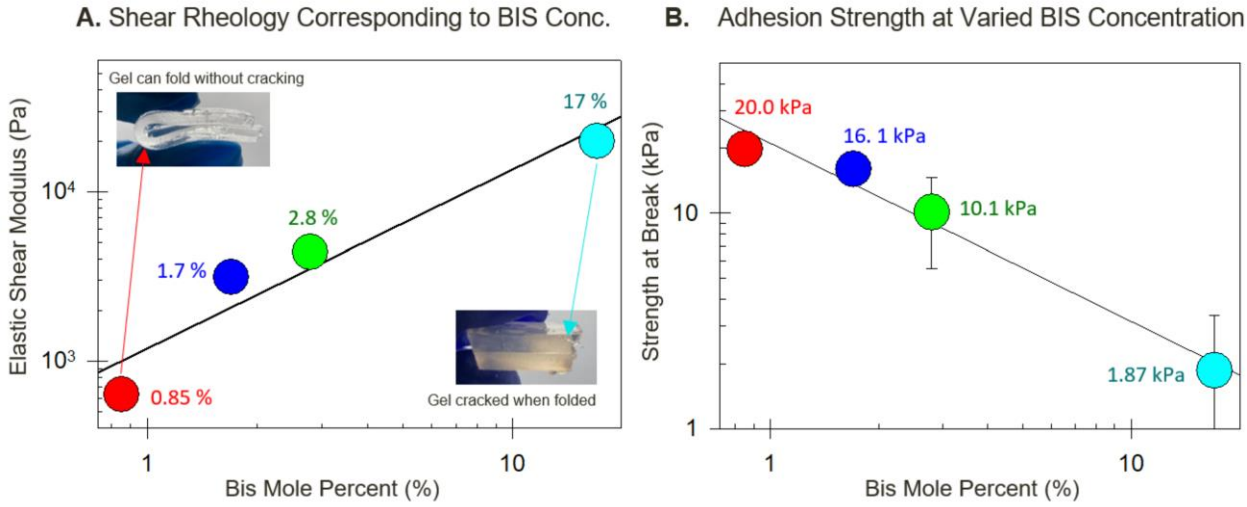

Figure 5.4. Effect of gel stiffness on electroadhesion strength. QDM gels (G^+) with varying crosslinker (BIS) concentration were prepared and these were stuck to identical SA gels (G^-) by EA (10 V, 30 s). (A) The elastic shear modulus of QDM gels increases (i.e., the gels become stiffer) with increasing BIS content. The photo inserts show a soft gel with low BIS concentration that can fold without breaking, while a high BIS gel cracks when folded (B) Adhesion strength from pull-off tests for the QDM/SA pairs decreases with increasing BIS content. Error bars in (B) correspond to standard deviations from $n \geq 4$ measurements.

Next, we examine the effect of gel rheology (stiffness) on EA. For this, we prepared QDM gels with the same charge density (i.e., the same QDM mol%) but increased the density of

crosslinker (BIS). As the BIS content is increased, the gels become stiffer (Figure 5.4A), as seen from the 100-fold increase in the elastic shear modulus (although the stiff gels do tend to be more brittle).[93] Photo inserts show a low concentration BIS gel that can fold easily, while a high concentration BIS gel cracks when folded. These gels were then adhered to identical SA gels by EA (using 10 V DC for 30 s) and the adhesion strength between the gel/gel pairs was measured using pull-off tests. Figure 5.4B shows that this strength decreases as the QDM gel increases in stiffness.

5.3.5 The Higher the Polymer Concentration, the Stronger the Electroadhesion

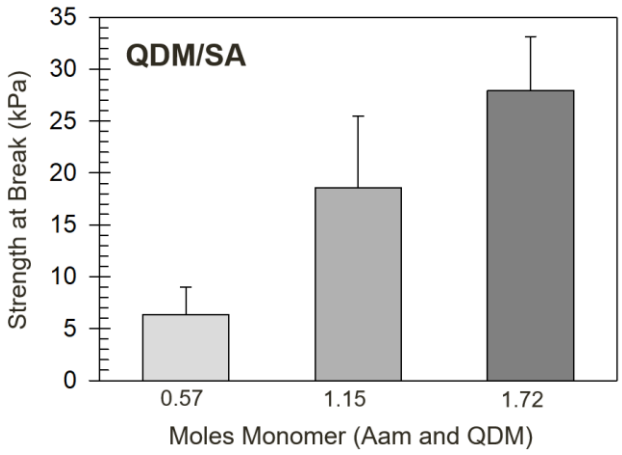

Figure 5.5. Effect of polymer concentration in the gel on electroadhesion strength. QDM gels (G^+) with varying polymer content were prepared and these were stuck to identical SA gels (G^-) by EA (10 V, 30 s). Adhesion strength from pull-off tests increases with increasing polymer content. Error bars correspond to standard deviations from $n \geq 4$ measurements.

Next, we examine the effect of polymer concentration on EA strength. For these experiments, we fixed both the charge density (QDM = 14 mol%) and the extent of crosslinking in QDM gels, while increasing the total monomer concentration. As the total monomer is

increased, the gels become stiffer (higher shear moduli), but they are also quite tough and strong (whereas the high-BIS gels in Figure 5.4 were increasingly brittle). The QDM gels were then adhered to identical SA gels by EA (using 10 V DC for 30 s). The pull-off adhesion strength between the pairs was measured. Figure 5.5 shows that as the polymer concentration increases, so does the adhesion strength. The same result was observed when the experiment was done in different ways. Instead of preparing gels with different monomer content, we took a "regular" QDM gel and then either (a) partially dried it for some time (under ambient conditions); or (b) swelled it in water for a prescribed time.[55] As the QDM gel dries, the polymer content in it increases, and in turn, its electroadhesion to SA also increased. Conversely, a swollen QDM gel showed weaker electroadhesion to SA compared to an unswollen control.

5.3.6 Counterion Migration Polarizes the Interface and Initiates Electroadhesion

In the previous sections, we have discussed the basic features of EA as well as ways to increase the strength of adhesion induced by EA. We now move on to discuss experiments designed to uncover the mechanism for EA. One intriguing aspect of EA is that adhesion is achieved *within just 10 s* of applying the field.[19] If EA was mainly due to the movement (by electrophoresis) of charged polymer chains,[18] would that not require more than 10 s to achieve sufficient adhesion? We hypothesized that the *counterions* for the QDM and SA chains had a role to play in the mechanism. Counterions (i.e., Na^+ and Cl^-) are much smaller (diameters of ions are 0.98 Å and 1.81 Å respectively) than the polymer chain segments between crosslinks, which were calculated by rheological measurements and elastic theory to be ~ 85 nm to 475 nm. Moreover, while the chain segments are constrained by the covalent crosslinks, the counterions are free to move within the gels.[153] Note that the mesh sizes of the hydrogels studied here were estimated by

rheological measurements and elastic theory to be between 6 to 19 nm, which is much larger than the counterion sizes. Thus, appreciable movement of counterions could happen within seconds of applying the field.[48,52,54]

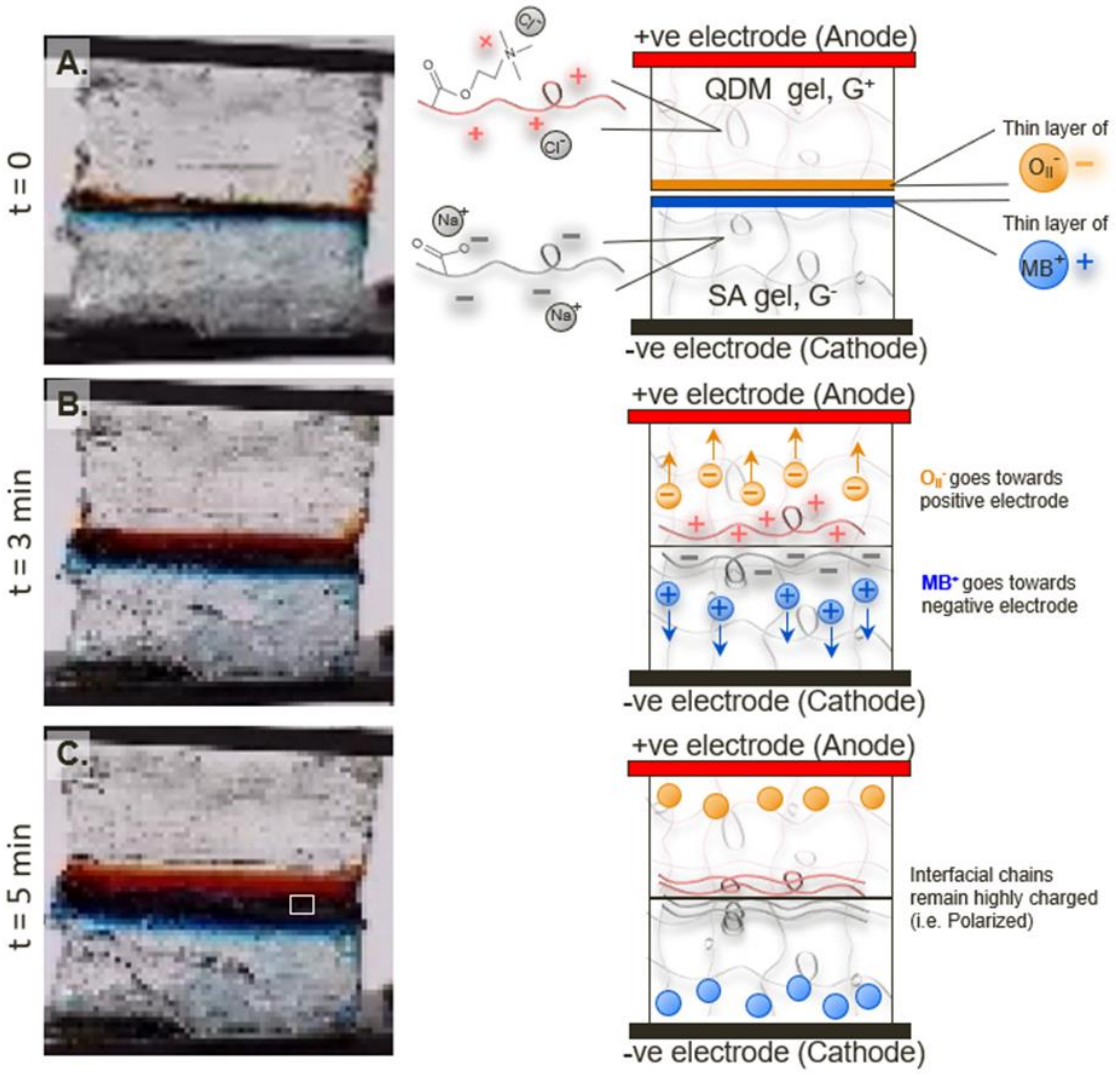

Figure 5.6. Counterion migration profiles during electroadhesion. The schematics show the setup at t = 0 and the subsequent changes at the molecular level. In the cationic QDM gel, as a visual surrogate for the Cl^- counterions, O_{II}^- dye is loaded over ~ 1 mm region next to the interface. Likewise, the SA gel has MB^+ dye to mimic the Na^+ counterions. In the EA orientation ($E^+G^+G^-E^-$ with 20 V), rapid electrophoresis of O_{II}^- upward (to E^+) and MB^+ downward (to E^-) are seen visually within minutes. This suggests that counterions move away from the interface, leaving behind strongly charged (i.e., polarized) chains at the interface. Pictures correspond to t_0, t = 3 mins and t = 5 mins of the G^+/G^- pair in the electric field.

To test this, we conducted the experiment depicted in Figure 5.6 using water-soluble ionic dyes in each gel that are chosen to simulate the respective counterions. Figure 5.6A shows the setup at $t = 0$: we have a QDM gel atop an SA gel, with both gels being ~1 cm in height. The end of the QDM (~ 1 mm in thickness) at the interface with the SA is infused with the anionic dye, Orange II (labeled in the schematic as O_{II}^-). Note that the amines along the QDM chain segments will be ionized (to $-N(CH_3)_3^+$)[23,129] and in turn will release chloride (Cl^-) counterions. Thus, the O_{II}^- is a mimic of the Cl^-. Likewise, the end of the SA gel is infused with the cationic dye, methylene blue (labeled in the schematic as MB^+). The MB^+ mimics the Na^+ counterions released when the carboxylates along SA chains get ionized (to $-COO^-$).[55] Further details of the setup are given in the Experimental Section.

At $t = 0$, a voltage of 20 V is applied across the gels with the electrodes in the adhesion orientation ($E^+G^+G^-E^-$) and we leave it on for 5 min. Over this time, we can visibly see the movement of both the O_{II}^- and MB^+ dyes (Figure 5.6B and C). The orange-red O_{II}^- dye in the QDM gel moves upward, i.e., it is attracted towards the E^+ electrode. Conversely, the MB^+ dye in the SA gel moves downward because it is attracted towards the E^- electrode. From the figures, we measured that the O_{II}^- and MB^+ dye fronts moved by ~ 1.3 mm in 5 min and ~ 1.5 mm in 5 min respectively. This suggests an electrophoretic velocity v ~ 1.3 – 1.5 mm/min or ~ 4.33 - 5 μm/s – which means that ion migration by electrophoresis is indeed rapid within the gels. Because the dyes were chosen to simulate counterions, we can expect a similar migration of counterions away from the gel-gel interface. The result of such migration will be to *polarize* the QDM and SA chains at the interface, i.e., the QDM chains will become strongly cationic and the SA chains strongly anionic.[128] Such polarization for chains that are right next to the interface, i.e., over a zone of 1 to

10 μm in each gel, can be achieved even in 5 to 10 s. Similar polarization has been suggested by the literature in polyelectrolyte diode.[154-156] Velev et al report that in the EA orientation, the current does not flow. This is because counterions are attracted to the nearby electrodes, leaving the polyelectrolyte gel highly charges at the interface. [154-156] On the other hand, when the field is switched to the reversed orientation, the current flows because the counterions are now attracted to the far end electrode.[154-156] In this reverse EA orientation, the polyelectrolyte chains at the interface are in equilibrium with the bulk of the gel.

5.3.7 Polarized Gels Adhere Electrostatically ("Zipping Experiments")

If at the interface the gels are polarized, do they experience an electrostatic attraction? Does this indeed cause adhesion? To shed light on this point, we conducted the usual EA experiment between QDM and SA gels in the adhesion orientation ($E^+G^+G^-E^-$), but at a much higher DC voltage (90 V). The striking findings from these experiments are reported in Figure 5.7. First, we contact QDM and SA gels with graphite electrodes (Figure 5.7A1). The moment the gels touch, the circuit is completed and current will flow. We make the gels touch at their bottom end, marked by the red dotted line (Figure 5.7A2). As soon as they touch, the gels *lock together* at this end indicating their adhesion. Then the rest of each gel "springs" into contact and the interface locks over the entire gel-gel interface (see the elongation of the red dotted line in Figure 5.7A3-5). A similar observation occurred when we replaced the SA gel with a slice of carrot, in Figure 5.7B. We refer to this phenomenon as "zipping" because the closure of the gel-gel interface seems to mimic the closure of a zip from one end. Note that as the gels spring into contact, the attraction to their opposite counterpart is so powerful that the gel "jumps" away from its electrode (note the gap to the electrode in 5.7A4-5, and 5.7B4-5). A movie of this zipping phenomenon clearly reveals

the features noted here. The conclusion we reach is that there is a definite electrostatic attraction between the interfaces.

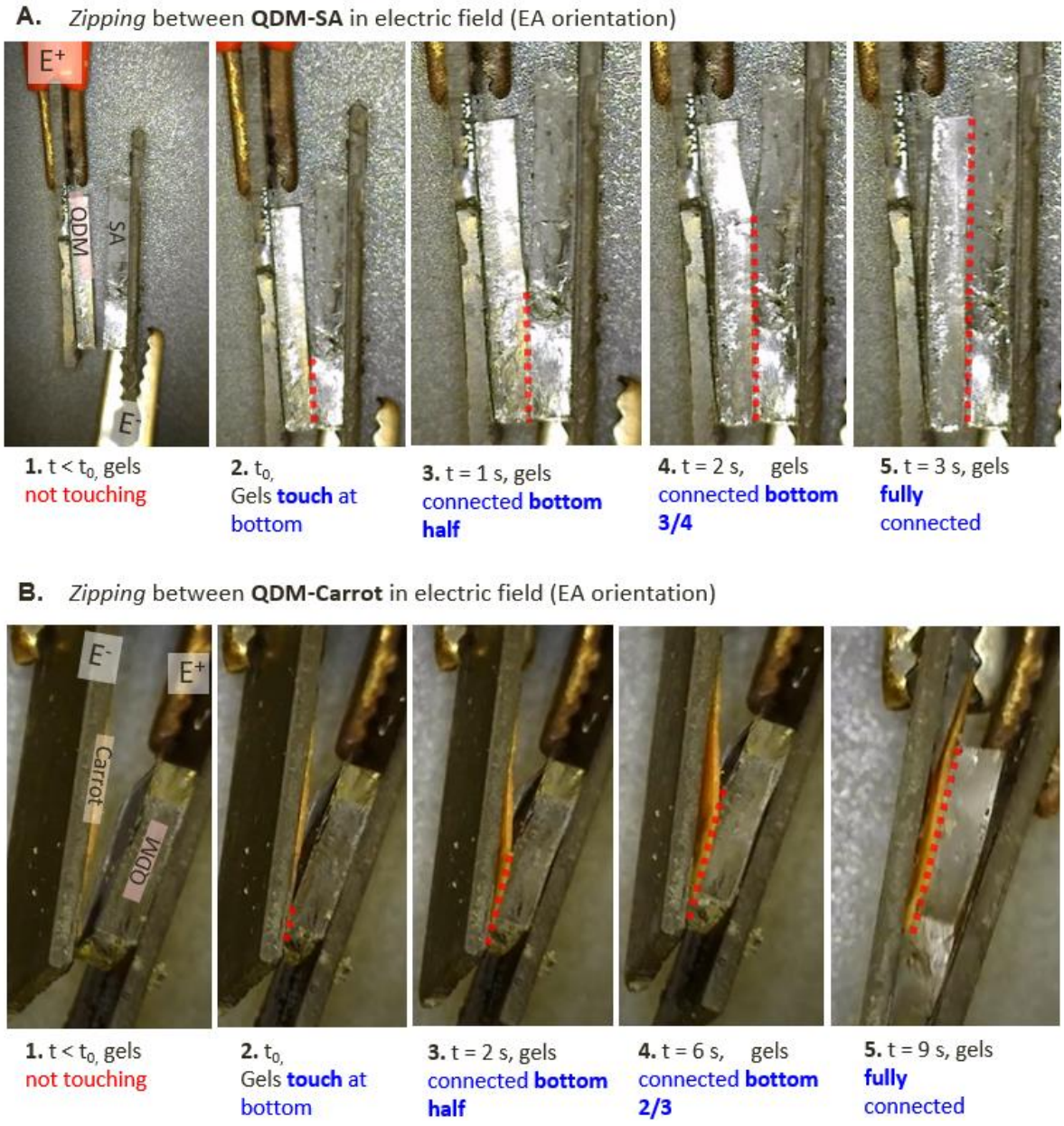

Figure 5.7. Zipping experiment showing the electrostatic attraction of QDM and carrot to SA gels. (A) Zipping of QDM to SA and (B) Zipping of QDM to carrot tissues. (A1) Gels of QDM (left) and SA (right) are placed in the EA orientation and are contacted at their bottom end at t = 0. A high DC field (90 V) is applied. (A2) When the gels touch, they instantly lock together over the bottom 0.5 cm (red line). (A3) After 1 s, the adhesion zone has extended up to 1 cm as the gels attract each other. (A4) After 2 s, the adhesion zone has advanced to 1.5 cm. (A5) After 3 s, the gels are adhered over the full 2 cm. The closure of the gel-gel interface resembles the closure of a zip from the bottom end; hence the term "zipping". Note that in (A4) and (A5), the gel-gel

attraction causes the QDM gel to jump and detach from the E^+ electrode, indicating a strong electrostatic attraction to the SA gel. The gel-pair is left in the field for ~ 5 s more and then the field is switched off – at this point, the gels are permanently adhered. The same process occurs with QDM-carrot tissue pair in (B1-B5).

The above zipping behavior of QDM and SA gels is seen at high voltages (90 V for QDM-SA and 50 V for QDM-carrot) but not at our usual condition of 10 V. Nor is there any such zipping if the gels are simply contacted without a field. This is understandable because the higher voltage likely causes the strong polarization needed to observe the zipping. Also, importantly, when 100 V are used, the gels need to be in contact for just ~ 5 s before they achieve permanent EA, i.e., adhesion that persists long after the field is removed. For comparison, at the lower voltage of 10 V, we keep the gels in contact for around 10 s to achieve such adhesion.

Zipping is not seen with gels of the same charge, either QDM-QDM or SA-SA. In those cases, when 100 V is applied, we see an adhesion while the gels are in the field.[129] When the field is removed, this adhesion dissipates within 30 to 60 s and the gels can be separated.[148] A movie of the SA-SA and QDM-QDM case shows these points. This weak, temporary adhesion may correspond to the JR effect with hydrogels. Consider the SA-SA case. As per JR, under the field, strongly charged SA chains will collect at the interface in one gel while an excess of counterions will collect across the interface in the other gel.[129] The chains and counterions will experience a weak electrostatic attraction, which can explain why SA-SA gels adhere under the field. However, when the field is switched off, the counterions will quickly equilibrate and move away from the interface, which can explain the loss of adhesion.

5.3.8 Putting it all Together: A Mechanism for Electroadhesion

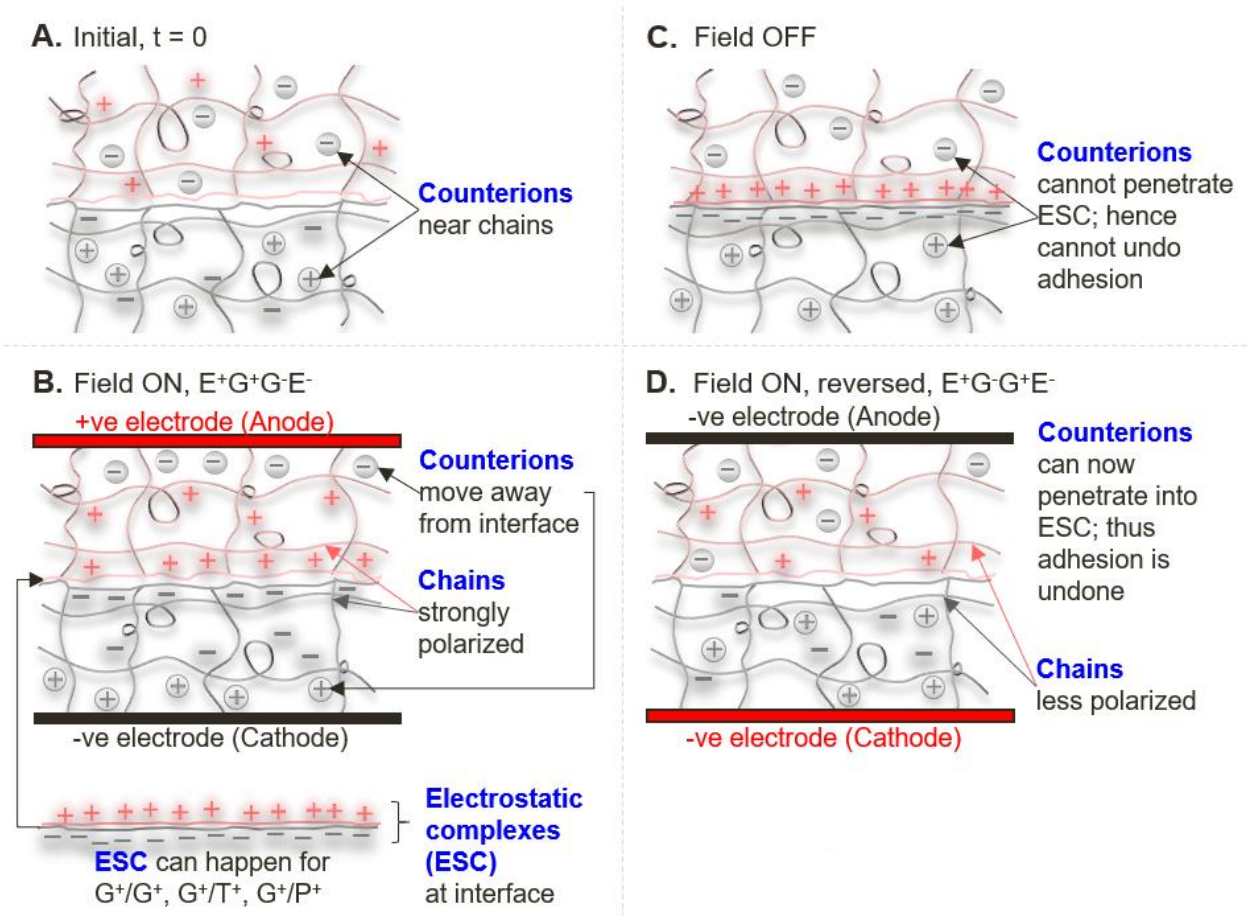

Figure 5.8. Mechanism for electroadhesion. Schematics of a cationic (G^+) and an anionic (G^-) gel are shown. (A) Initially, the counterions in each gel are randomly distributed. (B) When the field is applied in the adhesion orientation ($E^+G^+G^-E^-$), the counterions are pulled away from the gel-gel interface, which strongly polarizes the chains at the interface. These chains then form a dense electrostatic complex (ESC), leading to adhesion. (C) When the field is turned off, the ESC persists because counterions have weak affinity for the chains in the ESC. Hence, the adhesion remains strong. (D) When the field is applied in the reverse orientation ($E^+G^-G^+E^-$), counterions are induced to penetrate the ESC, thereby unbinding the chains and breaking apart the ESC – and thus reversing the adhesion.

The challenge in coming up with a mechanism for EA is to explain all its hallmarks (Section 5.3.1) as well as all the findings reported in Figures 5.2 to 5.7. Our hypothesis for the mechanism is illustrated by Figure 5.8. The schematics refer to EA between a cationic (G^+) and an

anionic (G^-) gel, but the same mechanism also applies to gel-tissue EA. Initially, the G^+ and G^- gels are brought into contact, but no field is applied (Figure 5.8A). At this stage, all chains in the gel are uniformly charged and the counterions are evenly distributed. When the field is applied in the adhesion ($E^+G^+G^-E^-$) orientation (Figure 5.8B), we have shown in Figure 5.6 that the chains near the interface in both gels get polarized – this occurs because the counterions are pulled away from the interface via electrophoresis. As a result, we are left with *strongly cationic* chains in the G^+ gel right next to *strongly anionic* chains in the G^- gel. We postulate that these chains form a dense **electrostatic complex** (ESC) at the interface, leading to adhesion under the field. Evidence for ESC formation comes from the zipping experiments in Figure 5.7. It is clear that the gels are strongly attracted to each other, and this must be due to electrostatic interactions, i.e., the presence of strongly charged molecules of opposite charge on either side of the interface. Within 10 s in the field, the ESC develops further, and the gels are strongly bound to each other, i.e., we see EA between the gels.

Next, we need to explain why the EA is persistent (and potentially permanent) when the field is switched off. To explain this, we postulate that, once the ESC is induced, it is a stable, non-equilibrium structure in which the chains remain bound to each other. For the ESC to be dissolved, the counterions must re-distribute around the chains in the ESC. In the absence of the field, the counterions that were pulled away towards the electrodes will revert to a more uniform distribution in the two gels via thermal energy. However, we suggest that the ESC will resist the insertion of counterions because the bound ionic chains are in a favorable, low-energy state.[157] This is suggested by Figure 5.8C. We can make the analogy to layer-by-layer (LbL) assemblies of cationic

and anionic polymers.[157,158] Although LbL assemblies are in a non-equilibrium state, they do not disintegrate when suspended in water with salt – and in fact, they can persist indefinitely.[157,159]

Does the ESC involve the *interpenetration* of cationic and anionic chain segments? Interpenetration implies that some cationic segments from the G^+ gel will cross over into the $G^–$ gel and vice versa.[24] If so, the polymers will form a coacervate (polyion complex) in which the chain segments will be entangled with each other, in addition to their electrostatic binding.[160] Although we cannot rule it out, we do not believe interpenetration occurs in *all* ESCs. While it can happen across a gel-gel ($G^+/G^–$) interface, we believe it is unlikely across gel-tissue ($G^+/T^–$ and $G^+/P^–$) interfaces. In particular, if a tissue is composed of close-packed cells, as is the case in vegetables or in epithelial tissues from animals, it will not expose free anionic chains that could cross into the G^+ gel. We envision ESCs as a *feature common to all systems that show EA*, and in that regard, the key is that it arises via *electrostatic interactions*. The precise structure of the ESC still needs to be elucidated, and we leave open the possibility that the ESC structure varies from one pair of materials to another.

Lastly, Figure 5.8D explains why EA is reversed when a DC field of opposite polarity is applied. When the field is applied in the reverse orientation ($E^+G^–G^+E^–$), counterions undergo electrophoresis in directions towards the gel-gel interface.[128,154] Thus, both sets of counterions will be induced to penetrate the ESC that previously existed at the interface. Once the counterions enter the ESC, they will induce the chains to unbind (i.e., the counterions will compete favorably with the oppositely charged chains). When the chains unbind, the ESC falls apart and this reverses the adhesion. The key point here is that the counterions will not *spontaneously enter into the ESC*[157]

(Figure 5.8C), but the reverse electric field will *force them into the ESC*. This can explain why the adhesion persists in the absence of the field but is reversed under the reverse field.

5.4 Conclusions

In this chapter, we have successfully answered what is the mechanism behind EA. EPA relies on interpenetration of polymers across the boundary of the gel-anionic material's interface. However, given the very different of classes of soft materials in which we see EA, EPA becomes a less likely mechanism.

We have shown that the counterions in the gel-anionic material are what initiates the EA process, and not polymer migration. We have done this by "visualizing" the migration of counterions using dyes with the same charge as the cunterions' charge. Further, we have shown that this diffusion causes interfacial polarization at the interface-of-adhesion, by conducting "zipping" experiments. The strong polarization leads to formation of ESC at the interface between both gels. These ESC complexes function in establishing permanent adhesion after the field is removed, in line of thermodynamically stable LbL complexes.

Such a mechanism is in-line with the Coulombic-like electric field driven adhesion called the Johnsen-Rahbak effect (JR). This is a bulk adhesion mechanism driving adhesion between hydrogels of the same charge. JR is non-permanent when the electric field is removed. Here, ESCs "pin" the gel-anionic material pair causing the non-permanent JR to become permanent. We conclude that JR and EPA have the same initiation process caused by counterion migration and interfacial polarization.

Chapter 6
Conclusions and Recommendations

6.1 Conclusions

In this dissertation, we have *described the phenomenon of electroadhesion and the many natural materials that can undergo EA, including all classes of animal, various plants, and fungi.* These findings were discovered after we observed EA to bovine tissues and asked whether EA is present in other classes of soft material? We began with describing our initial findings regarding EA in bovine tissues, and the potential applications of these findings in sutureless tissue repair. We have then illustrated EA was not limited to one animal but was present in many cellular organisms in nature. We also hypothesized that EA depends on the presence of anionic biopolymers in the natural systems. Additionally, we came up with a mechanism that described EA across gel-gel, gel-animal tissue and gel-plant tissue. This deeper understanding of the mechanism will allow an engineer to adjust the parameters needed for a surgical patch.

In Chapter 3, we presented a simple technique to adhere a cationic gel patch to an animal tissue by using electric fields as a stimulus. The electric field applied was 10 V DC for ~ 20 s in the EA orientation ($E^+G^+T^-E^-$). Using our technique, we showed we can adhere gel patches to various organs including, aorta, cornea, lung, skeletal muscle, tendon, and cartilage. We have also preformed model experiments in gel-gel systems to describe potential applications of EA in repairing tissue defects and even full end-to-end anastomoses. We measured the adhesion strength of EA and the weaker contact adhesion between gel-gel and gel-tissue, and in both cases, EA was significantly stronger. EA was ~ 20 kPa for both gel-gel and gel-cow tissues. The findings in this

chapter are a *groundbreaking achievement, with great clinical potential in surgical repair.* These findings also led us to assess whether EA was present in other classes of naturally occurring materials.

In Chapter 4, we surveyed a variety of natural soft materials and found EA in all classes of animal: vertebrates and invertebrates, EA was present in many plants, including fruit, vegetables, and stems, and in fungi, specifically mushrooms. We have shown *EA occurs in the same tissue across many animals,* for example, EA occurs in skeletal muscle in cow, pig, mouse, chicken, lizard, salmon fish, shrimp, scallop, and cicada. This *widespread occurrence of EA with all classes of animals suggests it will occur even in those animals not tested, such as with human tissues.* Further, we have shown that EA can occur in interfaces composed of cells with ECM (such as aorta or muscle) or close-packed cells (such as cornea and plant tissues). In all cases there are anionic biopolymers present at the adhesion interface. We have then shown that tissue anisotropy influences EA. In some tissues such as skeletal muscle and strawberry, depending on the orientation, EA may yield strong adhesion or no adhesion at all. Finally, we have shown that EA can occur in materials with different properties such as tissues that are soft (such as muscle) or hard (such as carrot). Because EA happened with such different tissues, we found the current explanation of EA to be lacking and asked, what is the common mechanism behind EA?

In Chapter 5, we discuss the mechanism. We systematically tested different components of the gel and tissues and arrive at a mechanism governing electroadhesion in all gel-anionic material pairs. We have demonstrated that increase charge in the gel increases adhesion strength. We were able to “visualize” the movement of counterions in the gel by inserting a dye of same charge as

the counterion. This experiment illustrated that the counterion initiate the process of EA. Diffusion of counterions out of the interface also polarizes the material's interface, causing a strong electrostatic attractions between both surfaces. We have shown this attraction by a series of "zipping" experiments. This polarization and attraction while in the electric field is similar to the JR effect, however with JR adhesion was non-permanent. Here the adhesion lasts indefinitely after the electric field is removed. The difference is that we use a cationic and an anionic material, where as JR had two materials with the same backbone charge. We hypothesized that after polarization, the materials form ESC that "pin" the surfaces together. The ESC is stable thermodynamically and is not disturbed or dissolved by presence of counterions in a similar way that LbL complexes are stable. However, when the field is turned back on in reversed polarity, the counterions are forced into the ESC causing it to dissolve and the adhesion is reversed. This mechanism can explain EA with gel-gel as well as other more complex pairs such as gel-animal and plant tissues.

6.2 Recommendations for Future Work

There are a couple of on-going projects that are not included in this thesis. These will be discussed briefly in Sections 6.2.1 – 6.2.2. Addition projects that have just begun or are in the plan for the future will be discussed in Sections 6.2.3- 6.2.7.

6.2.1 Electric field optimization and medical device fabrication for enhanced adhesion strength

Electroadhesion throughout this thesis has been applied using flat plate electrodes with the electric field transcending from the positive electrode, through the pair of soft material, to the negative electrode. This geometrical set-up is shown in Figure 6.1A. The most basic relationship between voltage V (electric field potential), the current I, and the resistance R, is given by Ohm's law in Equation 6.1.[161]

$$V = IR \tag{6.1}$$

When tissues and gels that undergo EA have a bulk resistance associated with them, it implies that part of the potential applied in the setup in Figure 6.1A does not travel from one electrode to the other, rather get absorbed in the tissue. This energy dissipates in the form of heat or another chemical or mechanical process. We have tested temperature increase and observed a slight ΔT of ~ 3-4°C. Temperature increase is not ideal for tissues, and a temperature increases above ~ 5°C begins to become detrimentally to biological systems.

Additionally, whenever there was a resistance associated with a gel-tissue system, adhesion was typically harder to achieve. In order to get adhesion, we had to increase the potential to get a better current I, which in turn led to polarizing the interfaces between the gel-tissue pair and achieving adhesion. Moreover, when the tissues had higher osmolarity, or when tissues were

segmented into very thin layers, we observed a current range of 10 mA to 80 mA even while applying only 10 V DC. In both cases were we artificially increased the current or that current increased by default of the system's parameter, the tissue can be affected negatively. In fact, in our early animal studies, we had some unfavorable outcomes associate with high currents, such as tissue damage and tissue death.

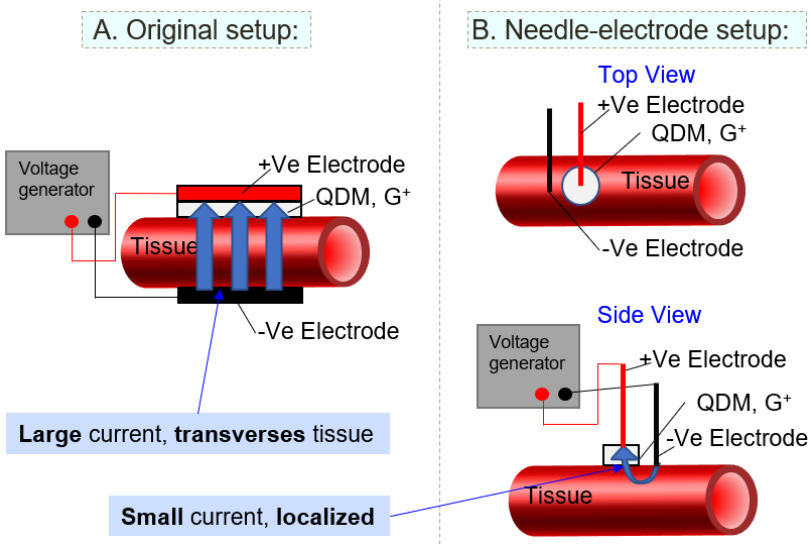

Figure 6.1. Old and new set-up for EA. (A) In the initial studies and in all work presented in this thesis a parallel plate electrode system encased the EA pair. This cause organs incased to begin to die after exposure to high electric fields. (B) In the updated needle-electrode setup, both electrodes are placed from the same direction. The positive needle-electrode is placed on the gel and the negative needle-electrode is placed right outside the gel onto the tissues. This allows for the patches to stick with much less current applied, and the current that does pass through the tissue is localized to the patch and tissue surface.

High currents in biological systems can lead to irreversible and damaging processes. Each cell has ion gates that function and provide the cell a resting potential. When an external current disturbs this resting potential, ion gates open and the cells and tissues can begin to die because homeostatic is disturbed significantly. In our early animal studies, we saw this " advancing wave of death" occur after application of EA, when we reopened the animals on day 3. This brought us

to reassess our electrode set up, with the aims: (1) to reduce the current applied to the biological system, (2) develop an electrode pathway that does not require current to transverse an entire organ, and (3) have the animal and organ survive following EA application.

In collaboration with the White lab in BioE, we developed a needle-electrode system that applies both needle electrodes from the same tissue surface direction. This set up is presented in Figure 6.1B. The positive needle is placed on the cationic gel patch and the negative needle is placed right outside the gel patch onto the tissue, but not touching the gel patch. Such a set up provides us with (1) lower current. We now observed currents between 1.2 mA and 5 mA at the highest in all animal studies. Recall in comparison that with the flat plate geometry the current range was 10 mA to 80 mA. In all animal studies we used a 7 - 10 V DC potential. (2) The pathway the current passes through the tissues is localized to tissue surface. Meaning, only the local tissue is affected by the electric field as current becomes weaker with distance from electrodes. (3) Animals subjected to the needle-electrode set up did not show any signs of injury at day 0 during EA application or at day 6 post operation (PO).

This needle set-up has evolved into a hand-held medical device prototype for surgery. We are currently developing it for clinical use in the operating room. A picture of this medical device is provided in Figure 6.2A. Several features have been implemented in the medical device for easy user experience. The device is operated on a 9V standard battery, as shown in Figure 6.2B. The device will have a removable head unit that has the ability to adjust the electrodes to various distances from one another. This allows for patch application of various diameters. This device will also include an LED that lights up while current is passing through the patient, to give the

surgeon a signal when the electric field is on. As future work, we would like to include different shaped electrodes, for example for EA to be applied to a patch on a round artery, we would like to be able to connect a semicircle electrode. We also would like the device to have an auto suggested time for EA based on calculating the integral of current and having some formula associating conductivity of tissue system and time the field needs to be applied.

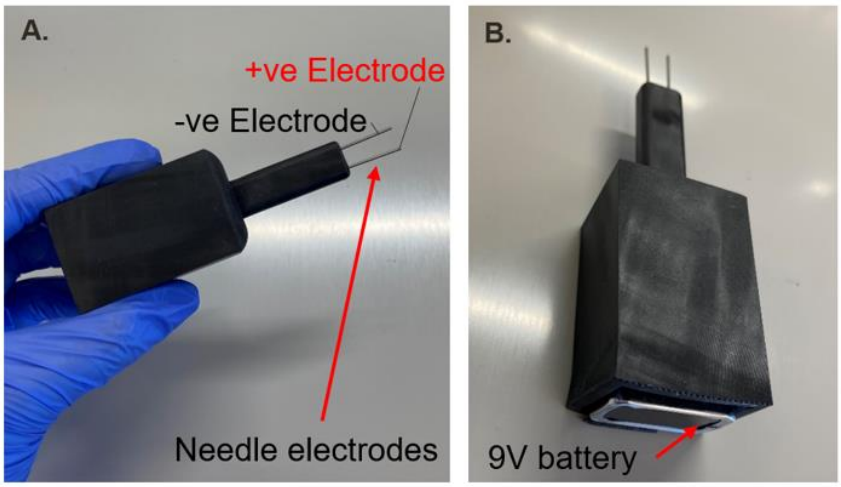

Figure 6.2. Hand-held medical device prototype for EA. (A) a small user-friendly hand-held device. Fits comfortably in the user's hand. The device contains a positive and negative electrode in the form of a thin needle. In the future we would like to make these needles adjustable in distance from one another as well as have various head attachments. (B) The device operates on a simple regular V battery. In the future it will contain an LED light that indicates when current is passing.

Additional parameters are being optimized in regard to the electric field including an understanding of how the voltage and the current affect EA, how to reduce the current in biological system while optimizing adhesion, and understanding how long we need to apply the field to achieve adhesion in various tissue systems and patch diameters.

6.2.2 Small animal study for electroadhesion intestine puncture repair

A small animal study has been in progress with Dr. Anthony Sandler Surgeon-in-Chief and Dr. Michele Saruwatari of Children's National Hospital. We are currently in the midst of analysis of a 25-mouse study, IACUC study number 30703. Our groups (n = 5) include: (1) Control 1: open the abdomen and reclose it to assess general surgical detrimental effects. (2) Standard-of-care: open abdomen, puncture cecum and repair puncture using sutures. The cecum is a component of the intestine that stores waste, akin to appendix in human. See Figure 6.3A for healthy mouse cecum after opening the abdomen. Figure 6.3B shows the puncture and gel-patch placement location. (3) EA, 9V DC applied for 30 s. A small gel patch (prepared in sterile conditions, diameter 5 mm, height 1.5 mm) is applied to the puncture location and electroadhered to the puncture site (enterotomy) by the conditions specified. The application of EA using the hand-held device is shown in Figure 6.3C. The adhered gel patch is presented in Figure 6.3D. (4) EA 7V DC applied for 60 s. Similar as case (4) but different electric field conditions. (5) Control 2: puncture of cecum and placement of gel patch by contact alone. The EA currents from EA 9V group had an average of 2.1 mA while current from EA 7V group had an average current of 1.6 mA.

On day 6 when we reopened the animals in the classes specified above, we assessed (1) adhesion of gel patch to puncture location, (2) surgical adhesions and (3) we harvested tissue and blood samples for pathology and immunology testing. All patches from the EA groups were stuck on day 6 PO. Figure 6.3E shown an abdominal cavity with the gel patch adhered to the cecum on day 6 PO. Surgical adhesions (a surgical detrimental outcome associated with the tissue's self-repair process) within the animal were assessed at day 6 PO. The best score is 0 with no adhesion and the worst score is 5 with severe adhesions. Group 2 or standard-of-care had an adhesion score

of 0.6 (±0.89), EA 9V's adhesion score of 1.4 (±0.55), EA 7V's adhesion score of 1.6 (±0.55), control 1 had an adhesion score of 0 (±0) and control 2 or contact adhesion had a score of 3.25 (±1.71). All animals survived besides one animal from control 2 group. *EA repair animals had significantly better outcomes compared to contact animals.* In the contact group, one animal died, one animal had an intestinal burst, see Figure 6.3F. and the remaining had varying degrees of surgical adhesions. Results from this study need are still being analyzed.

Figure 6.3. Testing EA for intestinal enterotomy repairs. (A-D) Are all pictures from day 0. (A) A healthy cecum in a mouse. The cecum is a compartment in the mouse that stores waste. (B) Puncture and patch placement location. (C) EA repair using the hand-help medical device prototype. (D) The cecum with a gel patch following EA. (E-F) Results from day 6 PO. (E) The gel patch is adhered on day 6 PO to a punctured cecum in an animal that received 9V DC applied for 30 s. (F) In comparison, an animal with a puncture and contact patch, had an intestinal rupture. The yellow is bowel waste spread throughout the abdomen.

The best outcomes are that gel patch applied by EA does maintain a good adhesion despite biological osmolarity, see Figure 6.3E for adhesion on day 6 PO. Additionally, the patch seems to have better indication than contact adhesion, which is equivalent to no treatment, by a statistical margin (obtained by ANOVA testing). Figure 6.3F shows some complications associated with no treatment to an intestinal puncture, such as the intestine bursting. However, standard-of-care is still better than EA. Therefore, some optimization will need to be done to reduce the surgical adhesions of the EA groups and bring its results closer to the standard-of-care by sutures. We will also need to increase the negative outcome observed by the contact group, possibly by increasing the puncture size.

6.2.3 Electroadhesion to repair liver injuries

The optimized medical device has resulted in favorable EA results. With this device we achieved EA to organs that are reported to have no adhesion in Chapters 3 and 4. Some (mouse) organs that had EA with the needle electrode set up include kidney epithelium, liver epithelium, heart epithelium (epicardial tissue), and mouse skin (shaved with all fur removed). All these organs had no EA with the flat plate electrode set-up.

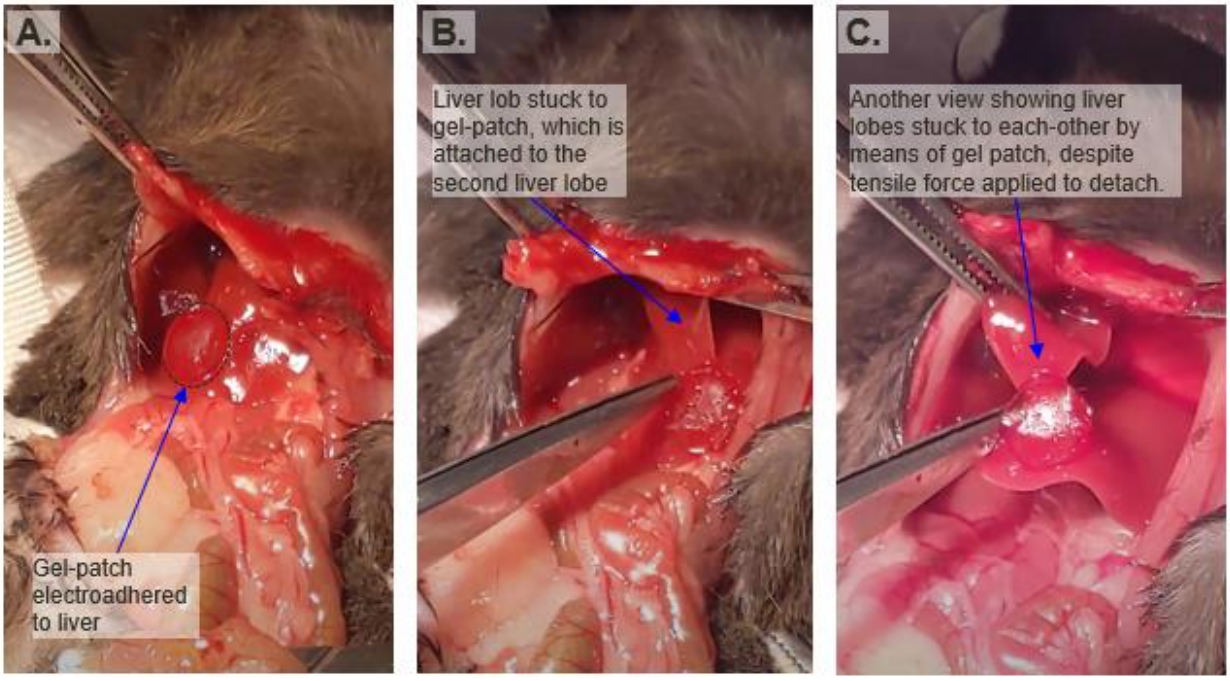

Figure 6.4. EA to liver by means of needle-electrode setup. (A)The QDM gel patch is electroadhered to the liver of a live mouse (under Anastasia). (B and C) We attempted to remove the gel patch by pulling the liver lobes apart. The gel patch got stuck on both liver lobes and stuck them together. A tensile strain is applied, and the tissue remain adhered until a strong force was applied.

It is very difficult to stop bleeding from liver injuries. The current standard of care utilized cautery, or application of an AC high frequency electric field to either coagulate the blood or to "cut" or in other words "burn or cook" the tissue in order to stop the bleeding. Various homeostatic products are in development or used but there is still a need for an alternative method to stop the bleeding. Since EA adheres strongly to liver epithelium, tested by how difficult it was to tear the adhered gel patch off the liver, Dr. Sandler proposed creating a liver injury animal model that utilized EA to stop bleeding. The gel patch will form a barrier on the external liver epithelium, similar to applying localized pressure, which will help the liver reach hemostasis. In Dr. Sandler's own words: "We can use this [EA] to save lives!" Figure 6.4A shows a QDM gel patch adhered to mouse liver. Following EA we attempted to remove the gel patch by force. Figure 6.4 B and Figure

6.4C show how the gel patch is holding two lobes of the liver together despite the tensile stain we are applying to the tissues. This indicated a strong adhesion has been reached with QDM-liver tissues by means of EA using the needle electrodes set-up.

One way to improve the strength of EA patches for liver injury (and for all other kind of EA applications as well), is to incorporate a thin wire mesh within the gel. The surface of the patch will be only made of gel alone, but a supportive interior mesh would allow for stronger support, higher burst pressure loads and higher tensile stress at rupture.

6.2.4. Electrophoretic drug delivery using electroadhesion with skin patches

As mentioned in Section 6.2.3, with the needle electrode set up, we are able to obtain EA to mouse skin. This opens a variety of work possible with EA to skin, some include treatment for burns and dermal forced drug delivery by electrophoresis. In our earlier work from Chapter 5 regarding dye diffusion as surrogates to counterions, we also explored co-ion electrophoresis. We observed that with electric fields we can force co-ions across the interface between both gels. For example, we loaded a thin layer of MB^+ dye into QDM gel. MB^+ has a cationic charge. We then inserted the QDM-MB^+ gel and an SA gel into the electric field in the EA orientation, See Figure 6.5A for the initial set up. We observed that after about 3 s some of the blue dye already traversed from the QDM gel into the SA gel, as can be seen in Figure 6.5B. On the other hand, as shown in Figure 6.5C no dye transfers to the SA gel by diffusion alone even after 30 s.

We are developing a study in which we would contain a molecule of interest within a cationic vesicle. We would like to see if a physical gel network would allow for electrophoretic delivery of such cationic vesicles to the skin surface. Previous work suggested that vesicles diffuse out of physical networks over the course of days. Would EA expediate this process and could this be a method for drug delivery?

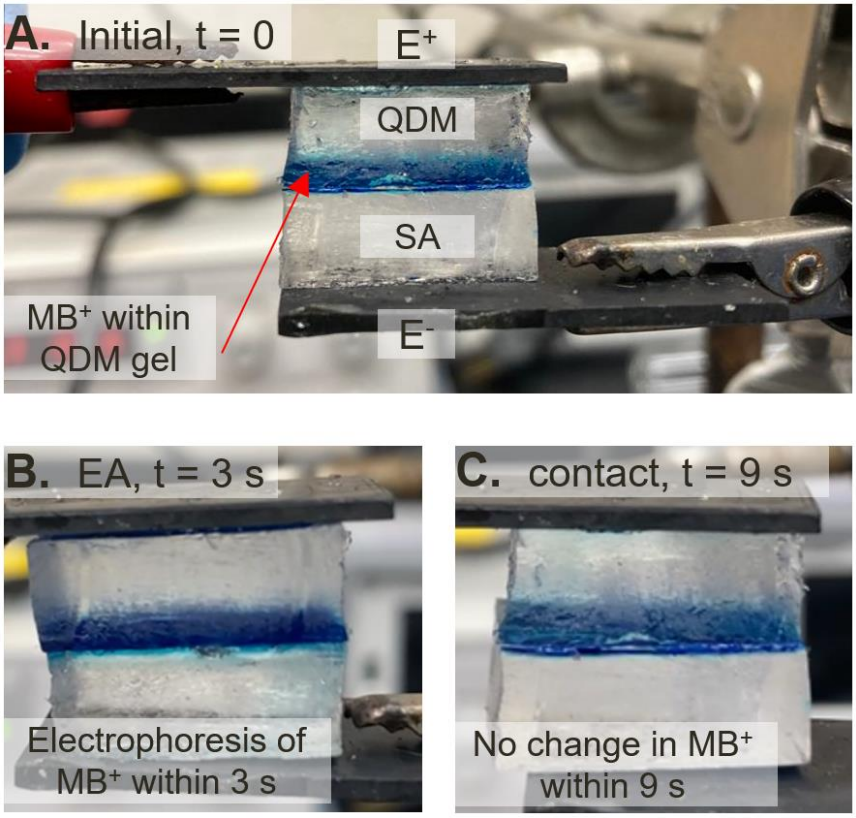

Figure 6.5. Set up for electrophoretic drug delivery (A) QDM gel with a thin layer of MB^+ dye at its interface comes in contact with SA. They are placed in the electric field. (B) within 3 s we see some dye cross the interface into the SA gel. (C) When no electric field is applied, no transfer of dye is seen even at 30 s.

6.2.5. Electroadhesion to human arteries for anastomosis repair

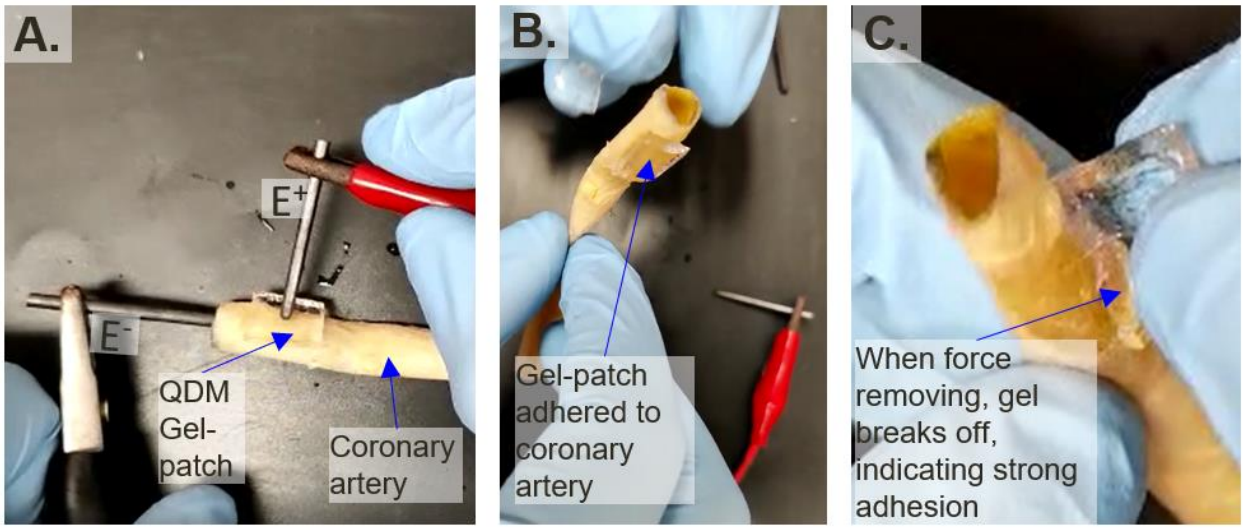

Figure 6.6. EA for repair of carotid artery implants for bypass surgery. (A) A QDM gel patch is applied on top a segment of a clinical grade bovine carotid artery, used for bypass surgery. EA is applied in the EA orientation using needle-electrodes. (B) The QDM gel adheres to the artery. (C) With forced probing the gel breaks off leaving gel adhered to the artery, indicating the gel adhesion is strong.

In collaboration with Dr. Raj Sarkar from the Baltimore Medical School, we are exploring EA for arterial anastomosis. We would like to try various patch types for different anastomosis repairs, such as end-to-end (create a cylindrical gel-patch), end-to-side (create a flange-like gel-patch). We have already completed EA on a bovine carotid artery used in bypass surgery with success. In Figure 6.6A we show the process of EA of QDM gel to a bovine graft used in bypass surgery. Figure 6.6B shows the artery is held up and the patch is stuck. In Figure 6.6C we attempt to pull of the QDM gel and it breaks in the process, indicating a strong adhesion was achieved.

Next, we were invited to test EA on human cadaver artery tissue at the Baltimore medical school. We will complete some experiments with human tissues in our next steps. EA to human tissue will bring this technology one step closer to a clinical setting.

6.2.6. Cardiac patches adhered with EA

As mentioned in 6.2.3, EA using the needle electrode set up achieves adhesion of QDM gel to heart epithelium. We would like to develop a cardiac patch that would provide either an electrical signal, a medical therapeutic, or localized stem cells to the heart. This cardiac patch would get adhered using EA. In our studies on anisotropic nature of muscle, we came to understand that the heart too has an anisotropy associated with its muscles. A big issue with heart injury leading to inefficient blood pumping out of the heart's left chamber is caused by stresses expanding the left heart. This is known as *left ventricular hypertrophy*. We would like to use our cardiac patch to address some of these issues by making it from a tough material that can counter the anisotropic nature of heart injury. This work would be done in collaboration with Dr. Ellen Roche from Material Science at MIT and Laurie Boyer from biological engineering at MIT.

6.2.7. Tissue and organ assembly from smaller units of pre-tissue

The last idea that is still in its infancy is using EA for assembling units of tissue to more complex 3D structures. The concept relies on the fact that to grow large tissues, a system of perfusion is needed (blood vessels to transport nutrients to the larger system). Tissues can get nutrient by diffusion only up to ~ 150 μm from a blood vessel. This limitation allows tissue engineers to create organ models that are either very small or have complex microfluidic channels for perfusion. We propose a unit gel made with a capillary for blood flow and cells incorporated within an ECM-like gel. We envision these units as "legos" or "bio-blocks" that can assemble in a specific order, connecting the capillaries as the units assemble to a larger connected tissue system.

Such a technique may affectively allow for building specific types of tissues from granular elements. With some growth, the tissues may become functional and in the far future may become a method for organ growth. The ECM-like gel work will be done in collaboration with Dr. Laurie Boyer from biological engineering at MIT. The assembly work may be a project I work on in the future, as faculty, when I begin a lab of my own.

References

[1] Regert, M.; Rodet-Belarbi, I.; Mazuy, A.; Le Dantec, G.; Dessì, R. M.; Le Briz, S.; Henry, A.; Rageot, M. "Birch-bark tar in the Roman world: The persistence of an ancient craft tradition?" *Antiquity* **2019**, *93*, 1553-1568.

[2] Abbott, S.; Destech Publications, I. *Adhesion science : principles and practice*; DEStech Publications: Lancaster, Pennyslvania, 2015.

[3] Lee, L.-H. *Fundamentals of adhesion*; Plenum Press: New York, 1991.

[4] Wake, W. C. "Theories of adhesion and uses of adhesives: A review." *Polymer* **1978**, *19*, 291-308.

[5] Zilhão, J. "Tar adhesives, Neandertals, and the tyranny of the discontinuous mind." *Proc. Natl. Acad. Sci.* **2019**, *116*, 21966-21968.

[6] Nam, S.; Mooney, D. J. "Polymeric tissue adhesives." *Chem. Rev.* **2021**, *121*, 11336-11384.

[7] Ahmadi, Z. "Nanostructured epoxy adhesives: A review." *Prog. Org. Coat.* **2019**, *135*, 449-453.

[8] Jovanović, R.; Dubé, M. A. "Emulsion-based pressure-sensitive adhesives: A review." *J. Macromol. Sci.* **2004**, *44*, 1-51.

[9] Khan, I.; Poh, B. T. "Natural rubber-based pressure-sensitive adhesives: A review." *J. Polym. Environ.* **2011**, *19*, 793-811.

[10] Li, W.; Bouzidi, L.; Narine, S. S. "Current research and development status and prospect of hot-melt adhesives: a review." *Ind. Eng. Chem. Res.* **2008**, *47*, 7524-7532.

[11] Stewart, R. J.; Ransom, T. C.; Hlady, V. "Natural underwater adhesives." *J. Polym. Sci. B Polym. Phys.* **2011**, *49*, 757-771.

[12] Hofman, A. H.; van Hees, I. A.; Yang, J.; Kamperman, M. "Bioinspired underwater adhesives by using the supramolecular toolbox." *Adv. Mater.* **2018**, *30*, 1704640.

[13] Li, Y.; Krahn, J.; Menon, C. "Bioinspired dry adhesive materials and their application in robotics: A review." *J. Bionic Eng.* **2016**, *13*, 181-199.

[14] Roberts, A. D.; Finnigan, W.; Wolde-Michael, E.; Kelly, P.; Blaker, J. J.; Hay, S.; Breitling, R.; Takano, E.; Scrutton, N. S. "Synthetic biology for fibres, adhesives and active camouflage materials in protection and aerospace." *MRS Commun* **2019**, *9*, 486-504.

[15] Aksak, B.; Murphy, M. P.; Sitti, M. “Gecko inspired micro-fibrillar adhesives for wall climbing robots on micro/nanoscale rough surfaces”; 2008 IEEE International Conference on Robotics and Automation, 2008.

[16] Yuk, H.; Wu, J.; Sarrafian, T. L.; Mao, X.; Varela, C. E.; Roche, E. T.; Griffiths, L. G.; Nabzdyk, C. S.; Zhao, X. “Rapid and coagulation-independent haemostatic sealing by a paste inspired by barnacle glue.” *Nat. Biomed. Eng.* **2021**, *5*, 1131-1142.

[17] King, D. R.; Bartlett, M. D.; Gilman, C. A.; Irschick, D. J.; Crosby, A. J. “Creating gecko-like adhesives for “real world” surfaces.” *Adv. Mater.* **2014**, *26*, 4345-4351.

[18] Asoh, T. A.; Kikuchi, A. “Electrophoretic adhesion of stimuli-responsive hydrogels.” *Chemical communications* **2010**, *46*, 7793-5.

[19] Borden, L. K.; Gargava, A.; Raghavan, S. R. “Reversible electroadhesion of hydrogels to animal tissues for suture-less repair of cuts or tears.” *Nat. Commun.* **2021**, *12*, 4419.

[20] Asoh, T. A.; Kawamura, E.; Kikuchi, A. “Stabilization of electrophoretically adhered gel-interfaces to construct multi-layered hydrogels.” *RSC Adv.* **2013**, *3*, 7947-7952.

[21] Asoh, T. A.; Nakamura, M.; Shoji, T.; Tsuboi, Y.; Uyama, H. “Electrophoretic adhesion of conductive hydrogels.” *Macromol. Rapid Comm.* **2020**, *41*, 2000169.

[22] Asoh, T. A.; Kawai, W.; Kikuchi, A. “Electrophoretic adhesion of biodegradable hydrogels through the intermediary of oppositely charged polyelectrolytes.” *Soft Matter* **2012**, *8*, 1923-1927.

[23] Morales, D.; Palleau, E.; Dickey, M. D.; Velev, O. D. “Electro-actuated hydrogel walkers with dual responsive legs.” *Soft Matter* **2014**, *10*, 1337-1348.

[24] Xin, A.; Zhang, R. R.; Yu, K. H.; Wang, Q. M. “Mechanics of electrophoresis-induced reversible hydrogel adhesion.” *J. Mech. Phys. Solids* **2019**, *125*, 1-21.

[25] Ryou, M.; Thompson, C. C. “Tissue adhesives: A review.” *Tech. Gastrointest. Endosc.* **2006**, *8*, 33-37.

[26] Bhagat, V.; Becker, M. L. “Degradable adhesives for surgery and tissue engineering.” *Biomacromolecules* **2017**, *18*, 3009-3039.

[27] Bruns, T. B.; Worthington, J. M. “Using tissue adhesive for wound repair: A practical guide to Dermabond.” *Am. Family Physician* **2000**, *61*, 1383-1388.

[28] Sanders, L.; Nagatomi, J. “Clinical applications of surgical adhesives and sealants.” *Crit. Rev. Biomed. Eng.* **2014**, *42*, 271-92.

[29] Behrens, A. M.; Lee, N. G.; Casey, B. J.; Srinivasan, P.; Sikorski, M. J.; Daristotle, J. L.; Sandler, A. D.; Kofinas, P. "Biodegradable-polymer-blend-based surgical sealant with body-temperature-mediated adhesion." *Adv. Mater.* **2015**, *27*, 8056-8061.

[30] Daristotle, J. L.; Zaki, S. T.; Lau, L. W.; Torres, L.; Zografos, A.; Srinivasan, P.; Ayyub, O. B.; Sandler, A. D.; Kofinas, P. "Improving the adhesion, flexibility, and hemostatic efficacy of a sprayable polymer blend surgical sealant by incorporating silica particles." *Acta Biomater.* **2019**, *90*, 205-216.

[31] Duarte, A. P.; Coelho, J. F.; Bordado, J. C.; Cidade, M. T.; Gil, M. H. "Surgical adhesives: Systematic review of the main types and development forecast." *Prog. Polym. Sci.* **2012**, *37*, 1031-1050.

[32] Ahmed, E. M. "Hydrogel: Preparation, characterization, and applications: A review." *J. Adv. Res.* **2015**, *6*, 105-121.

[33] Tanaka, T. "Gels." *Sci. Am.* **1981**, *244*, 124-36, 138.

[34] Osada, Y.; Gong, J.-P. "Soft and wet materials: Polymer gels." *Adv. Mater.* **1998**, *10*, 827-837.

[35] Laftah, W. A.; Hashim, S.; Ibrahim, A. N. "Polymer hydrogels: A review." *Polym. Plast. Technol. Eng.* **2011**, *50*, 1475-1486.

[36] Kopeček, J. "Hydrogels from soft contact lenses and implants to self-assembled nanomaterials." *J. Polym. Sci. A Polym. Chem.* **2009**, *47*, 5929-5946.

[37] Sannino, A.; Demitri, C.; Madaghiele, M. "Biodegradable cellulose-based hydrogels: Design and applications." *Materials* **2009**, *2*, 353-73.

[38] Fonkwe, L. G.; Narsimhan, G.; Cha, A. S. "Characterization of gelation time and texture of gelatin and gelatin–polysaccharide mixed gels." *Food Hydrocoll.* **2003**, *17*, 871-883.

[39] Musgrave, C. S. A.; Fang, F. "Contact lens materials: A materials science perspective." *Materials* **2019**, *12*, 261.

[40] Kim, S. H.; Marmo, C.; Somorjai, G. A. "Friction studies of hydrogel contact lenses using AFM: Non-crosslinked polymers of low friction at the surface." *Biomaterials* **2001**, *22*, 3285-3294.

[41] Escobedo, F. A.; de Pablo, J. J. "Molecular simulation of polymeric networks and gels: phase behavior and swelling." *Phys. Rep.* **1999**, *318*, 85-112.

[42] Anseth, K. S.; Bowman, C. N.; Brannon-Peppas, L. "Mechanical properties of hydrogels and their experimental determination." *Biomaterials* **1996**, *17*, 1647-1657.

[43] Kim, C. S.; Oh, S. M. “Performance of gel-type polymer electrolytes according to the affinity between polymer matrix and plasticizing solvent molecules.” *Electrochim. Acta* **2001**, *46*, 1323-1331.

[44] Richbourg, N. R.; Peppas, N. A. “The swollen polymer network hypothesis: Quantitative models of hydrogel swelling, stiffness, and solute transport.” *Prog. Polym. Sci.* **2020**, *105*, 101243.

[45] Myung, D.; Waters, D.; Wiseman, M.; Duhamel, P. E.; Noolandi, J.; Ta, C. N.; Frank, C. W. “Progress in the development of interpenetrating polymer network hydrogels.” *Polym. Adv. Technol.* **2008**, *19*, 647-657.

[46] Sperling, L. H. “Interpenetrating polymer networks: An overview.” in *Interpenetrating polymer networks*; American Chemical Society, 1994; Vol. 239; pp 3-38.

[47] Gong, J. P. “Why are double network hydrogels so tough?” *Soft Matter* **2010**, *6*, 2583-2590.

[48] Wanasingha, N.; Dorishetty, P.; Dutta, N. K.; Choudhury, N. R. “Polyelectrolyte gels: Fundamentals, fabrication and applications.” *Gels* **2021**, *7*, 148.

[49] Kwon, H. J.; Osada, Y.; Gong, J. P. “Polyelectrolyte gels-fundamentals and applications.” *Polym. J.* **2006**, *38*, 1211-1219.

[50] Viovy, J. L. “Electrophoresis of DNA and other polyelectrolytes: Physical mechanisms.” *Rev. Mod. Phys.* **2000**, *72*, 813-872.

[51] Lankalapalli, S.; Kolapalli, V. R. “Polyelectrolyte complexes: A review of their applicability in drug delivery technology.” *Indian J. Pharm. Sci.* **2009**, *71*, 481-7.

[52] Lee, C.-J.; Wu, H.; Hu, Y.; Young, M.; Wang, H.; Lynch, D.; Xu, F.; Cong, H.; Cheng, G. “Ionic conductivity of polyelectrolyte hydrogels.” *ACS Appl. Mater. Interfaces* **2018**, *10*, 5845-5852.

[53] Bret, M. L.; Zimm, B. H. “Distribution of counterions around a cylindrical polyelectrolyte and manning's condensation theory.” *Biopolymers* **1984**, *23*, 287-312.

[54] Li, H.; Erbaş, A.; Zwanikken, J.; Olvera de la Cruz, M. “Ionic conductivity in polyelectrolyte hydrogels.” *Macromolecules* **2016**, *49*, 9239-9246.

[55] Cipriano, B. H.; Banik, S. J.; Sharma, R.; Rumore, D.; Hwang, W.; Briber, R. M.; Raghavan, S. R. “Superabsorbent hydrogels that are robust and highly stretchable.” *Macromolecules* **2014**, *47*, 4445-4452.

[56] Ebnesajjad, S.; Lanck, A. H.“Adhesives technology handbook.” **2014**.

[57] Autumn, K.; Sitti, M.; Liang, Y. A.; Peattie, A. M.; Hansen, W. R.; Sponberg, S.; Kenny, T. W.; Fearing, R.; Israelachvili, J. N.; Full, R. J. "Evidence for van der Waals adhesion in gecko setae." *PNAS* **2002**, *99*, 12252-12256.

[58] Ochi, M.; Takahashi, R.; Terauchi, A. "Phase structure and mechanical and adhesion properties of epoxy/silica hybrids." *Polymer* **2001**, *42*, 5151-5158.

[59] Gordon, T. L.; Fakley, M. E. "The influence of elastic modulus on adhesion to thermoplastics and thermoset materials." *Int. J. Adhes. Adhes.* **2003**, *23*, 95-100.

[60] Meredith, H. J.; Wilker, J. J. "The interplay of modulus, strength, and ductility in adhesive design using biomimetic polymer chemistry." *Adv. Funct. Mater.* **2015**, *25*, 5057-5065.

[61] Houston, S.; Hodge Jr., J. W.; Ousterhout, D. K.; Leonard, F. "The effect of α-cyanoacrylates on wound healing." *J. Biomed. Mater. Res.* **1969**, *3*, 281-289.

[62] Okada, M.; Hara, E. S.; Yabe, A.; Okada, K.; Shibata, Y.; Torii, Y.; Nakano, T.; Matsumoto, T. "Titanium as an instant adhesive for biological soft tissue." *Adv. Mater. Interfaces* **2020**, *7*, 1902089.

[63] Li, J.; Celiz, A. D.; Yang, J.; Yang, Q.; Wamala, I.; Whyte, W.; Seo, B. R.; Vasilyev, N. V.; Vlassak, J. J.; Suo, Z.; Mooney, D. J. "Tough adhesives for diverse wet surfaces." *Science* **2017**, *357*, 378-381.

[64] Zhou, J. J.; Defante, A. P.; Lin, F.; Xu, Y.; Yu, J. Y.; Gao, Y. H.; Childers, E.; Dhinojwala, A.; Becker, M. L. "Adhesion properties of catechol-based biodegradable amino acid-based poly(ester urea) copolymers inspired from mussel proteins." *Biomacromolecules* **2015**, *16*, 266-274.

[65] Lu, S. C.; Zhang, X. H.; Tang, Z. W.; Xiao, H.; Zhang, M.; Liu, K.; Chen, L. H.; Huang, L. L.; Ni, Y. H.; Wu, H. "Mussel-inspired blue-light-activated cellulose-based adhesive hydrogel with fast gelation, rapid haemostasis and antibacterial property for wound healing." *Chem. Eng. J.* **2021**, *417*, 129329.

[66] Fullenkamp, D. E.; Barrett, D. G.; Miller, D. R.; Kurutz, J. W.; Messersmith, P. B. "pH-dependent cross-linking of catechols through oxidation via Fe3+ and potential implications for mussel adhesion." *RSC Adv.* **2014**, *4*, 25127-25134.

[67] Hong, Y.; Zhou, F.; Hua, Y.; Zhang, X.; Ni, C.; Pan, D.; Zhang, Y.; Jiang, D.; Yang, L.; Lin, Q.; Zou, Y.; Yu, D.; Arnot, D. E.; Zou, X.; Zhu, L.; Zhang, S.; Ouyang, H. "A strongly adhesive hemostatic hydrogel for the repair of arterial and heart bleeds." *Nat. Commun.* **2019**, *10*, 2060.

[68] Spotnitz, W. D. "Fibrin sealant: The only approved hemostat, sealant, and adhesive-a laboratory and clinical perspective." *ISRN Surg.* **2014**, *2014*, 203943.

[69] Lopezcarasa-Hernandez, G.; Perez-Vazquez, J.-F.; Guerrero-Naranjo, J.-L.; Martinez-Castellanos, M. A. "Versatility of use of fibrin glue in wound closure and vitreo-retinal surgery." *Int. J. Retina Vitr.* **2021**, *7*, 33.

[70] Miyawaki, O.; Omote, C.; Matsuhira, K. "Thermodynamic analysis of sol-gel transition of gelatin in terms of water activity in various solutions." *Biopolymers* **2015**, *103*, 685-91.

[71] Xiang, L.; Cui, W. "Biomedical application of photo-crosslinked gelatin hydrogels." *J. Leather Sci. Eng.* **2021**, *3*, 3.

[72] Zosel, A. "Adhesive failure and deformation behaviour of polymers." *J. Adhes.* **1989**, *30*, 135-149.

[73] Kashihara, Y.; Okada, S.; Urahama, Y.; Hikasa, S.; Makuta, S.; Fujiwara, K.; Fujii, S.; Nakamura, Y. "Effects of the degree of crosslinking and test rate on the tensile properties of a crosslinked polyacrylic pressure-sensitive adhesive and vulcanized rubber." *J. Appl. Polym. Sci.* **2019**, *136*, 47272.

[74] Wang, Y.; Yang, X.; Nian, G.; Suo, Z. "Strength and toughness of adhesion of soft materials measured in lap shear." *J. Mech. Phys. Solids* **2020**, *143*, 103988.

[75] Erdi, M.; Rozyyev, S.; Balabhadrapatruni, M.; Saruwatari, M. S.; Daristotle, J. L.; Ayyub, O. B.; Sandler, A. D.; Kofinas, P. "Sprayable tissue adhesive with biodegradation tuned for prevention of postoperative abdominal adhesions." *Bioeng. Transl. Med.* **2022**, *n/a*, e10335.

[76] Liu, J.; Lin, S.; Liu, X.; Qin, Z.; Yang, Y.; Zang, J.; Zhao, X. "Fatigue-resistant adhesion of hydrogels." *Nat. Commun.* **2020**, *11*, 1071.

[77] Eitner, U.; Rendler, L. C. "The mechanical theory behind the peel test." *Energy Procedia* **2014**, *55*, 331-335.

[78] ASTM-F2255-05 *Standard test method for strength properties of tissue adhesives in lap-shear by tension loading.*; ASTM International: West Conshocken, PA, 2015.

[79] Campbell, F. C. "Adhesive bonding and integrally coccured structure: A way to reduce assembly costs through parts integration." in *Manufacturing processes for advanced composites*; Campbell, F. C., Ed.; Elsevier Science: Amsterdam, 2004; pp 241-301.

[80] Pandey, V.; Fleury, A.; Villey, R.; Creton, C.; Ciccotti, M. "Linking peel and tack performances of pressure sensitive adhesives." *Soft Matter* **2020**, *16*, 3267-3275.

[81] von Fraunhofer, J. A. "Adhesion and cohesion." *Int. J. Dent.* **2012**, *2012*, 951324.

[82] Asoh, T. A.; Kikuchi, A. "Rapid fabrication of reconstructible hydrogels by electrophoretic microbead adhesion." *Chem. Commun.* **2012**.

[83] Bamber, T.; Guo, J.; Singh, J.; Bigharaz, M.; Petzing, J.; Bingham, P. A.; Justham, L.; Penders, J.; Jackson, M. "Visualization methods for understanding the dynamic electroadhesion phenomenon." *J. Phys. D* **2017**, *50*, e205304.

[84] Asoh, T. A. "Electrophoretic hydrogel adhesion for fabrication of three-dimensional materials." *Polym. J.* **2016**, *48*, 1095–1101.

[85] Taguchi, T. "Assembly of cells and vesicles for organ engineering." *Sci. Technol. Adv. Mater.* **2011**, *12*, 064703.

[86] Javvaji, V.; Dowling, M. B.; Oh, H.; White, I. M.; Raghavan, S. R. "Reversible gelation of cells using self-assembling hydrophobically-modified biopolymers: Towards self-assembly of tissue." *Biomater. Sci.* **2014**, *2*, 1016-1023.

[87] Annabi, N.; Tamayol, A.; Shin, S. R.; Ghaemmaghami, A. M.; Peppas, N. A.; Khademhosseini, A. "Surgical materials: Current challenges and nano-enabled solutions." *Nano Today* **2014**, *9*, 574-589.

[88] Smith, D. J.; Brat, G. A.; Medina, S. H.; Tong, D. D.; Huang, Y.; Grahammer, J.; Furtmuller, G. J.; Oh, B. C.; Nagy-Smith, K. J.; Walczak, P.; Brandacher, G.; Schneider, J. P. "A multiphase transitioning peptide hydrogel for suturing ultrasmall vessels." *Nat. Nanotechnol.* **2016**, *11*, 95-+.

[89] Godoy-Gallardo, M.; Labay, C.; Trikalitis, V. D.; Kempen, P. J.; Larsen, J. B.; Andresen, T. L.; Hosta-Rigau, L. "Multicompartment Artificial Organelles Conducting Enzymatic Cascade Reactions inside Cells." *ACS Appl. Mater. Interfaces* **2017**, *9*, 15907-15921.

[90] Apostolakis, E. E.; Leivaditis, V. N.; Anagnostopoulos, C. "Sutureless technique to support anastomosis during thoracic aorta replacement." *J. Cardiothoracic Surg.* **2009**, *4*, 1749-8090.

[91] Gargava, A.; Ahn, S.; Bentley, W. E.; Raghavan, S. R. "Rapid electroformation of biopolymer gels in prescribed shapes and patterns: A simpler alternative to 3-D printing." *ACS Appl. Mater. Interfaces* **2019**, *11*, 37103-37111.

[92] ASTM-D1002-10 *Standard test method for apparent shear strength of single-lap-joint adhesively bonded metal specimens by tension loading (metal-to-metal).* ASTM International: West Conshocken, PA, 2019.

[93] Gharazi, S.; Zarket, B. C.; DeMella, K. C.; Raghavan, S. R. "Nature-inspired hydrogels with soft and stiff zones that exhibit a 100-fold difference in elastic modulus." *ACS Appl. Mater. Interfaces* **2018**, *10*, 34664-34673.

[94] Fu, Z. F.; Chen, R. "Study of complexes of tannic acid with Fe(III) and Fe(II)." *J. Anal. Methods Chem.* **2019**, 3894571.

[95] Bird, R. B.; Stewart, W. E.; Lightfoot, E. N. *Transport Phenomena*, 2nd ed.; Wiley: New York, 2002.

[96] OpenStaxCollege *Biology*; Downloadable at: http://cnx.org/content/col11448/latest/, 2013.

[97] Neuman, R. E.; Logan, M. A. "The determination of collagen and elastin in tissues." *J. Biol. Chem.* **1950**, *186*, 549-556.

[98] Bendall, J. R. "Elastin content of various muscles of beef animals." *J. Sci. Food Agric.* **1967**, *18*, 553-558.

[99] Tsamis, A.; Krawiec, J. T.; Vorp, D. A. "Elastin and collagen fibre microstructure of the human aorta in ageing and disease: A review." *J. Royal Soc. Interface* **2013**, *10*, 20121004.

[100] Tseng, S. C. G.; Smuckler, D.; Stern, R. "Comparison of collagen types in adult and fetal bovine corneas." *J. Biol. Chem.* **1982**, *257*, 2627-2633.

[101] Yin, J. H.; Xia, Y.; Lu, M. "Concentration profiles of collagen and proteoglycan in articular cartilage by fourier transform infrared imaging and principal component regression." *Spectrochim. Acta A* **2012**, *88*, 90-96.

[102] Feneck, E. M.; Lewis, P. N.; Ralphs, J.; Meek, K. M. "A comparative study of the elastic fibre system within the mouse and human cornea." *Exp. Eye Res.* **2018**, *177*, 35-44.

[103] Taylor, Z. D.; Garritano, J.; Sung, S. J.; Bajwa, N.; Bennett, D. B.; Nowroozi, B.; Tewari, P.; Sayre, J.; Hubschman, J. P.; Deng, S.; Brown, E. R.; Grundfest, W. S. "THz and mm-wave sensing of corneal tissue water content: Electromagnetic modeling and analysis." *Ieee T. Thz. Sci. Techn.* **2015**, *5*, 170-183.

[104] Mitchell, H. H.; Hamilton, T. S.; Steggerda, F. R.; Bean, H. W. "The chemical composition of the adult human body and its bearing on the biochemistry of growth." *J. Biol. Chem.* **1945**, *158*, 625-637.

[105] Mansfield, J.; Yu, J.; Attenburrow, D.; Moger, J.; Tirlapur, U.; Urban, J.; Cui, Z. F.; Winlove, P. "The elastin network: its relationship with collagen and cells in articular cartilage as visualized by multiphoton microscopy." *J. Anat.* **2009**, *215*, 682-691.

[106] Sophia Fox, A. J.; Bedi, A.; Rodeo, S. A. "The basic science of articular cartilage: Structure, composition, and function." *Sports health* **2009**, *1*, 461-8.

[107] Aparecida de Aro, A.; Vidal Bde, C.; Pimentel, E. R. "Biochemical and anisotropical properties of tendons." *Micron* **2012**, *43*, 205-14.

[108] Divoux, A.; Tordjman, J.; Lacasa, D.; Veyrie, N.; Hugol, D.; Aissat, A.; Basdevant, A.; Guerre-Millo, M.; Poitou, C.; Zucker, J. D.; Bedossa, P.; Clement, K. "Fibrosis in human adipose tissue: Composition, distribution, and link with lipid metabolism and fat mass loss." *Diabetes* **2010**, *59*, 2817-25.

[109] Spencer, M.; Unal, R.; Zhu, B.; Rasouli, N.; McGehee, R. E., Jr.; Peterson, C. A.; Kern, P. A. "Adipose tissue extracellular matrix and vascular abnormalities in obesity and insulin resistance." *J. Clin. Endocrinol. Metab.* **2011**, *96*, E1990-8.

[110] Pearse, G. "Normal structure, function and histology of the thymus." *Toxicol. Pathol.* **2006**, *34*, 504-14.

[111] Shoulders, M. D.; Raines, R. T. "Collagen structure and stability." *Annu. Rev. Biochem.* **2009**, *78*, 929-958.

[112] Highberger, J. H. "The isoelectric point of collagen." *J. Am. Chem. Soc.* **1939**, *61*, 2302-2303.

[113] Scott, J. E. "Proteoglycan fibrillar collagen interactions." *Biochem. J.* **1988**, *252*, 313-323.

[114] Dalziel, C. F.; Mansfield, T. H. "Effect of frequency on perception currents." *Trans. Am. Inst. Elec. Eng.* **1950**, *69*.

[115] Miklavčič, D.; Pavšelj, N.; Hart, F. H. "Electric properties of tissues." in *Wiley Encyclopedia of Biomedical Engineering: John Wiley & Sons, Inc.*; John Wiley & Sons, Inc., 2006; Vol. 6; pp 3578-3589.

[116] Hronik-Tupaj, M.; Kaplan, D. L. "A review of the responses of two- and three-dimensional engineered tissues to electric fields." *Tissue. Eng. Part B Rev.* **2012**, *18*, 167-80.

[117] Mezzenga, R.; Schurtenberger, P.; Burbidge, A.; Michel, M. "Understanding foods as soft materials." *Nat. Mater.* **2005**, *4*, 729-740.

[118] Li, J.; Wong, W.-Y.; Tao, X.-M. "Recent advances in soft functional materials: Preparation, functions and applications." *Nanoscale* **2020**, *12*, 1281-1306.

[119] Guimarães, C. F.; Gasperini, L.; Marques, A. P.; Reis, R. L. "The stiffness of living tissues and its implications for tissue engineering." *Nat. Rev. Mater.* **2020**, *5*, 351-370.

[120] Poon, W.; McLeish, T.; Donald, A. "Soft condensed matter: Where physics meets biology." *Phys. World* **2001**, *14*, 33-38.

[121] de Gennes, P.-G. "Soft Matter (Nobel Lecture)." *Angew. Chem., Int. Ed. Engl.* **1992**, *31*, 842-845.

[122] Gonzalez-Rodriguez, D.; Guevorkian, K.; Douezan, S.; Brochard-Wyart, F. “Soft matter models of developing tissues and tumors.” *Science* **2012**, *338*, 910-7.

[123] Guo, J. L.; Leng, J. S.; Rossiter, J. “Electroadhesion technologies for robotics: A comprehensive review.” *IEEE Trans. Robot.* **2020**, *36*, 313-327.

[124] Monkman, G. “Electroadhesive microgrippers.” *Ind. Rob.* **2003**, *30*, 326-330.

[125] Nakamura, T.; Yamamoto, A. “Modeling and control of electroadhesion force in DC voltage.” *Robomech. J.* **2017**, *4*, 18.

[126] Shultz, C. D.; Peshkin, M. A.; Colgate, J. E. “Surface haptics via electroadhesion: Expanding electrovibration with Johnsen and Rahbek”; 2015 IEEE World Haptics Conference (WHC), 2015.

[127] Shintake, J.; Rosset, S.; Schubert, B.; Floreano, D.; Shea, H. “Versatile soft grippers with intrinsic electroadhesion based on multifunctional polymer actuators.” *Adv. Mater.* **2016**, *28*, 231-238.

[128] Kim, H. J.; Paquin, L.; Barney, C. W.; So, S.; Chen, B.; Suo, Z.; Crosby, A. J.; Hayward, R. C. “Low-voltage reversible electroadhesion of ionoelastomer junctions.” *Adv. Mater.* **2020**, *32*, e2000600.

[129] Ladd, C. D. “Design and characterization of electroresponsive polymers based on the Johnsen-Rahbek effect”, 2016.

[130] Koch, K.; Ensikat, H.-J. “The hydrophobic coatings of plant surfaces: Epicuticular wax crystals and their morphologies, crystallinity and molecular self-assembly.” *Micron* **2008**, *39*, 759-772.

[131] Zullo, L.; Bozzo, M.; Daya, A.; Di Clemente, A.; Mancini, F. P.; Megighian, A.; Nesher, N.; Röttinger, E.; Shomrat, T.; Tiozzo, S.; Zullo, A.; Candiani, S. “The diversity of muscles and their regenerative potential across animals.” *Cells* **2020**, *9*, 1925.

[132] Ju, Y. H.; Lee, H.-J.; Han, C. J.; Lee, C.-R.; Kim, Y.; Kim, J.-W. “Water-responsive pressure-sensitive adhesive with reversibly changeable adhesion for fabrication of stretchable devices.” *Mater. Des.* **2020**, *195*, 108995.

[133] Witter, K.; Tonar, Z.; Schöpper, H. “How many layers has the adventitia? - structure of the arterial tunica externa revisited.” *Anat. Histol. Embryol.* **2017**, *46*, 110-120.

[134] Cooper, G. M. *The cell: A molecular approach*; Sinauer Associates: Sunderland (MA), 2000; Vol. .

[135] Sridhar, M. S. “Anatomy of cornea and ocular surface.” *Indian J. Ophthalmol.* **2018**, *66*, 190-194.

[136] Schnetler, R.; Gillan, W. D. H.; Koorsen, G. “Immunological and antimicrobial molecules in human tears: A review and preliminary report.” *S. Afr. Optom.* **2012**, 10.

[137] Johnstone, M. A. “Aqueous humor outflow system overview.” in *Becker-Shaffer's Diagnosis and Therapy of the Glaucomas (Eighth Edition)*; Stamper, R. L., Lieberman, M. F., Drake, M. V., Eds.; Mosby: Edinburgh, 2009; pp 25-46.

[138] Braidwood, L.; Breuer, C.; Sugimoto, K. “My body is a cage: Mechanisms and modulation of plant cell growth.” *New Phytol.* **2014**, *201*, 388-402.

[139] Prasanna, V.; Prabha, T. N.; Tharanathan, R. N. “Fruit ripening phenomena-an overview.” *Crit. Rev. Food Sci. Nutr.* **2007**, *47*, 1-19.

[140] Daher, F. B.; Braybrook, S. A. “How to let go: Pectin and plant cell adhesion.” *Front. Plant Sci.* **2015**, *6*, 523.

[141] Kuravi, R.; Leichsenring, K.; Trostorf, R.; Morales-Orcajo, E.; Böl, M.; Ehret, A. E. “Predicting muscle tissue response from calibrated component models and histology-based finite element models.” *J. Mech. Behav. Biomed. Mater.* **2021**, *117*, 104375.

[142] Soliman, M.; Atteia, S.; Kefafy, M.; Ali, A.; Radwan, E. “Histological study on the effect of rosuvastatin (Crestor) on the skeletal muscle of adult male albino rats and the possible protective effect of coenzyme Q10.” *Menoufia Med. J.* **2017**, *30*, 1117-1124.

[143] Guerriero, G.; Hausman, J. F.; Cai, G. “No stress! Relax! Mechanisms governing growth and shape in plant cells.” *Int. J. Mol. Sci.* **2014**, *15*, 5094-114.

[144] Johnsen, A.; Rahbek, K. L. “A physical phenomenon and its applications to telegraphy, telephony, etc.” *J. Electr. Eng.* **1923**, *61*, 713-725.

[145] Prahlad, H.; Pelrine, R.; Stanford, S.; Marlow, J.; Kornbluh, R. “Electroadhesive robots—wall climbing robots enabled by a novel, robust, and electrically controllable adhesion technology”; 2008 IEEE International Conference on Robotics and Automation, 2008.

[146] Schein, L. B. “Recent progress and continuing puzzles in electrostatics.” *Science* **2007**, *316*, 1572-1573.

[147] Sogard, M. R.; Mikkelson, A. R.; Nataraju, M.; Turner, K. T.; Engelstad, R. L. “Analysis of Coulomb and Johnsen-Rahbek electrostatic chuck performance for extreme ultraviolet lithography.” *J. Vac. Sci. Technol. B* **2007**, *25*, 2155-2161.

[148] Shim, G. I.; Sugai, H. “Dechuck operation of coulomb type and johnsen-rahbek type of electrostatic chuck used in plasma processing.” *J. plasma fusion res. ser.* **2008**, *3*, 051-051.

[149] Jana, S.; Hu, M.; Shen, M.; Kassiri, Z. “Extracellular matrix, regional heterogeneity of the aorta, and aortic aneurysm.” *Exp. Mol. Med.* **2019**, *51*, 1-15.

[150] Kim, Y.; Ko, H.; Kwon, I. K.; Shin, K. “Extracellular matrix revisited: Roles in tissue engineering.” *Int. Neurourol. J.* **2016**, *20*, S23-29.

[151] González-Díaz, E. C.; Varghese, S. “Hydrogels as extracellular matrix analogs.” *Gels* **2016**, *2*, e2030020.

[152] Kurn, H. D., D.T.; *Histology, epithelial cell.* ; StatPearls Publishing: Treasure Island (FL), 2021.

[153] Miller, C. C.; Walker, J. “The Stokes-Einstein law for diffusion in solution.” *Proc. R. soc. Lond. Ser. A-Contain. Pap. Math. Phys. Character* **1924**, *106*, 724-749.

[154] Cayre, O. J.; Chang, S. T.; Velev, O. D. “Polyelectrolyte diode: Nonlinear current response of a junction between aqueous ionic jels.” *J. Am. Chem. Soc.* **2007**, *129*, 10801-10806.

[155] Yamamoto, T.; Doi, M. “Electrochemical mechanism of ion current rectification of polyelectrolyte gel diodes.” *Nat. Commun.* **2014**, *5*, 4162.

[156] Nyamayaro, K.; Triandafilidi, V.; Keyvani, P.; Rottler, J.; Mehrkhodavandi, P.; Hatzikiriakos, S. G. “The rectification mechanism in polyelectrolyte gel diodes.” *Phys. Fluids* **2021**, *33*, 032010.

[157] Cuomo, F.; Lopez, F.; Miguel, M. G.; Lindman, B. “Vesicle-templated layer-by-layer assembly for the production of nanocapsules.” *Langmuir* **2010**, *26*, 10555-10560.

[158] Correa, S.; Boehnke, N.; Deiss-Yehiely, E.; Hammond, P. T. “Solution conditions tune and optimize loading of therapeutic polyelectrolytes into layer-by-layer functionalized liposomes.” *ACS Nano* **2019**, *13*, 5623-5634.

[159] Zhang, L.; Zheng, M.; Liu, X.; Sun, J. “Layer-by-layer assembly of salt-containing polyelectrolyte complexes for the fabrication of dewetting-induced porous coatings.” *Langmuir* **2011**, *27*, 1346-1352.

[160] Wang, Q. M.; Schlenoff, J. B. “The polyelectrolyte complex/coacervate continuum.” *Macromolecules* **2014**, *47*, 3108-3116.

[161] Urone, P. P. H., R.;. “College Physics.” 2e ed.; OpenStax: Houston, Texas, 2022.

List of Publications

Publications that have appeared in print:

1. **L. K. Borden,** A. Gargava and S. R. Raghavan
   Reversible Electroadhesion of Hydrogels to Animal Tissues for Suture-less Repair of Cuts or Tears.
   Nature Communications, 12, 4419 (2021). DOI: 10.1038/s41467-021-24022-x

2. S. Jafilan, **L. K. Borden,** C. Hyun and J. Florian
   Intermolecular Base Stacking of Dinucleoside Monophosphate Anions in Aqueous Solution.
   The Journal of *Physical Chemistry B*., 116,11:3613-3618 (2012). DOI: 10.1021/jp209986y

Publications that have been submitted and under review:

1. S. Ahn, **L. K. Borden**, S. N. Subraveti, W. Bentley and S. R Raghavan
   Multicompartment Capsules with Smart Inner Compartments Responsive to Enzyme, ROS and Light.
   Manuscript submitted to *Small,* on October 30th, 2022

2. **L. K. Borden**†**,** A. Gargava†, U. Kokilepersaud and S. R. Raghavan
   Electroadhesion in Capsule-Capsule and Capsule-Gel Systems: A New Way to Reversibly Connect and Assemble Diverse Soft Materials.
   Manuscript submitted to *Matter,* on November 10th, 2022.

Publications that will be submitted:

3. **L. K. Borden**, U. Kokilepersaud, F. Burni, M. Saruwatari, M. Erdi, P. Kofinas, A. Sandler and S. R. Raghavan
   Electroadhesion of Gels to Various Animal and Plant Tissues
   Manuscript will be submitted to *PNAS*. Tentative submission December 15th, 2022

4. U. Kokilepersaud, **L. K. Borden**, and S. R. Raghavan
   Tough and Biocompatible Hydrogels for Ex-Vivo Sutureless Repair of Intestinal Cuts and Tears.
   Manuscript will be submitted to *Biomaterials*. Tentative submission December 15th, 2022

5. **L. K. Borden,** M. Nadar, S. Grasso, M. Erdi, P. Kofinas, and S. R. Raghavan
   Mechanism for Electroadhesion: Why Gels can be Permanently Adhered to Tissues by Applying a DC Electric Field
   Manuscript will be submitted to *XXX*. Tentative submission February 2023

6. **L. K. Borden**†**,** D. Boegner†, M. Wheeler, S. R. Raghavan and I. White
   Electric Field Parameter Optimization for Electroadhesion Risk Minimization in Survival

Studies
Manuscript will be submitted to *XXX*. Tentative submission February 2023

7. **L. K. Borden**[†]**,** M. Saruwatari[†], D. Boegner, I. White, A. Sandler, and S. R. Raghavan
Electroadhesion of Gel-Patches to Mouse Intestine for Anastomosis Repairs
Manuscript will be submitted to *Science Advances*. Tentative submission February 2023

Patents

1. **Borden, L. K.**; Raghavan, S. R.
Reversible Electroadhesion of Hydrogels to Animal Tissues for Suture-Less Repair of Cuts or Tears.
PCT application No. PCT/US2022/073562, filed on July 8, 2022

2. **Borden, L. K.**; Boegner, D.; White, I
Medical Device and Electric Field Optimization for Intestinal Repairs Using Electroadhesion.
Patent to be filed December 2022

List of Presentations

<u>Presentations that have been delivered:</u>

Invited Talks:

1. **University of Minnesota, Department of Biomedical Engineering - Departmental Seminar (Given on 03/16/2022)**
   Adhesion and Assembly of Hydrogels and Tissues Using Electric Fields: Aims at Tissue Repair and Construction

Conference (Oral) Presentations:

2. **L. K. Borden** and S. R. Raghavan
   Advances in Replacement of Sutures and Surgical Glues by Switchable Electroadhesion of Polyelectrolyte Hydrogel to Animal Tissue.
   Society For Biomaterials, Baltimore MD, 2022
   <u>Received Honorable Mention</u>

3. **L. K. Borden,** A. Gargava, A and S. R. Raghavan
   Stimuli Responsive Reversible Adhesion between Physical and Chemical Networks.
   AICHE annual meeting, Boston MA, 2021

4. **L. K. Borden** and S. R. Raghavan
   Electroadhesion of Polyelectrolyte Hydrogels to Animal Tissues: A Simple Way to Reseal Cut or Damaged Tissues without Sutures.
   AICHE annual meeting in Boston MA, 2021

5. **L. K. Borden** and S. R. Raghavan
   Electroadhesion of Polyelectrolyte Hydrogels to Tissues: Prospects for Suture-less Surgery.
   Pacifichem, HI, 2021

6. **L. K. Borden** and S. R. Raghavan
   Deciphering the Mechanism of Electrically Triggered Adhesion in Gel-Gel, Gel-Tissue and Gel-Plant Systems.
   Pacifichem, HI, 2021

7. **L. K. Borden** and S. R. Raghavan
   Reversible Electroadhesion of Hydrogels to Animal Tissues for Suture-Less Repair of Cuts or Tears
   BMES Annual Meeting, Orlando FL, 2021

8. **L. K. Borden** and S. R. Raghavan
   Reversible Electroadhesion of Polyelectrolyte Hydrogels to New Classes of Soft Matter.
   Virtual Adhesion Science Gathering, August 2021

9. **L. K. Borden,** A. Gargava, A and S. R. Raghavan

Electroadhesion of Polymer Capsules to Hydrogels: A New Way to Manipulate Soft Materials.
ACS annual meeting, Surface, Interface and coating Materials. and Fall 2021

10. **L. K. Borden,** U. J. Kokilepersaud and S. R. Raghavan
Electroadhesion in Polymer-Polymer, Polymer-Tissue and Polymer-Plant Systems: Deciphering the Mechanism.
ACS annual meeting, Biomaterials and Biointerfaces. Fall 2021

11. **L. K. Borden** and S. R. Raghavan
Stimuli Responsive Reversible Adhesion Between Physical and Chemical Networks.
95th Colloid and Surface Science Symposium, Wetting and Adhesion, Virtual. June **2021**

12. **L. K. Borden,** A. Gargava, A and S. R. Raghavan
Electroadhesion of Polyelectrolyte Hydrogels to Animal Tissues: A Simple Way to Reseal Cut or Damaged Tissues Without Sutures.
95th Colloid and Surface Science Symposium, Interfacing Biology with Materials, Virtual. June **2021**

13. **L. K. Borden** and S. R. Raghavan
Electrically Induced Adhesion of Polyelectrolyte Hydrogels to Animal and Plant Tissues.
Fall 2020 meeting of Material Research Society (MRS), Hydrogel Technology for Humans and Machines, Virtual. Dec **2020**

14. **L. K. Borden,** A. Gargava, A and S. R. Raghavan
Electrical "Suturing" of Polyelectrolyte Hydrogels to Reseal Cut or Damaged Tissues.
Spring 2019 Meeting of the American Chemical Society (ACS), Biomaterial and Biointerfaces session of the Division of Colloid and Surface Chemistry, Orlando. April 2019
Awarded best presentation in session

15. **L. K. Borden** and S. R. Raghavan
Electrical Suturing of Polyelectrolyte Hydrogels to Reseal Cut or Damaged Tissues.
The 21st Mid-Atlantic Soft Matter Workshop, Rockville MD. Feb 2019

Presentations that have been submitted:

16. **L. K. Borden** and S. R. Raghavan
Universal Way to 'Glue' Capsules, Gels, and Tissues, in 3D Using Electric Fields
MRS Spring, San Francisco, CA, 2023

17. **L. K. Borden** and S. R. Raghavan
Electroadhesion of Hydrogels to Tissues: A Simple Way to Perform Suture-Less Surgical Repair
Adhesion Society, Orlando FL, 2023